

2007

Using Hurricane Ivan as a modern analog in paleotempestology: lake sediment studies and environmental analysis in Gulf Shores, Alabama

Thomas Bianchette

Louisiana State University and Agricultural and Mechanical College, tbianc1@lsu.edu

Follow this and additional works at: https://digitalcommons.lsu.edu/gradschool_theses



Part of the [Social and Behavioral Sciences Commons](#)

Recommended Citation

Bianchette, Thomas, "Using Hurricane Ivan as a modern analog in paleotempestology: lake sediment studies and environmental analysis in Gulf Shores, Alabama" (2007). *LSU Master's Theses*. 3312.

https://digitalcommons.lsu.edu/gradschool_theses/3312

This Thesis is brought to you for free and open access by the Graduate School at LSU Digital Commons. It has been accepted for inclusion in LSU Master's Theses by an authorized graduate school editor of LSU Digital Commons. For more information, please contact gradetd@lsu.edu.

USING HURRICANE IVAN AS A MODERN ANALOG IN PALEOTEMPESTOLOGY:
LAKE SEDIMENT STUDIES AND ENVIRONMENTAL ANALYSIS IN GULF SHORES,
ALABAMA

A Thesis

Submitted to the Graduate Faculty of the
Louisiana State University and
Agricultural and Mechanical College
in partial fulfillment of the
requirements for the degree of
Master of Science

in

The Department of Geography and Anthropology

by
Thomas Bianchette
B.S., Western Michigan University, 2005
August 2007

Acknowledgements

There are many, many people to whom I am completely indebted for the help and support needed to receive this degree. I would like to begin with my loving family which has been a tremendous support system throughout the years. They were sad to see me leave the Wolverine State, but they prodded me to follow my heart and trust my gut. I love you all!

Secondly, I would like to thank Dr. Kam-biu Liu for his tremendous help with this degree. His door was always open, and he has always been a trusted and reliable leader. I would also like to thank him for giving me the opportunity to study at Louisiana State University, the place I had my heart set on all along, over certainly many comparable applicants. This research was supported by grants from the National Science Foundation (DEB-0213884; BCS-0612477) and the Risk Prediction Initiative (RPI) of the Bermuda Biological Station for Research, of which Dr. Liu was the principal investigator (P.I.). Special thanks also go to Dr. Nina Lam and Dr. Robert Rohli, the other members of my thesis committee, for their advice and support.

In addition, I would like to thank all of the members of the Global Change and Coastal Paleocology lab. That includes Jason Knowles, Jennifer Hathorn, Terry McCloskey, Larry Kiage, Jon Breaux, and Yun Huang. All of these members were an unbelievable help through the thesis process, whether aiding in data analysis, or making me smile and laugh when I was stressed out. All of them possess distinctive specialties and strengths, making this lab a truly unique working and learning environment, and I respect and admire everyone mentioned due to their own intrinsic qualities.

A special thanks also goes to the Department of Geography and Anthropology, for awarding me the R.J. Russell Field Research Grant, aiding in the finances of traveling to Gulf Shores, purchasing accessories, etc.

I cannot forget about the other professionals and graduate students at LSU who spent time on this project, and I would like to send them my deepest appreciations. This includes Dr. Brian Marx (Experimental Statistics), Ryan Langlois (graduate student – Experimental Statistics), Amit Kulkarni (graduate student – Geography), Chris Pennington (graduate student – Geography), Mr. Dewitt Braud (Geography), and Dr. Bill Platt (Biological Sciences). Dr. Greg Veeck (Western Michigan University) introduced me to the idea of entering the graduate department at LSU (his first love), and I thank him for that. Additionally, I will never forget my very first geography class at the ‘lowly’ community college level with Mr. Andrew Huddy, another truly inspirational individual. Finally, I thank everyone at Gulf State Park, Alabama, particularly Ms. Kelly Reetz, and Scott Phipps at Weeks Bay Natural Estuarine Research Reserve, for their logistical support.

Table of Contents

Acknowledgements	ii
List of Tables	vi
List of Figures.....	vii
Abstract.....	ix
Chapter 1: Introduction	1
Chapter 2: Literature Review.....	3
2.1 Hurricanes	3
2.1.1 Hurricane Formation.....	3
2.1.2 Hurricane Characteristics.....	4
2.2 Paleotempestology	5
2.2.1 Case Studies.....	11
2.3 Oceanic Interactions.....	13
2.4 Geomorphic Effects	15
2.5 Impacts on Vegetation	17
2.5.1 Wind Damage	17
2.5.2 Flooding and Water Damage	21
2.5.3 Recovery	21
2.5.4 Case Studies.....	25
Chapter 3: Gulf Shores Hurricane Activity	28
3.1 Hurricane Ivan	28
3.2 Past Regional Hurricane Activity	30
Chapter 4: Survey of Tree Mortality Patterns.....	35
4.1 Methodology.....	35
4.2 Statistical Methods.....	39
4.3 Results and Discussion	41
4.4 Conclusion	46
Chapter 5: Remote Sensing.....	49
5.1 Introduction.....	49
5.1.1 Landsat 5 Images	50
5.1.2 Vegetation Indices	50
5.1.3 Land Cover Classification.....	51
5.1.4 Tasseled Cap Transformation	52
5.1.5 Accuracy Assessment	53
5.1.6 Research Question	55
5.2 Methodology.....	55
5.3 Results and Discussion (Pre-hurricane).....	61

5.3.1 NDVI.....	61
5.3.2 Tasseled Cap Transformation	62
5.3.3 Land Cover Classification.....	62
5.3.4 Accuracy Assessment	66
5.4 Results and Discussion (Post-hurricane)	68
5.4.1 NDVI.....	68
5.4.2 Image Differencing.....	70
5.4.3 Tasseled Cap Transformation	70
5.4.4 Land Cover Classification.....	70
5.4.5 Accuracy Assessment	73
5.4.6 Matrix Image/Major Changes in Land Cover.....	75
5.5 Sources of Error	75
Chapter 6: Sedimentary Impacts	80
6.1 Introduction.....	80
6.2 Methodology	82
6.3 Results.....	85
6.3.1 Lake Shelby – Western Transect	85
6.3.2 Lake Shelby – Eastern Transect.....	88
6.3.3 Lake Shelby – Southern Transect	88
6.3.4 Middle Lake.....	89
6.3.5 Little Lake.....	94
6.3.6 Non-forested Wetland.....	96
6.3.7 Swale Lakes	96
6.4 Discussion.....	96
6.4.1 Lake Shelby	96
6.4.2 Middle Lake.....	101
6.4.3 Little Lake.....	106
6.4.4 Non-forested Wetland.....	111
6.4.5 Swale Lakes	111
6.4.6 The Role of Winter Storms.....	111
6.5 Summary	114
Chapter 7: Conclusions	115
Bibliography	118
Vita	125

List of Tables

Table 1: Saffir -Simpson intensity scale	6
Table 2: GPS coordinates of the center of each tree plot.....	37
Table 3: Basic statistics from the tree mortality survey.....	42
Table 4: Cross-tabulation of complete binary statistics.....	44
Table 5: Odds ratio estimate results are shown	47
Table 6: Accuracy assessment results for the pre-hurricane classified image.....	67
Table 7: Accuracy assessment results for the post-hurricane classified image	76
Table 8: Comparing total land area of pre-hurricane to post-hurricane.....	78
Table 9: Radiocarbon dating results..	109

List of Figures

Figure 1: Diagram depicting how hurricane intensity and hurricane positioning can alter the amount of sand depositing in a lake.....	8
Figure 2: Diagram depicting sand layers eventually thinning out with distance from the sandy beach.....	9
Figure 3: Previous Lake Shelby core locations.....	14
Figure 4: Catastrophic damage to vegetation caused by storm surge flooding (between Lake Shelby and Middle Lake).....	22
Figure 5: Catastrophic damage to vegetation caused by storm surge flooding (north end of campground).	23
Figure 6: Catastrophic damage to vegetation caused by storm surge flooding (between Lake Shelby and Middle Lake).....	24
Figure 7: Winds along Ivan’s path.....	29
Figure 8: Rainfall totals attributed to Hurricane Ivan, with its track.....	31
Figure 9: “Before” and “after” effects of Hurricane Ivan in Orange Beach, Alabama	32
Figure 10: All Category 3-5 hurricanes from 1851-current to make landfall near Gulf Shores, Alabama.....	34
Figure 11: Locations of 13 tree plots and their elevations.....	38
Figure 12: Scatterplot with elevation (ft) and the percent of trees dead.....	43
Figure 13: Pre-hurricane raw image (4,5,3 band combination).....	57
Figure 14: Post-hurricane raw image (4,5,3 band combination).	58
Figure 15: Pre-hurricane NDVI.....	63
Figure 16: Pre-hurricane – Tasseled cap transformation	64
Figure 17: Pre-hurricane classification.....	65
Figure 18: Post-hurricane NDVI.....	69
Figure 19: Image differencing (NDVI).....	71

Figure 20: Post-hurricane – Tasseled Cap Transformation	72
Figure 21: Post-hurricane land cover classification.....	74
Figure 22: Matrix image	79
Figure 23: Sand supply (between Gulf of Mexico and Shelby Lakes).....	81
Figure 24: Lake Shelby core locations.....	86
Figure 25: Lake Shelby LOI results (eastern and western transect).....	87
Figure 26: Lake Shelby LOI results (southern transect).....	90
Figure 27: Lake Shelby LOI results (southern transect).....	91
Figure 28: Middle Lake (and vicinity) coring locations.....	92
Figure 29: Middle Lake LOI results.....	93
Figure 30: Little Lake (and vicinity) core locations.....	95
Figure 31: Little Lake LOI results.....	97
Figure 32: Non-forested wetland/swale lake LOI results.....	98
Figure 33: Location of cores taken from Lake Shelby in 1989 and the early 1990s	100
Figure 34: Core ML-06.....	102
Figure 35: Core ML-01.....	103
Figure 36: Core ML-TV2.....	104
Figure 37: Core ML-10.....	105
Figure 38: Cores taken from Middle Lake in September 1989	107
Figure 39: Loss on ignition results for core M2D.....	108
Figure 40: Radiocarbon dating results and possible storm correlations.....	110
Figure 41: Core LL-06.....	112
Figure 42: Core GS-3-6	113

Abstract

Paleotempestology is a young field in the science community, aimed at discovering evidence of past catastrophic hurricanes by analyzing geological proxy records, mostly overwash sand layers derived from barrier beach inundation. Gulf State Park in Gulf Shores, Alabama, is an ideal location to study this emerging science due to its unique geography of having three coastal lakes just north of a long beach system.

Hurricane Ivan, a Category 3 storm, made landfall at Gulf Shores, Alabama, on 16 September 2004, with 130 mph winds. It was expected that the overwash fan created by the storm surge was sufficient to reach the lakes and create a storm signature which could be useful as a modern analog.

A vegetation survey was done to examine Ivan's ecological damage to the forest around the Shelby Lakes. The results suggest quantitatively that elevation was a major factor in tree mortality. This study establishes that most damage to the forest was from storm surge and not high winds, as the latter would have led to a more continuous spatial pattern of destruction. Remote sensing work with Landsat 5 images was performed to reveal the spatial pattern of ecological damage to the forest at the landscape scale.

Cores taken near the center of Lake Shelby do not contain a sand layer at the top attributable to Ivan, primarily due to the lake's large size. Cores from Middle Lake do show visible sand layers at the top (ML-10, ML-06, ML-01, and ML-TV2). Little Lake, the easternmost lake, had two cores with a visible Ivan layer (LL-06 and LL-08).

Loss-on ignition data and radiocarbon dating results from core ML-TV2 indicate a minimum return period of 213 years. This estimate is comparable to results in Liu et al. (2003), who reported a return period of 180 years for Little Lake. The fact that Ivan left a sedimentary

signature in both Middle Lake and Little Lake supports the interpretation that sand layers in cores taken from the southern ends of both lakes represent direct hits by major hurricanes of Category 3 or higher intensity according to the Saffir-Simpson intensity scale.

Chapter 1: Introduction

This study aims at understanding the ecological and sedimentary impacts of Hurricane Ivan, an intense hurricane that made landfall near Gulf Shores, Alabama, on 16 September 2004. Ivan had significant geological and biophysical impacts in and around all three coastal lakes (Lake Shelby, Middle Lake, Little Lake) in Gulf State Park because this Category 3 hurricane made a direct hit at Gulf Shores. Therefore, it is interesting to examine the sedimentary impact of Hurricane Ivan in each lake, and to compare and contrast the stratigraphies within each lake and among the three lakes. From this sedimentary work, a modern analog can be established to aid the reconstruction of prehistoric hurricane strikes from sedimentary proxy records derived from these coastal lakes (Liu and Fearn, 1993). Paleotempestology, an emerging field of science (Liu, 2004a, 2004b) is becoming extremely important, mainly due to the increasing need to understand the return periods of many recent, powerful storms, such as Hurricanes Katrina and Rita. Paleotempestological data and results are extremely important to engineers, insurance companies, and policy-makers, to understand the frequency of hurricane activity during historic and prehistoric time periods to determine future risk. These data and results can best be analyzed and dissected if a proper modern analog is found. By finding a modern analog, logical interpretations can be made concerning the strength and impacts of past storms.

Remote sensing is a useful tool for studying the biophysical or environmental impacts of recent hurricanes. Specifically, Landsat 5 images can not only reveal how an intense storm alters the landscape, but can also allow the analyst to determine quantitatively the degree of change in certain land cover categories. Remote sensing can also be a useful tool to delineate patterns and boundaries of the storm surge inundation, based on the degree of tree mortality. In order to interpret the remote sensing data accurately, ground truthing must be performed at the study site,

and vegetation plots were analyzed to receive a more thorough “hands-on” understanding of any underlying patterns associated with tree mortality.

This thesis consists of six chapters. Following a brief introduction (Chapter 1), Chapter 2 is a literature review, outlining basic information on hurricanes, paleotempestology, and other relevant topics. Chapter 3 presents an overview of Hurricane Ivan, and other storms that have recently affected the Gulf Shores area. Chapter 4 reports on a vegetation survey to assess the degree of tree mortality within Gulf State Park. Chapter 5 is dedicated to a remote sensing analysis. The main purpose of Chapter 5 is to understand the impact of Ivan to this area. Changes in different land cover categories were calculated by comparing a pre-storm image to a post-storm image. These pre- and post-storm images are discussed in detail, along with interpretation of the land cover changes stemming from Ivan. Chapter 6 deals with the sedimentary impacts on the three lakes in Gulf State Park. Stratigraphic data from a large number of sediment cores are discussed in that chapter, and these data are correlated among cores taken from the same lake and between different lakes. The methodology and analysis are discussed regarding the sediment core findings and spatial relationships they contain with surrounding cores. Chapter 7 presents the summary of results and conclusions derived from this investigation.

Chapter 2: Literature Review

2.1 Hurricanes

According to Emanuel (2005), hurricanes have been discussed and interpreted in contrasting fashions for the past few centuries. Spanish explorers actually coined the term *hurricane* (initially called *Huracán*, *Hunraken*, or *Jurakan*) when they visited the New World. These three names were associated with tales of a god full of sinister actions, and even the potential to inflict harm on others. Caribbean peoples were so afraid of these gods that they often partook in out-of-character mannerisms, involving constant drum tapping or even ceremonies to save themselves from the potential winds and rain. The term *cyclone* was invented from a Greek word implicating “coil of a snake” by Henry Piddington, a curator at the Calcutta Museum in 1848. A *cyclone* is a word that is synonymous throughout the scientific world for a:

“Nonfrontal synoptic-scale (200-2,000 km in diameter) low-pressure system originating over tropical or subtropical waters with organized convection (i.e., rain shower or thunderstorm activity) and definite cyclonic surface wind circulation” (Emanuel, 2005: Pg. 21).

A *hurricane* is the term used for a tropical cyclone located in the South Pacific (east of 160°), Northeast Pacific (east of International Date Line), and the North Atlantic (Emanuel, 2005). A hurricane’s formal definition is:

“A tropical cyclone with maximum sustained surface winds of at least 33 m/s (74 mph).” (Emanuel, 2005: Pg. 21).

2.1.1 Hurricane Formation

A hurricane is a truly complex storm system, which should be understood in terms of its internal structure and characteristics upon landfall in order to comprehend the damage it can inflict. According to Simpson and Riehl (1981), a hurricane forms when a “rain system” hovers

over an ocean with a surface temperature at or over 26-27° Celsius, with an absence of temperature inversions in the vicinity. When these conditions occur, surface flow can speed up, causing cold air to sink into a central core area. Clouds eventually rise in circular bands, causing a surface pressure decrease and an increase in temperature around these cloud regions, equipped with vast amounts of water vapor. Outflow can eventually be greater than inflow, due to the quickly rising air (Simpson and Riehl, 1981).

According to Simpson and Riehl (1981), the air “follows successively warmer ascent paths” as it finally begins to rise from the rather choppy ocean (due to the storm’s high winds), and this instability creates a clear temperature contrast between the core and the outside edge of this storm. The pressure could plummet to 990-980 millibars at the center of the hurricane. Potentially, this pressure can drop to as low as 950 millibars, corresponding to the degree of temperature difference between the core and the outside of the hurricane (Simpson and Riehl, 1981).

Once the hurricane is formed over an ocean, it moves slowly. It can potentially make landfall at the nearest landmass in its path. According to Anthes (1982), as cited in Boose et al. (1994), once a hurricane is over land, it loses latent heat and sensible heat, while it experiences an increase in surface friction. Furthermore, according to Dunn and Miller (1964), as cited in Boose et al. (1994), changes in geography such as a mountain range can also alter the hurricane’s degree of influence, causing extreme dissipation potentially in a few hours.

2.1.2 Hurricane Characteristics

The storm’s *eye* is the most tranquil portion of the hurricane and is usually 5-60 kilometers in diameter. A lack of clouds and precipitation are indicative of this region (Simpson and Riehl, 1981). The *eyewall* surrounds the eye of the hurricane. This region has the strongest

winds and most intense rainfall, along with the greatest potential for damage when it reaches land (Emanuel, 2005). The average width of this area is approximately one to two kilometers (Simpson and Riehl, 1981). According to Emanuel (2005), the *moat* is the region just outside the eyewall. It is characterized by decreased precipitation and weaker winds than the eyewall. Some hurricanes have an *outer eyewall*, an area outside of the *moat* with similar conditions to the *eyewall* (Emanuel, 2005). Overall, the most destruction and the strongest activity is found at a radius of 100 kilometers from the center (Simpson and Riehl, 1981). Therefore, the positioning of a forest or a lake relative to the eye or eyewall of the hurricane is an important factor affecting the degree of geological or biophysical impact, especially because of the differing sizes and characteristics of the *eye*, *eyewall*, *outer eyewall*, and *moat*.

According to Emanuel (2005), storm surge is triggered by low pressure over the water surface. The storm surge increases roughly one centimeter for every millibar drop in surface pressure. Strong hurricanes can lift sea levels by a meter or more. Also, storm surge is precipitated by strong winds, especially at shallow water areas. These strong winds can push ocean currents to a few meters per second. Overall, the storm surge is large if the storm has a low central pressure and/or a substantial eye. Also, the storm surge is generally large if the seafloor becomes shallower closer to the shore, or the coastline is a section of the bay (in which the eye is larger than the bay) (Emanuel, 2005).

2.2 Paleotempestology

Paleotempestology is a rather new field in the science community. It studies past hurricane activity by analyzing geological proxy records (Liu, 2004a). During a strong hurricane landfall (typically Category 3-5 intensity – Table 1), sand is transported from a sandy beach into a backbarrier lake due to the storm surge overtopping the beach ridge. The overwash deposits in

Table 1: Saffir -Simpson intensity scale

<u>Description</u>	<u>Category</u>	<u>Pressure (mb)</u>	<u>Winds (knots)</u>	<u>Winds (km/hr)</u>	<u>Winds (mph)</u>	<u>Surge (m)</u>	<u>Surge (ft)</u>
Depression	TD	N/A	<34	<63	<39	N/A	N/A
Tropical Storm	TS	N/A	34-63	63-117	39-73	N/A	N/A
Hurricane	1	> 980	64-82	119-153	74-95	~1.5	4-5
Hurricane	2	965-980	83-95	154-177	96-110	~2.0-2.5	6-8
Hurricane	3	945-965	96-113	179-209	111-130	~2.5-4.0	9-12
Hurricane	4	920-945	114-135	211-249	131-155	~4.0-5.5	13-18
Hurricane	5	<920	>135	>249	>155	>~5.5	>18

the lake will appear as sand layers in a core taken from the lake, and they can provide evidence of past hurricane strikes in the area, covering the last 5,000 years or more (Liu, 2004a, 2004b; Liu and Fearn 2000a).

According to Liu and Fearn (2000b) the shape and size of these overwash deposits vary with each hurricane and/or geomorphic setting of the lake. Hurricane intensity, storm surge height, and coastal positioning are also vital factors. In addition, tidal height, duration of hurricane conditions, amount of barrier beach sand, and positioning of incoming hurricanes are also important factors (Figure 1). Therefore, sediment cores taken from a lake might have contrasting storm signatures, depending on the location of the coring sites relative to the size and shape of past overwash deposits (Liu and Fearn, 2000b).

According to Liu (2004a), overwash sand layers and other sediment deposits from storm surges identified from coastal lakes are the most useful proxy records for paleotempestology. During a hurricane strike, the beach barrier may be overtopped by the storm surge and sand is washed into the backbarrier lake, creating an overwash fan. Sand layers will generally be thicker near the coast and thinner toward the center and far end of the lake (Figure 2). Also, thicker sand layers tend to be caused by stronger hurricanes, such as catastrophic hurricanes of Category 4 and 5 intensity according to the Saffir-Simpson intensity scale. However, the height of the sand barrier is pertinent, since it takes a stronger hurricane to create an overwash fan in the lake with a higher sand barrier than one with a lower sand barrier. The paleotempestological sensitivity of a lake is the minimum intensity a potential hurricane needs to create an overwash sand layer in the lake, which is ultimately related to the overwash threshold, or the height of the sand barrier (Liu, 2004a).

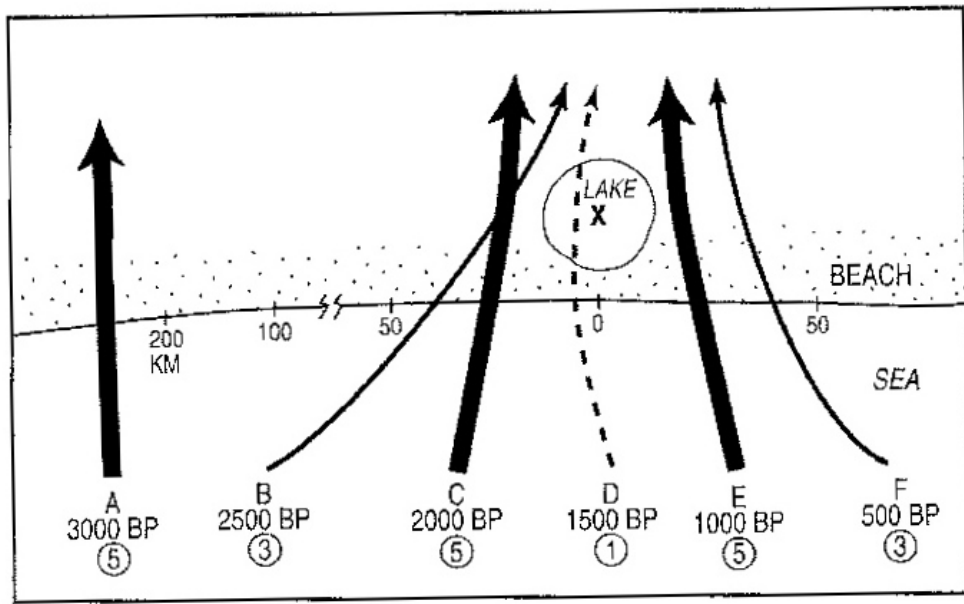
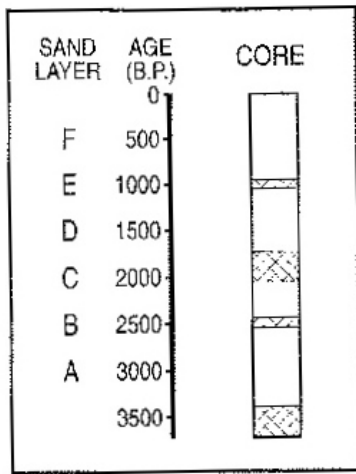


Figure 1: Diagram depicting how hurricane intensity and hurricane positioning can alter the amount of sand depositing in a lake (Liu, 2004a).

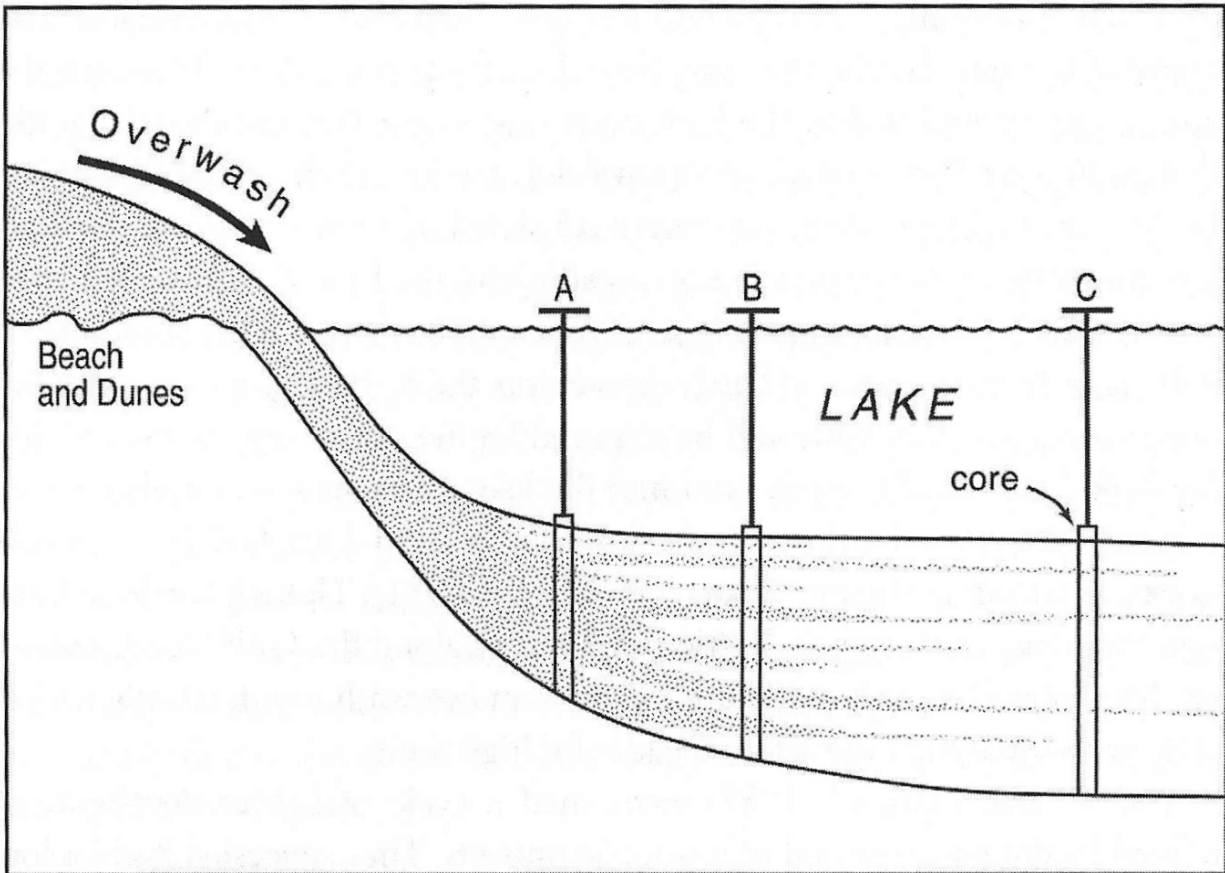


Figure 2: Diagram depicting sand layers eventually thinning out with distance from the sandy beach (Liu, 2004a).

Donnelly and Webb (2004) also provide an insightful synopsis of the factors involved in the formation of an overwash fan in a backbarrier marsh. They suggest that the degree to which a storm layer can be deposited at a particular site depends on numerous factors at a historic timescale, such as sediment amount, barrier height and position, sea level changes, wave energy, astronomical tide stage, and elapsed time from the last barrier breaching (Donnelly and Webb, 2004). Also, according to Donnelly and Webb (2004), these barrier beaches can either migrate landward or seaward through time. Seaward migration tends to follow a decrease in sea level, or an increase in sediment. On the contrary, if sea level rise is high compared to sediment supply, the barrier beach usually migrates landward (Donnelly and Webb, 2004).

In addition to the importance of sand layers as a useful proxy technique for paleotempestological research, other promising means exist to infer the landfall of hurricanes in historic and prehistoric time periods. Liu (2007) summarized these additional proxies and archives. Marine microfossils, such as dinoflagellates, foraminifera, and marine diatoms can be useful indicators, because an increase in these microfossils in a core can indicate saltwater intrusion from the storm surge, even if sand layers are not present. Fossil pollen can also be studied to detect salinity changes in a coastal plant community resulting from a storm surge. Other potential indicators of historic and prehistoric hurricane strikes are tree rings, storm-generated beach ridges, oxygen isotopic ratios from corals and speleothems, and sedimentary structures in marine sediments (Liu, 2007). Therefore, sedimentary evidence of a hurricane strike by a sand layer can be supplemented by evidence from pollen or marine microfossils to confirm the reconstruction.

These geological proxy records are essential for estimating the frequency of catastrophic hurricane strikes in a particular area. Such estimates cannot be obtained from the historical

written record because instrumental records of hurricane activity only go back approximately 150 years (Liu, 2004b). During the historical period, many areas have never been directly struck by a catastrophic Category 4 or 5 hurricane (Liu, 2004a).

More importantly, geological proxy records can reveal long-term changes in the prehistoric hurricane strikes, such as the occurrence of quiet and active periods. From the historical record of the last 100-150 years, it has been shown that hurricane activity exhibits marked interannual and multidecadal variability that is related to Sub-Saharan drought, El Niño-Southern Oscillation events, or other climatic phenomena occurring at a local to hemispheric scale (Elsner and Kara, 1999). According to Liu and Fearn (2000b), around 6,000 ¹⁴C years before present during the mid-Holocene thermal maximum, the jet stream was north of its position today, while the Bermuda High drifted to the northeast toward the mid-Atlantic. Anticyclonic air flow from around the Bermuda High directed more hurricanes toward the U.S. However, around 3,000 ¹⁴C years before present, the jet stream shifted to the south and the Bermuda High retreated to the southwest. Therefore, the predominant tracks of moist air and hurricanes were directed toward the Gulf of Mexico (Liu and Fearn, 2000b).

2.2.1 Case Studies

A sedimentary record from Western Lake in northwestern Florida reveals interesting results in paleotempestology. A sand barrier about 150 to 200 meters wide separates Western Lake from the Gulf of Mexico (Liu and Fearn, 2000b; Liu, 2004b). A sand layer attributable to Hurricane Opal, a Category 3 storm making landfall on 4 October 1995, was detected from a core taken from the nearshore zone near the south shore of Western Lake. The sand layer was composed of white sand similar to the sand exposed on sand dunes along the lakeshore (Liu and Fearn, 2000b).

Evidence from Western Lake indicates that frequent hurricane activity occurred from 1000-3400 ¹⁴C years ago, yet the last 1000 years have been remarkably quiet in terms of hurricane frequency. During the ‘hyperactive period,’ the Florida Panhandle had a 0.5% per year probability of being struck by a catastrophic hurricane. Data also indicated that the sand layers’ frequency and grain size increased in a period from 1400 to 3400 ¹⁴C years before present (BP). Conversely, the sand layers are rare or absent in the period from 3400 to 5000 ¹⁴C years BP. It has been determined that changes in global circulation patterns, especially the positions of the jet stream and Bermuda High, caused frequent hurricane activity between 1000 and 3400 ¹⁴C before the present, as well as rather inactive periods between 3400 and 5000 ¹⁴C years BP and in the past millennium from 1000 ¹⁴C BP to today. (Liu and Fearn, 2000b).

Lake Shelby, in coastal Alabama, also yields remarkable results from the groundbreaking paleotempestological work conducted by Liu and Fearn (1993). Their aim was to find evidence of Hurricane Frederic, a Category 3 hurricane that struck the Alabama Gulf Coast in 1979. The storm surge of Frederic was 4.8 meters high, sufficient to completely overwash the barrier beach and create an overwash fan. Hurricane Frederic’s wind gusts reached 145 miles per hour, and numerous locations in southern Alabama and southern Mississippi received between 22 and 28 inches of rain. Despite the strong Category 3 nature of Hurricane Frederic, a sand or layer attributable to this storm was not found in three cores taken near the center of the lake. However, two cores taken toward the southwestern shore showed the imprint of Hurricane Frederic. In core L (Figure 3), taken approximately 100 meters from the southernmost shore, a 9 cm thick band of white sand occurring toward the top of the core was attributed to the overwash event due to Frederic. Above the sand layer was a thin layer of gyttja deposited in the ten years

since the hurricane landfall. Frederic's sand layer was also found in Core S derived 325 meters from the shore, but the sand layer is much thinner, less than 0.1 cm (Liu and Fearn, 1993).

Information from other cores with no apparent storm signature of Hurricane Frederic permitted the reconstruction of the environmental history of the lake, according to Liu and Fearn (1993). Cores A, B, and E (Figure 3) were taken from the middle of the lake, and were out of reach from the overwash fan created by Hurricane Frederic. The cores had 55-85 cm of gyttja, overlying gray lagoonal clay. This stratigraphic boundary dated to 2,190 ¹⁴C years ago, while the bottom of core E dated back to 4,760 ¹⁴C years ago. Therefore, it may be determined that the freshwater lake was established around 2,200 ¹⁴C years ago, and it was a lagoon prior to that time. These cores did show older sand layers however, probably from more powerful catastrophic hurricanes of Category 4 or 5 intensity. By analyzing the sand layers and by using radiocarbon dating, it was determined that hurricanes of either a Category 4 or 5 intensity hit this area 3,200-3,000, 2,600, 2,200, 1,400, and 800 ¹⁴C years ago. Interestingly, sand layers were absent in sediments older than 3,200 ¹⁴C years ago. The possible explanation can rest in the Bermuda High hypothesis, similar to the results of the data from Western Lake (Liu and Fearn, 1993, 2000b).

2.3 Oceanic Interactions

ENSO cycles have a profound effect on hurricane landfall patterns for the United States. This is clear after analyzing trends from El Niño (warming of tropical eastern Pacific) and La Niña (cooling of tropical eastern Pacific). From 1900-1997, the probability of two or more hurricanes hitting the United States in the same season varied greatly with the different phases of the ENSO cycle. The percentages were: 66% for La Niña, 48% for neutral years, and 28% for El Niño (Bove et al., 1998). In addition, the chances of one random major hurricane (winds of at

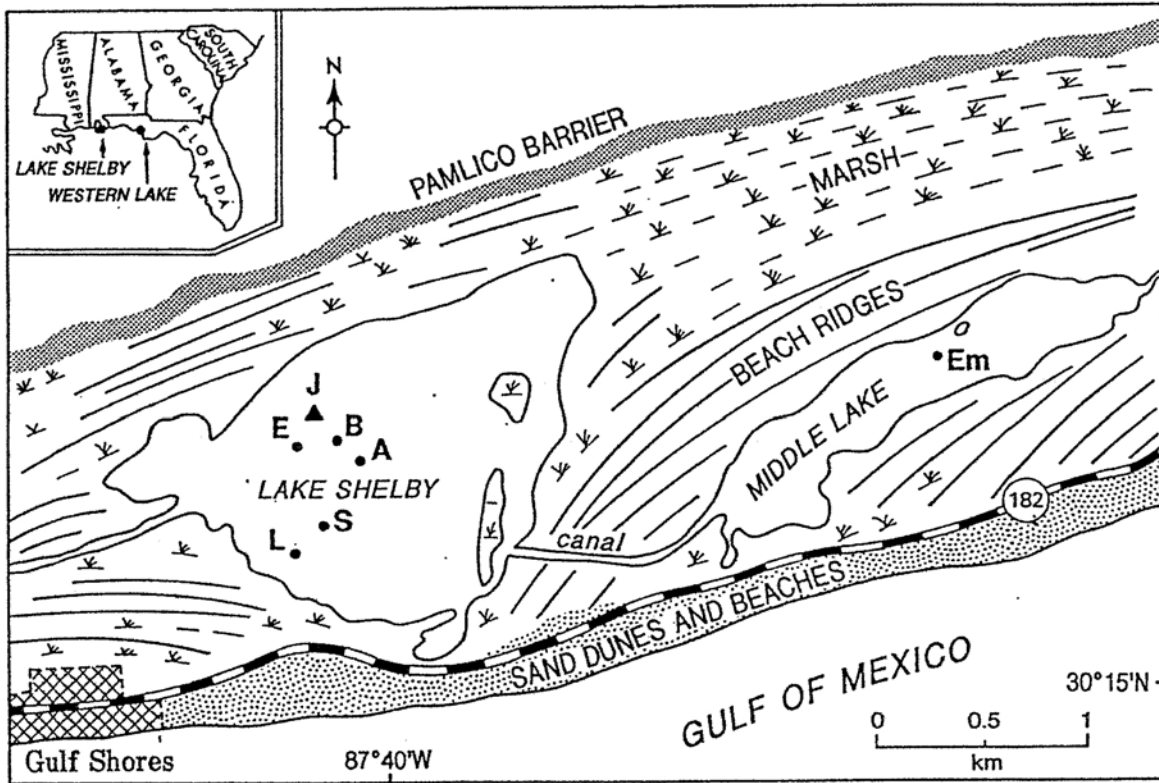


Figure 3: Previous Lake Shelby core locations. Only cores L and S showed a top sand layer attributed to Hurricane Frederic (Liu and Fearn, 1993).

least 96 knots, or 110 mph) making landfall during the ENSO cycles were also analyzed. These percentages were: 63% during a La Niña, 58% during a neutral cycle, and 23% during an El Niño (Bove et al., 1998). Interestingly, during September 2004 (the month of Ivan's landfall) the Oceanic Niño Index showed a warming trend (over the +/- 0.5° C threshold), indicative of an El Niño event (0.8, 0.9, and 0.9°C for three-month means of June-August-September, August-September-October, and September-October-November, respectively) (Climate Prediction Center, 2007).

2.4 Geomorphic Effects

Hurricanes can have significant effects on the geomorphology of a region. The geomorphology of a region can increase or decrease the effects of a hurricane. According to Cahoon et al. (1995), hurricanes can bring sediment into wetlands, thereby decreasing any potential land loss. However, hurricanes can also negatively affect wetland status by quickly eroding sediment surfaces. The rate of erosion depends upon many factors, including the meteorological characteristics of the hurricane. Also, the relative position of the wetland or landmass in relation to the hurricane is important (Cahoon et al., 1995).

Sediment deposition is a frequent occurrence after a hurricane event, with numerous examples from the landfall of Hurricane Andrew in 1992. Certain locations on Louisiana's Gulf Coast were affected by that storm, including Bayou Chitigue, Bayou Blue, and Jug Lake. Jug Lake and Bayou Chitigue received higher rates of sediment deposition than Bayou Blue. This may be related to the proximity of Jug Lake to the storm track, along with the location of Bayou Chitigue near many coastal bays and other tidal systems conducive to sediment transport (Cahoon et al., 1995).

Even after a hurricane's landfall, sediment deposition can still occur. According to Otvos (2004), as waves eventually die down, if the tide remains rather high, beach aggradation can still occur due to sand or sediment deposition. Overall, the sand accumulation leading to beach aggradation during a hurricane can be the result of sand derived from nearby bluffs, artificial or natural sand dunes, or the shallow portion of seafloor approaching the land. This scenario has been documented during Hurricane Georges, a Category 2 hurricane hitting central Mississippi in 1998 (Otvos, 2004).

Also, the speed of the storm can have an effect on coastline erosion or degradation. For instance, Hurricane Andrew was a rather fast-moving hurricane. Therefore, throughout the Straits of Florida and surrounding beaches the wave attack and wave scour were rather low. The onshore surge was strong, but short-lived. Therefore, a slower-moving hurricane, such as Rita in 2005, would have brought a strong wave attack for a longer period of time before the incoming hurricane winds (Tedesco et al., 1995).

Many beaches were affected by Hurricane Andrew, whether they were positioned on the eastern or western coast of Florida. According to Tedesco et al. (1995), southern Key Biscayne (facing the incoming hurricane from the Atlantic) was situated in Andrew's northern eyewall. Beaches located in the north-central region of southern Key Biscayne had overwash sand lobes carried to the island, while onshore surge approached the land perpendicularly. However, the storm surge moved toward the southern beaches at an oblique angle. Therefore, the backshore was not thoroughly inundated. Both northern and southern beaches developed a storm ramp, which was not steep. However, the land profile eventually drifted inward about 15 meters. This was due to rather powerful incoming waves from strong easterly winds (Tedesco et al., 1995). Furthermore, when Andrew moved offshore, the southern eyewall helped to transport sediment

to western coast beaches, lagoons, and coastal and interior bays, due to storm surge, onshore wind, and waves. The sediment carried by wind created a storm layer 1 to 10 kilometers from the western coast, high in organic and carbonate content (Risi et al., 1995).

2.5 Impacts on Vegetation

Damage to vegetation is quite common following periods of intense winds, especially during a hurricane. Not only do destructive hurricane winds damage plants and trees during the storm, but flooding due to storm surge can also harm coastal vegetation communities. Overall, the ferocity of a hurricane's winds, together with flooding from intense rainfall and storm surge can alter vegetation patterns by changing the structure of the forest, causing certain species to increase and others to decrease in population.

Numerous factors affect the damage to a forest, such as the hurricane size, intensity, and the positioning of the forest relative to the storm track. Furthermore, different topographies affect the outcome of a hurricane strike, together with the particular species composition and forest structure along the storm track (Boose et al., 1994).

2.5.1 Wind Damage

There are four major syndromes in terms of the population response of tree species after a hurricane strike: *resilient*, *usurper*, *resistant*, and *susceptible* (Bellingham et al., 1995).

According to Batista and Platt (2003), the syndrome that a tree population exhibits depends on a number of factors, such as the strength of the hurricane, the population configuration of the particular species in the forest, and the history of disturbance (such as a forest fire occurring prior to the storm, possibly killing recruits). Trends are occasionally seen when comparing the same species to other regions influenced by other hurricanes, since these species contain specific traits that either aid or impair its response to a hurricane (Batista and Platt, 2003). These

syndromes enable categorization and comparison among species, and are convenient for comparing and contrasting hurricane damage or tree species propensities.

Moreover, a hurricane affects the coastal plant communities in many contrasting ways. Strong winds can break limbs and defoliate trees. The specific location of a forest or a group of trees can be important when analyzing the area's potential for damage, or lack thereof. For example, when Hurricane Hugo rumbled through the island of St. John in the Virgin Islands, it destroyed the forests near streambeds at rather low elevations. These forested plots positioned on a narrow valley were affected more than higher elevated plots due to the former's exposure to stronger winds channeled through the valley (Reilly, 1991).

Certain circumstances involving a forest's specific geography can often affect its chances of survival. A forest growing on loose soils that can saturate easily is more susceptible to uprooting by strong winds. Bottomland hardwoods are shown to be more prone to windthrow on sandy soils than soils with high organic or clay content (Doyle et al., 1995). For example, the white pond pine (*Pinus serotina*), which usually grows on weak soils (Myers and van Lear, 1998), does not respond well to wind disturbance events (Gresham et al., 1991). Also, aerial surveys suggested that damage tends to be heavier on the windward side of a hill, plateau, or mountain than the leeward side, as suggested by the destruction to vegetation on the Luquillo Mountain in Puerto Rico from Hurricane Hugo (Brokaw and Walker, 1991). A dense forest is generally more resistant to wind damage due to the protection of the trees on the periphery, even though an incidence of canopy trees toppling subcanopy trees is common (Doyle et al., 1995).

Different tree species possess contrasting traits in response to hurricane disturbance. Certain traits enable trees to withstand a hurricane, while other traits can hinder resistance. Rainforest trees generally respond favorably after a hurricane, mainly due to an adaptation

allowing them to resprout after crown destruction (Boucher et al., 1990). In temperate forests, numerous factors must be considered. According to Doyle et al. (1995), hurricane damage to trees is more acute along an ecotone, such as in areas between two major biomes or land cover regions. Possessing a high crown ratio or having a low wood density are other factors potentially causing an increase in damage (Doyle et al., 1995). Tree survival also depends on the damage type and the stem size of the tree, as well as the actual tree species; these factors can be subsequently measured by crown regeneration following a disturbance event. The rate of re-leafing, however, is dependent upon the tree species (Cooper-Ellis et al., 1999). Moreover, wood characteristics are vital in determining the resistance to hurricane damage. Trees resistant to stem damage are more susceptible to branch damage, mainly due to the high wood density, leading to less pressure and an increase in branch stress (Zimmerman et al., 1994). Denser wood species have a very low chance of a stem break in a windstorm, because of the firmness and lack of flexibility characteristic of this type of wood. Since these woods are also stronger, the tree mortality rate decreases for these species as well (Zimmerman et al., 1994).

Tree uprooting is common during a hurricane. Despite the tree being killed, the uprooting brings important nutrients to the surface to be utilized by other surrounding vegetation (Myers and van Lear, 1998). Tree uprooting is not related to wood density, but to other factors such as changes in topography and wood composition characteristics (Zimmerman et al., 1994).

All in all, tree mortality is fairly rare in tropical forests after a hurricane. Additionally, tropical trees are more likely to re-grow branches after a hurricane than their temperate counterparts (Zimmerman et al., 1994). Understorey trees might develop increased growth and survival following a hurricane (Lugo and Scatena, 1996), while mature trees are fairly resilient against high winds (Boucher et al., 1990).

It is imperative to discuss how different tree species react in various ways to a hurricane. According to Doyle et al. (1995), numerous tree species, especially those residing in coastal locations prone to strong winds, possess special adaptations to withstand these disturbance events. For instance, the swamp tupelo (*Nyssa sylvatica*) and the bald cypress (*Taxodium distichum*) are wind resistant, due to their buttressed boles. Cypress also is fairly wind resistant, due to its deciduous characteristics leading to a decreased surface area in the brunt of the force. Bald cypress showed impressive resistance characteristics during Hurricane Andrew, from the Atchafalaya Basin in southern Louisiana. The bald cypress withstood impact quite well, due to its complex root system, increased root size, and weight (Doyle et al., 1995). Longleaf pine (*Pinus palustris*) has a fairly extensive root system, with roots that are six meters long and can reach two meters deep. Live oaks (*Quercus virginiana*) contain a rather sturdy, durable wood and are known for having a rather continuous canopy notorious for “branching out” (Gresham et al., 1991). Also, mahogany responds well to hurricanes and associated conditions such as fire, flooding, and extreme wind. Mahogany trees disperse their seeds which aids in population stability (Myers and van Lear, 1998).

A hurricane usually results in an abundance of woody debris on the forest floor. According to Rice et al. (1997), this woody debris is more common in an open rather than a closed canopy. Woody debris has an important function in these ecosystems. It stores vast amounts of nutrients, such as phosphorus and nitrogen. Decomposition slowly takes place once the debris is in contact with the soil, at which point the nutrients are slowly transferred into the soil beneath (Rice et al., 1997). Therefore, the forest can regenerate itself by means of having new understorey trees to replace those trees that have been uprooted and killed, rather than a complete depletion of all essential nutrients.

2.5.2 Flooding and Water Damage

Flooding represents a possible environmental impact from a hurricane strike (Figures 4-6). Flooding brings disastrous effects to vegetation, such as reducing stomata activity, diminishing photosynthetic rates, and causing hormonal fluctuations, as well as consequences such as significantly condensed water and nutrient uptake (Pezeshki, 1994 - cited in Lopez and Kursar, 2003). According to Lopez and Kursar (2003), flooding engulfs the roots in saltwater, decreasing their oxygen uptake, leading to limited tree growth. Light-loving species have a much more complex metabolism than shade-tolerant species. Therefore, these species are more damaged in flood conditions than shade-tolerant vegetation types (Lopez and Kursar, 2003). Slow-moving hurricanes will potentially lead to more intense flooding, especially with riparian and upland forests (Myers and van Lear, 1998). Flooding can also occur inland during a hurricane strike. For example, Hurricane Agnes, which made landfall in 1972 in Apalachicola, Florida, caused \$3.5 billion in damage from inland river flooding over 1600 kilometers from the coast (Simpson and Riehl, 1981). Flooding response also depends on the type of species. For instance, *Tabebuia* had increased leaf growth during a series of floods, while *Pentaclethra* did not respond well in a seasonally flooded forest in Panama (Lopez and Kursar, 2003).

2.5.3 Recovery

In terms of forest recovery following the disturbance event, many species take advantage of the increase in sunlight and use the light to resprout. Certain other species have difficulty resprouting or regenerating a canopy following a disturbance. When this occurs, these species are often replaced by other species, similar to when hardwoods replaced most pines following central Massachusetts's 1938 hurricane (Cooper-Ellis et al., 1999). Resprouting rates can vary widely, but are dependent on certain factors. For instance, woody tissue traits, along with



Figure 4: Catastrophic damage to vegetation caused by storm surge flooding (between Lake Shelby and Middle Lake).



Figure 5: Catastrophic damage to vegetation caused by storm surge flooding (north end of campground).



Figure 6: Catastrophic damage to vegetation caused by storm surge flooding (between Lake Shelby and Middle Lake).

nutrient surplus such as phosphorus, potassium, and calcium on the soil surface, lead to rather expeditious growth in damaged trees and rapid resprouting of those uprooted trees.

Decomposition by woody debris can also accelerate growth or rate of resprouting, due to a transfer of nutrients (Whigham et al., 1991). Canopy gaps following a hurricane can promote vast seed recruitment, along with rapid growth, due to reduced competition to receive light or optimal soil resources from competing trees (Brokaw and Walker, 1991).

Seedlings and saplings must compete with surrounding trees in the disturbance area for resources to eventually reach the canopy. The number of seedlings which eventually reach the canopy depends on the degree of canopy damage and how quickly the canopy closes (Tanner et al., 1991). Normally, the forest composition will change minimally following a hurricane if tree mortality is generally low, along with a nominal presence of invasives (Whigham et al., 1991).

2.5.4 Case Studies

It is important to consider other case studies regarding specific hurricanes to understand how different forests in isolated regions respond to storms of differing characteristics and intensities. Hurricane Hugo hit approximately 20 kilometers east of Charleston, South Carolina on 22 September 1989. Hugo had sustained winds up to 222 km/hr (roughly 138 miles/hr), making it a Category 4 hurricane on the Saffir-Simpson scale. The forests of South Carolina that were affected by this storm possessed an extensive array of tree species. Live oak, pond cypress, and bald cypress have relatively high wind resistance. These species sustained very little damage due to the storm. However, loblolly pine, longleaf pine, southern red oak, and water oak, possessing a low resistance to breakage, sustained broken branches, damaged trunks, and high levels of defoliation (Gresham et al., 1991).

Furthermore, during Hurricane Hugo, most trees with the greatest diameter at breast height (dbh) values were damaged much more than trees with a smaller dbh value, which suffered minimal damage, such as the loblolly pine. The longleaf pine reacted slightly differently however, as this smaller species experienced substantial crown damage, while the larger pines were generally intact. Other coastal species, such as swamp tupelo, bald cypress, longleaf pine, and live oak were unharmed for approximately 80% or more of the basal area (Gresham et al., 1991). An interesting side note comes from the lower coastal plain of this region. This region is more “hurricane prone” than western regions farther from the coast. The species found in this region proved more resistant to hurricane damage than species found outside of this region. The question is posed whether these species are actually more resilient due to past hurricanes throughout the course of history; that is, did the stress of previous hurricanes enable these trees to withstand the damage by means of traits developed in order to resist these frequent storm strikes (Gresham et al., 1991)?

Hurricane Andrew also left a significant impact on the Gulf Coast. According to Loope and Duever (1994), the destruction created countless canopy openings of various sizes. These gaps allowed pine saplings to grow up to reach the overstorey, made possible by the increased sunlight. The Long Pine Key Hammocks, an area abundant with hardwood trees that are less resilient than pines, experienced a reduction in canopy cover reduction from 30% to 100%, with scattered gaps ranging from 10-20 meters wide (Loope and Duever, 1994). It must be noted that vines such as grape vines and poison ivy propagated due to the canopy disturbance. While such vines aid in the retention of soil moisture, they also stop seedling growth and can choke nearby trees by inhibiting their potential growth and prosperity. In terms of trees, the taller trees (specifically the live oaks) sustained far more damage than shorter trees from Hurricane Andrew.

These trees lost many branches, particularly the larger trees that can reach 15 meters in height and 75 centimeters in diameter. The palm trees, having adapted to hurricane-type climates, sustained minimal damage from Hurricane Andrew (Loope and Duever, 1994).

The canopy disturbance caused the microclimate to be altered dramatically. This change brought immeasurable debilitating effects, notably increased sunlight and a drop in relative humidity, leading to a subsequent decrease in soil moisture and ultimately a decrease in human-initiated burning (Loope and Duever, 1994). Canopy disturbance is also an avenue for pioneer species to develop and thereby completely alter the forest structure (Walker, 1991). It is predicted that forest composition will not vary after Andrew, specifically because tree mortality rates were found to be low. However, Hurricane Andrew brought many consequences to this area. This includes a loss or decrease in rare species, possible widespread dispersal of propagules and other invasive species, and the remote possibility of a large, catastrophic fire (Loope and Duever, 1994). The possibility of fire would come from the vast array of leaves and drying biomass on the forest floor, coupled with rapidly drying soil from the increase in sunlight. Also, an increase in wind would increase the probability and potential strength of these fires. However, in reality fires are unlikely to occur in modern times, due to human intervention (Whigham et al., 1991).

Chapter 3: Gulf Shores Hurricane Activity

3.1 Hurricane Ivan

Hurricane Ivan originated near Africa's west coast and subsequently strengthened to a tropical depression on 2 September 2004 (Franklin, 2005). According to the National Hurricane Center (2004), Ivan eventually became a tropical storm on 3 September and gathered strength, even though it was unusually close to the equator for a tropical storm, with a position of approximately 9.7°N. Ivan became a hurricane on 5 September 2004, about 1000 nautical miles east of Tobago, and continued moving westward, developing strength as it traveled. Ivan became severely weakened temporarily, due to disintegrated convection in the eyewall, caused by a sudden influx of dry air. Ivan then strengthened to Category 3 status, and hit Grenada with an eye diameter of 10 nautical miles (National Hurricane Center, 2004). Hurricane Ivan became a Category 5 storm on 9 September as the storm reached the Caribbean, just south of the Dominican Republic. The pressure plummeted to 910 millibars (mb) twice, and sustained winds reached approximately 160 mph (Franklin, 2005). According to the National Hurricane Center (2004), the storm weakened to Category 4 as it passed Jamaica, due to a disrupted eyewall. Ivan reached a catastrophic Category 5 status a second time and continued, strengthened by warm Gulf water and upper-tropospheric outflow, to clip Western Cuba. Ivan turned northward on 14 September weakened by vertical shear increase due to southwesterly flow from a mid to upper level trough (National Hurricane Center, 2004). Hurricane Ivan eventually reached the United States on 16 September (Franklin, 2005). At 1:50 A.M. local time, Hurricane Ivan entered eastern Mobile Bay as a Category 3 storm (Figure 7) with 130 mph winds (CNN, 2004). At landfall, the eye was 40-50 nautical miles long (National Hurricane Center, 2004). Torrential rains affected a great portion of the Gulf and Atlantic south, together with more than 100



Figure 7: Winds along Ivan's path (National Weather Service, 2006).

tornadoes (Franklin, 2005). This storm left over 1.1 million people with power outages in Florida, Mississippi, and Alabama (CNN, 2004). Franklin (2005) states that over the Delmarva Peninsula, the remainder of the storm joined a frontal system that ultimately led to the reformation of this once powerful storm; unconventionally, the extratropical low split from the frontal system and drifted from the western Atlantic to the Gulf of Mexico. Due to the typical hurricane-producing distinctiveness of the Gulf of Mexico, Ivan soon gained tropical storm strength on 22 September and eventually reaching tropical depression status, making its final landfall in southwestern Louisiana two days later (Franklin, 2005). The entire track and the rainfall totals are depicted in Figure 8.

According to Franklin (2005), the storm surge was approximately 10 to 15 feet along the Alabama Gulf Coast, while the heaviest rainfall amounted to 10 to 15 inches in certain areas. This assessment agrees with Stone et al. (2005), who claimed that Hurricane Ivan produced a storm surge of at least 3 meters (about 9.8 feet) along Gulf Shores, Alabama, despite a sudden decrease to a Category 3 storm. Twenty-six people died due to Hurricane Ivan (Franklin, 2005). To date, Hurricane Ivan is the 9th strongest Atlantic hurricane on record, with the minimum pressure falling to 910 mb (U.S. Department of Commerce, 2006). The damage inflicted on buildings could be seen throughout the Gulf Coast (Figure 9).

3.2 Past Regional Hurricane Activity

To understand the potential sand overwash imprints on Gulf State Park, it is vital to understand when and where intense storms hit this area, particularly Category 3 storms and higher. The NOAA Coastal Services Center (<http://maps.csc.noaa.gov/hurricanes/viewer.html>) inputs such information in a vast database. One can perform a search for a particular zip code, latitude/longitude, storm name, climatology, or place name.

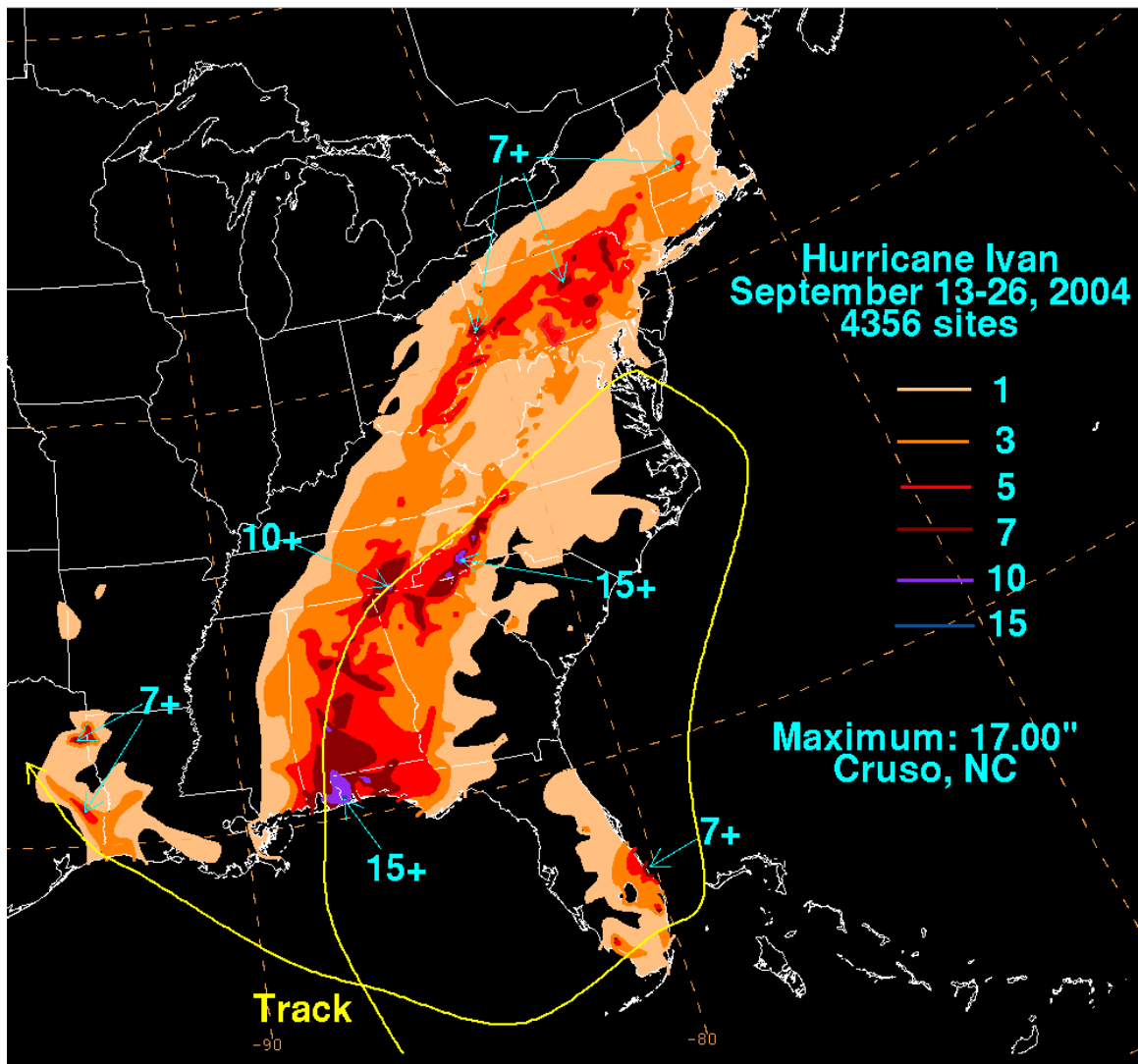


Figure 8: Rainfall totals attributed to Hurricane Ivan, with its track (National Oceanic and Atmospheric Administration, last accessed 16 Jan 2007).



Figure 9: “Before” and “after” effects of Hurricane Ivan in Orange Beach, Alabama (about 10 km east) of Gulf Shores – two buildings are severely damaged (United States Geological Survey, 2004).

Figure 10 indicates there were approximately 11 hurricanes of Category 3 or higher intensity making landfall within a 65-nautical mile buffer from Gulf Shores from 1851 to the current time. Hurricane Ivan (2004), a Category 3 storm, is most compelling due to the fact it was a direct hit on this area. Although other hurricanes were hits in close proximity to Gulf Shores, it was unclear (prior to lake coring and analysis) whether the positioning of the hurricane and/or strength of the storm had allowed a sand overwash imprint in the lakes at Gulf State Park. Two storms to consider in respect to a potential overwash are Frederic (1979), and Not Named (1916). This is due to storm positioning and strength (see Liu, 2004a). Frederic, a strong Category 3 storm, made landfall approximately 30 miles west of Ivan's path, while Not Named, a Category 3 storm, made landfall approximately 30 miles east of Ivan's path.

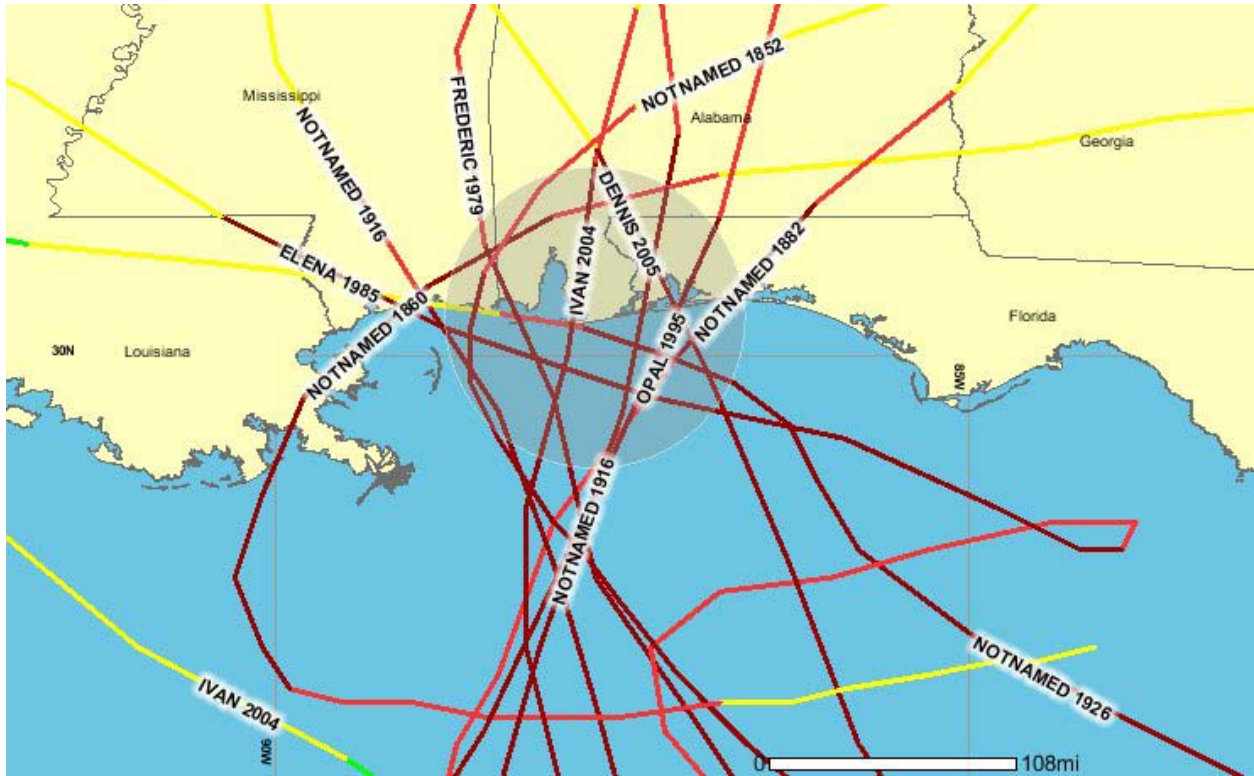


Figure 10: All Category 3-5 hurricanes from 1851-current to make landfall near Gulf Shores, Alabama. (gray circle indicates 65 nautical mile buffer) (NOAA Coastal Services Center, 2006).

Chapter 4: Survey of Tree Mortality Patterns

Analyzing the spatial pattern of the ecological damage caused by Ivan is an integral part of this research project, particularly in relation to the post-hurricane land cover classification (discussed in Chapter 5). This involves a survey of the spatial pattern of tree mortality as a function of differences in elevation within Gulf State Park. This research component also lends a loosely quantitative interpretation to the Landsat images and measures the extent of forest damage of different locations, thus providing the finalized ground truthing in support of the remote sensing component of this study.

A major objective for this analysis is to understand the spatial pattern of tree mortality as a function of elevation. It is hypothesized that the majority of the ecological damage inflicted upon this area was caused by flooding, not wind damage. Therefore, the damage was expected to be heaviest in low-lying areas subjected to storm surge inundation, unlike a continuous pattern that would be more typical of wind damage. Even a difference of only a few feet of elevation would then be a major factor in tree survival. By analyzing multiple reference images (TOPO software, Google Earth, topographical maps) in conjunction with the vegetation indices (Chapter 5) derived from ERDAS Imagine, it was clear how elevation represents a major factor affecting the survival of trees after the hurricane. Data collected from this tree mortality survey can be used to test the hypothesis that tree mortality pattern was highly related to elevation and that storm surge flooding, rather than wind, was the main cause of the ecological damage.

4.1 Methodology

The field survey was performed in October 2006 and January 2007. Tools such as a field notebook, tape measure, machete (to cut undergrowth), and GPS were used for this study. Areas of low (3-7 feet), medium (8-14 feet), and high elevation (15+ feet) were included in the

sampling design. These areas were found with the aid of National Geographic's TOPO software along with Google Earth, both of which give accurate elevation measurements.

Thirteen plots were used for this tree survey (Figure 11, Table 2). Because elevation is a primary focus in this analysis, tree plots were chosen on sites of contrasting topography. Once a site was chosen in the field, the GPS location was stored (Table 2), and the number of trees for the particular plot was determined. The tree plots were of contrasting sizes, because certain forests are denser than others. A minimum tree count of 25 was sought. For each plot, an arbitrary center tree was pinpointed and marked with chalk. The remaining trees of the respective plot were marked by emanating away from this center tree. Each tree was marked with chalk to eliminate any chance of being analyzed twice. For areas with dense undergrowth, 25-30 trees were counted. For most areas, the undergrowth was not dense. These particular plots had 50 trees. For each sampled tree the diameter at breast height (dbh) was determined, and it was considered whether:

- the tree was a pine or a hardwood;
- the tree was dead or alive;
- the tree was standing (or leaning), or broken;
- the tree branches were intact or not intact.

The records of the dichotomies were transported back to Louisiana State University for analysis. The data were imported into an Excel spreadsheet, with binary input for the nominal data. They were subsequently imported into a statistical software package (SPSS). The coding for each tree is the following:

- Dead = 0: Alive = 1 (categorical variable):
- Pine = 0: Hardwood = 1 (categorical variable):
- Standing/Leaning = 0: Broken = 1 (categorical variable):
- Branches Intact = 0: Not Intact = 1 (categorical variable):
- DBH = numeric value (continuous variable).

Table 2: GPS coordinates of the center of each tree plot.

Plot	Latitude (N)	Longitude (W)
1	30°15.961'	87°38.620'
2	30°16.264'	87°37.897'
3	30°16.629'	87°36.701'
4	30°16.210'	87°39.083'
5	30°16.146'	87°39.716'
6	30°16.461'	87°37.406'
7	30°16.573'	87°37.408'
8	30°16.858'	87°37.410'
9	30°16.533'	87°36.633'
10	30°15.883'	87°38.767'
11	30°16.000'	87°37.400'
12	30°16.083'	87°37.267'
13	30°16.433'	87°36.533'

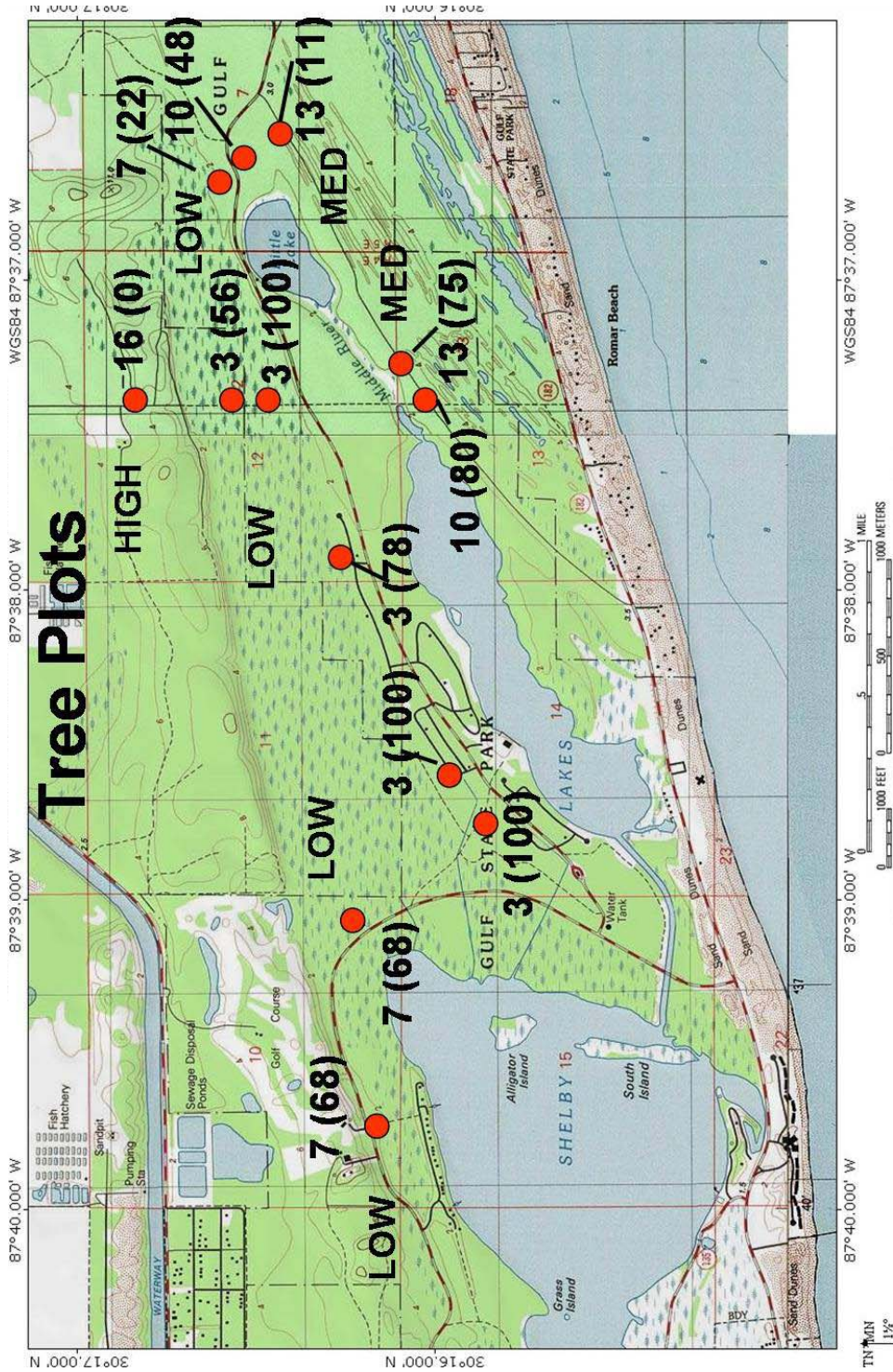


Figure 11: Locations of 13 tree plots and their elevations (number in feet). Areas of low (3-7 feet), medium (8-14 feet) and high (15+ feet) elevation are also indicated (National Geographic TOPO Software).

The elevation dummy variable was added as an additional column. For this column, each tree of the same plot is given the same elevation of the center point of the plot.

4.2 Statistical Methods

Logistic regression was chosen to indicate how odds of survivability increase when there is a one unit increase in dbh (for example). The most common method to interpret the results of a logistic regression is an odds ratio.

Odds ratios are explained in significant detail in Agresti (1996). An odds ratio is the probability of success divided by one minus the probability of success. This is best explained by first visualizing the equation for odds:

- $\text{Odds}_1 = \text{Probability}_1 / (1 - \text{Probability}_1)$.

Importantly, when the probability of a success is higher than the probability of failure, the value is over 1.0. For example, if 'Probability₁' is 0.9, then odds of success are 9 (0.9/0.1) (Agresti, 1996).

Furthermore, an odds ratio is a ratio of two odds, as defined above. The equation for an odds ratio, as stated in Agresti (1996) is:

- $\Theta = \text{Odds}_1 / \text{Odds}_2$

In applying the variables (discussed in Methodology section), it is important to analyze the odds of increase or decrease when increasing or decreasing the relevant variable by a fixed unit. For example, if analyzing dbh, the odds ratio would be: (odds alive | dbh + 1) / (odds alive | dbh).

This is equal to e^B , with B being the parameter value from the logistic regression model (discussed below - see Hosmer and Lemeshow, 2000). This odds ratio can be applied to discover differing survival (or death) rates when the particular variable in the regression model is increased by one unit (Platt et al., 2002). Therefore, when dbh (or any other continuous variable)

is increased by one unit (one cm in this scenario), the difference of survivability is portrayed by an odds ratio.

Logistic binary regression is discussed by DeCoster (2004). No assumptions are made toward dependent or independent variables being interval or ratio data (DeCoster, 2004). In addition, logistic regression is useful in the analysis of a dependent variable, by examining either categorical or continuous data (Garson, 1998). Logistic regression is most useful when the dependent variable is dichotomous (Garson, 1998). The independent variable values help create an equation analyzing the logarithm of these variables' odds (DeCoster, 2004). A coefficient B is derived for the independent variables in the model, in order to develop odds ratios, found by utilizing constant e and coefficient e^B (DeCoster, 2004; Hosmer and Lemeshow, 2000). Altering the independent variable is accomplished by increasing the quantity to reveal changes in odds (DeCoster, 2004). For a logistic regression, independent variables can be either polychotomous, dichotomous, or continuous. Confidence intervals can easily and efficiently be calculated for a logistic regression (Hosmer and Lemeshow, 2000).

Logistic regression is also discussed extensively by Christensen (1997). Correspondingly, logistic regression works well with a dependent variable with only two categories, since the odds of binary variable 1 occurring is p_1/p_2 , while the opposite (p_2/p_1) is true for odds of binary variable 0, with $p_1 + p_2 = 1$. Models are fit toward the statement $\log(p_1/p_2)$. For a simple regression analysis, the equation is:

- Logit (p_i) is defined as $\log(p_i/1 - p_i) = \beta_0 + \beta_1 V_1$, where
 - V_1 (or V_2, \dots, V_{24}) – Variables (dbh, elevation, etc.).
 - β_0, β_1 – intercept, slope parameters (Christensen, 1997).

Phi coefficients and Pearson's r statistics are also computed. Pearson's r is used to analyze the correlation between interval or ratio data, not categorical. This outcome can range

from -1 to 1, indicating a strong negative or positive correlation, respectively (Sheshkin, 1997).

A phi coefficient is similar to a Pearson's r value, but is used with 2 X 2 contingency tables, as in Table 4, with dichotomous variables with binary values (Sheshkin, 1997).

4.3 Results and Discussion

It is pertinent to discover the number of trees dead and alive in each plot, along with the basic statistics of these plots. This information is grouped by elevation and listed in Table 3. A pattern can be seen to how tree mortality increases as elevation decreases, and vice versa. Tree plots 1 and 6 (both 3 feet elevation) do not yield a living tree, while plot 8 (16 feet) yields 50 living trees and no dead trees. Elevations between these two plots yield differing results. Other obvious trends seen from Table 3 include more broken trees toward lower elevations and a lack of hardwood trees toward higher elevations.

The regression plot shows that tree mortality decreases with increasing elevation (Figure 12). The Pearson's r value of -0.697 shows a moderate to strong negative relationship between elevation and tree mortality, which is significant at the 0.01 level. According to Sheshkin (1997), a moderate correlation in strength is roughly $0.3 \leq |r| < 0.7$, while a strong correlation is 0.7 or higher. While these are admittedly arbitrary, it indicates a definitive relationship between these two variables. Many statistically significant correlations in scientific journals tend to be weak (r less than 0.3) or moderate in value (Sheshkin, 1997).

Table 4 analyzes the cross-tabulation between the mortality variable and the other binary (categorical) variables in the study. This is performed to understand relationships that cannot be visualized from Table 3. For instance, this shows that pines, broken trees, and trees with branches that are not intact have a higher percentage of dead trees than their binary counterparts. An interesting finding occurs when analyzing the statistics for pines/hardwoods (Tables 3,4).

Table 3: Basic statistics from the tree mortality survey. The plots are grouped by elevation.

Plot	Elev. (ft)	# of trees	# hardwood (%)	# pine (%)	# standing (%)	# broken (%)	# br. intact (%)	# br. not intact (%)	Avg. DBH (cm)	# dead (%)
1	3	50	6 (12)	44 (88)	41 (82)	9 (18)	30 (60)	20 (40)	13.62	50 (100)
2	3	50	12 (24)	38 (76)	43 (86)	7 (14)	40 (80)	10 (20)	10.24	39 (78)
6	3	25	3 (12)	22 (88)	24 (96)	1 (4)	23 (92)	2 (8)	8.64	25 (100)
7	3	25	17 (68)	8 (32)	22 (88)	3 (12)	23 (92)	2 (8)	15.64	14 (56)
10	3	25	1 (4)	24 (96)	23 (92)	2 (8)	5 (20)	20 (80)	30.04	25 (100)
3	7	50	27 (54)	23 (46)	47 (94)	3 (6)	44 (88)	6 (12)	19.21	11 (22)
4	7	50	34 (68)	16 (32)	47 (94)	3 (6)	40 (80)	10 (20)	15.04	34 (68)
5	7	50	24 (48)	26 (52)	45 (90)	5 (10)	39 (78)	11 (22)	23.9	34 (68)
9	10	27	20 (74)	7 (26)	24 (89)	3 (11)	16 (59)	11 (41)	31.93	13 (48)
11	10	25	0 (0)	25 (100)	23 (92)	2 (8)	3 (12)	22 (88)	32.04	20 (80)
12	13	28	0 (0)	28 (100)	26 (93)	2 (7)	25 (89)	3 (11)	27.14	21 (75)
13	13	28	2 (7)	26 (93)	27 (96)	1 (4)	23 (82)	5 (18)	21.36	3 (11)
8	16	50	4 (8)	46 (92)	50 (100)	0 (0)	50 (100)	0 (0)	15.1	0 (0)
Totals:		483	150	333	442	41	361	122	19.11	289

Comparing elevation with % tree mortality

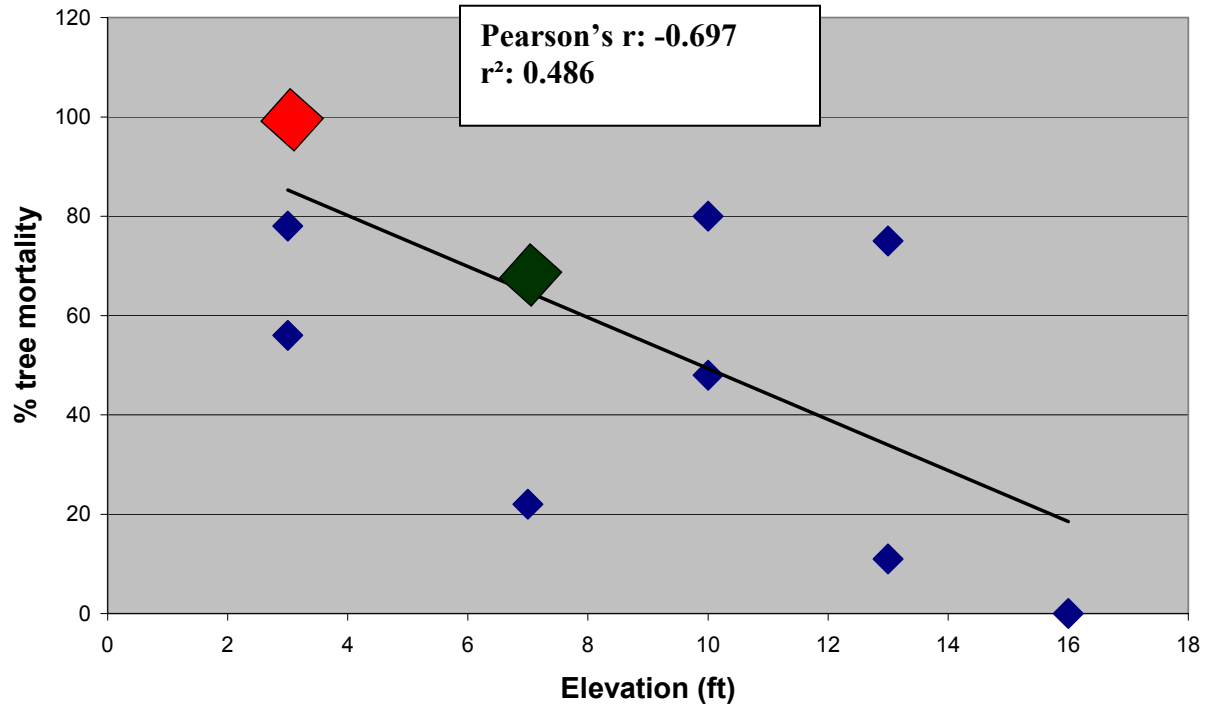


Figure 12: Scatterplot with elevation (ft) and the percent of trees dead. Each blue dot indicates a tree plot. The green dot indicates an area with two plots, and the red dot indicates an area with three plots. A trendline and the Pearson's r value are shown. The Pearson's r (significant at the 0.01 level) indicates a moderate/strong relationship between elevation and tree survivability.

Table 4: Cross-tabulation of complete binary statistics (pine/hardwood, standing/not standing, branches intact/not intact) and the dead/alive variable.

	Dead (0)	Alive (1)	% Dead	Totals	Phi	Significance
Pine (0)	205	128	62	333	0.052	0.249
Hardwood (1)	84	66	56	150		
Totals	289	194	60	483		
	Dead (0)	Alive (1)	% Dead	Totals		
Standing (0)	249	193	56	442	-0.234	0.000
Broken (1)	40	1	98	41		
Totals	289	194	60	483		
	Dead (0)	Alive (1)	% Dead	Totals		
Intact (0)	179	182	50	361	-0.36	0.000
Not intact (1)	110	12	90	122		
Totals	289	194	60	483		

Pines have a higher percentage of trees killed, even though they dominate the higher elevations. Neither tree responds well at lower elevations. Mortality is thought to be mostly due to location in the forest, more so than tree type.

Phi coefficients are listed for Table 4. For tree type, the significance level is too high (0.249). Therefore, there are no meaningful associations between these two variables. However, the low significance values (0.000) show tremendous fit with the other two variables. According to Cohen (1988), phi values range in “effect sizes.” Cohen made the following guidelines for interpreting effects:

- Small effect - $.10 \leq \Phi \leq .30$
- Medium effect - $.30 \leq \Phi \leq .50$
- Large effect - $\Phi \geq .50$ (Cohen, 1988).

The negative values (Table 4) indicate a relationship between the 0 and 1 values, such as *standing* and *alive*. However, this relationship (by using Cohen’s guideline) is small (-0.234). The association is slightly higher regarding the branches being intact or not (-0.36). A major reason for low values is the storm surge’s tendency to kill the trees without knocking them over, or causing them to lose their branches. Therefore, a large number of trees that are dead are still standing and have their branches.

For this analysis, one logistic model was created for the dbh variable. This was performed to discover if this predictor variable could be used to attribute increasing rates of survivability to an increase or decrease in one unit of dbh. The Hosmer-Lemeshow significance value for this model is 0.553. The baseline of 0.05 signifies that the observed and predicted values are similar for this Hosmer-Lemeshow test, a test used to analyze goodness of fit (Garson,1998). Therefore, the model is suitable for analysis.

According to the logistic regression analysis (Table 5), for every centimeter increase in dbh, odds of life increase by 1.4%. This is not statistically significant, however, as the significance (0.057) is higher than the 95% confidence threshold (0.05). In addition, the 95% confidence interval lower limit is 1.000. Confidence interval limits including 1.000 further indicate that dbh is not a useful predictor variable (see Garson, 1998), as a 1.000 odds ratio equals complete independence between the dependent variable (dead/alive) and the independent variable (dbh). Therefore, no association is ascribed to these variables, as increases or decreases in dbh cannot be attributed to an increase or decrease in odds of survivability. The results are contrary to findings in Gresham et al. (1991), where trees with higher dbh values were more severely damaged. The difference in results could also be an indicator of the degree of flooding damage at Gulf State Park, opposed to severe wind damage from Hurricane Hugo discussed in Gresham et al. (1991).

4.4 Conclusion

The basic statistics and regression results offer some interesting findings from this tree mortality survey. It is clear that a relationship between damage response variables and a tree's survivability exists, according to the cross tabulation and phi coefficients. This is not surprising, due to the major damage to the forest in Gulf State Park.

By tabulating the correlation between elevation and % tree mortality, the results support the previous hypothesis that storm surge flooding was a main cause of tree mortality. The storm surge created a fragmented landscape in terms of tree survivability, with areas of lower elevation more affected than areas of higher elevation. Wind damage would potentially be more geographically continuous, or create more damage at higher elevations. It also would not be concentrated in areas of low elevation and decrease dramatically with even minimal increases in

Table 5: Odds ratio estimate results are shown, along with the 95% confidence intervals.

Variable	Significance	Odds Ratio	95% Interval	Unit
DBH	0.057	1.014	1.000,1.029	cm

elevation. While other associations are apparent, such as an association between a tree being dead and broken, the elevation variable is the most important variable in this study that confirms the ecological impacts of storm surge at Gulf State Park.

Chapter 5: Remote Sensing

5.1 Introduction

Remote sensing is defined by Lillesand et al. (2004).

“Remote Sensing is the science and art of obtaining information about an object, area, or phenomenon through the analysis of data acquired by a device that is not in contact with the object, area, or phenomenon under investigation”
(Lillesand et al., 2004 – page 1).

Remote sensing science is based on the detection and measurement of electromagnetic energy.

Generally, the microwave, infrared, or visible portions are most useful for remote sensing analyses (Lillesand et al., 2004). Also of high interest is the respective reflectance and/or emittance of different wavelengths of electromagnetic energy on contrasting land cover types.

Accordingly, land cover types and other land characteristics can be detected and analyzed due to reflected energy. Generally, three microns ($3\mu\text{m}$) is the baseline separating reflected wavelengths and emitted infrared wavelengths (Lillesand et al., 2004).

For this project, visible wavelengths are of the utmost concern, due to the land covers at Gulf State Park, specifically forested areas. Basically, the equation below (Lillesand et al., 2004) states the relationship between incoming energy and its relationships with earth surfaces:

- $E_I(\lambda) = E_R(\lambda) + E_A(\lambda) + E_T(\lambda)$, in which
 - E_I = incident energy
 - E_R = reflected energy
 - E_A = absorbed energy
 - E_T = transmitted energy

Furthermore, spectral “response patterns” (Lillesand et al., 2004) are of concern for remote sensing work. This corresponds to different land covers having similar spectral signatures. Accordingly, many land cover features do contain emittance or reflectance individualities, or trends. Minor variations can occur for “response patterns” of similar land cover types in different areas, and therefore knowledge about the study area is important (Lillesand et al., 2004).

Importantly, remote sensing is a vital tool in any disturbance study (see Ramsey et al., 2001; Kovacs et al., 2001; Saksa et al., 2003; Ayala-Silva and Twumasi, 2004).

5.1.1 Landsat 5 Images

The Landsat 5 satellite system has a 16 day sequence of 705 kilometers above the earth's surface (Lillesand et al., 2004). Approximately 14.5 orbits are performed in a day, with each trajectory lasting 99 minutes. The Thematic Mapper (TM) is introduced, with additional geometric, spectral, and radiometric capabilities not found in the Multispectral Scanner, the main system of Landsat 1, 2, and 3. The Thematic Mapper is useful in distinguishing contrasting land cover types more accurately, due to the relative wavelengths of the TM bands. Furthermore, the implementation to seven bands (from four), along with new bands in many portions of the electromagnetic spectrum, such as a visible-blue band from 0.45-0.52 microns, greatly aids in spectral quality. The TM data have a 30-meter resolution, except for the thermal band (120-meter). (Lillesand et al., 2004).

5.1.2 Vegetation Indices

Vegetation indices are frequently used in disturbance ecology studies. According to Lillesand et al. (2004), two main vegetation indices are employed in vegetation analyses: a simple index (Vegetation Index, or VI) and a more complex index (Normalized Difference Vegetation Index, or NDVI). The equation for the vegetation index is the infrared band (IR), subtracted by the red band (R), or $(IR-R)$. The equation for NDVI is $(NIR-VIS)/(NIR+VIS)$ (NASA Earth Observatory, last accessed 01 March 2007). Due to its aid in correcting for such features as aspect, slope, and illumination, the NDVI is often preferred over the VI. While areas such as snow, water, and rock have low values due to small near-IR reflectance (0.7 to 1.1 microns) and high visible reflectance (0.4 to 0.7 microns), the opposite is true for areas of

vegetation with green, healthy leaves (Lillesand et al., 2004; NASA Earth Observatory, last accessed 01 March 2007). The NDVI values range from -1 to 1, while a value close to 1 is generally indicative of stands of healthy, dense leaves (NASA Earth Observatory, last accessed 01 March 2007).

Creating an image difference file between a pre-hurricane and post-hurricane NDVI image is often an effective means to discover the extent and degree of hurricane damage (Ramsey et al., 2001). Vegetation indices are implemented in many studies of differing scopes, from deforestation and vegetation moisture studies to hurricane disturbance ecology (see Ichii et al., 2003; Dilley et al., 2004; Ayala-Silva and Twumasi, 2004).

5.1.3 Land Cover Classification

Land cover classification is a common practice in remote sensing studies (see Latifovic et al., 2004; Tømmervik et al., 2003; Kuemmerle et al., 2006). It is especially significant in hurricane studies to depict changes in land cover and compare these changes to conditions before the storm.

There are two main types of classification schemes: supervised and unsupervised. These are both discussed in detail by Lillesand et al. (2004). Accordingly, during a supervised classification, three main stages occur:

- Training stage
- Classification Stage
- Output Stage

The training stage is synonymous with depicting training areas, or areas of interest, and assigning these areas to others with similar spectral characteristics. It is mandatory that the analyst has familiarity with the area (Lillesand et al., 2004), accomplished through ground truthing and

studying reference images. A maximum likelihood classifier is often implemented, effective in analyzing area “spectral response patterns” and the pattern variance and covariance for each analyzed pixel. For the classification stage, these pixels are assigned to land cover classes, while some pixels are labeled as ‘unknown,’ as they do not fit any land cover classes. Finally, the output stage is categorized by the final results being shown. This is generally done with thematic maps or a digital format for a GIS (Lillesand et al., 2004).

An unsupervised classification uses an algorithm to group pixels with similar values into clusters, as opposed to training areas or areas of interest (Lillesand et al., 2004). Therefore, this classification scheme is more appropriate for analysts with little knowledge of the study area. A hybrid classification method, which utilizes both supervised and unsupervised classification methods, is quite common as it integrates the strengths of both methods. For example, this is employed by Kuemmerle et al. (2006) in their study of Eastern Europe in part due to a lack of reliable aerial photos, along with the intricacy of the mountainous terrain in the region. Other research projects also use a hybrid methodology due to its strengths (see Latifovic et al., 2004; Tømmervik et al., 2003).

5.1.4 Tasseled Cap Transformation

The Tasseled Cap Transformation is a powerful tool used frequently in vegetation analysis. This transformation, according to Healey et al. (2005), creates three orthogonal directories from the original six Landsat bands. These directories (greenness, brightness, and wetness) are termed to enable them to be useful in depicting many land cover changes/conditions (Healey et al., 2005). The Tasseled Cap Transformation is used in numerous research projects of various scopes (see Jin and Sader, 2005; Dymond et al., 2002).

The three orthogonal axes used in the Tasseled Cap Transformation (as stated above) are brightness (weighted sum of each band), wetness (useful for even spot moisture such as on soil), and greenness (aids in viewing the greenness in an image, a cross of the visible band and the near-infrared band) (Leica Geosystems, 2003a, 2003b). These data axes are shown with a 1,2,3 layer color combination (red, green, and blue respectively) for Landsat 5 data, as the #1 layer is the brightness layer (high albedo), while layers #2 and #3 show greenness and wetness, respectively (Leica Geosystems, 2003b).

Dymond et al. (2002) used this Tasseled Cap Transformation to analyze an outwash plain and loess plain in northern Wisconsin. They discovered that utilizing the tasseled cap directory was useful for analysis. Accordingly, using the tasseled cap was more accurate in classifying certain vegetation covers. It was less likely to group harvested stands to unharvested stands. In addition, it was more accurate than a data file of TM bands or NDVI bands in identifying deciduous shrubs. These improvements in analyzing plant configuration, phenology, and even shadows are ideal for many remote sensing projects (Dymond et al., 2002). Due to its propensity of analyzing forests, water bodies, and beaches/sandy areas, the Tasseled Cap Transformation image was a fitting complement for the land cover classification.

5.1.5 Accuracy Assessment

An accuracy assessment is essential for all land cover classifications. This topic is discussed by Congalton and Green (1999). A main reason for performing an accuracy assessment is to discover the correctness of a classification, especially when results are mandatory for any laws, regulations, or resolutions to problems. An accuracy assessment assures clarity as to errors, making adjustments or corrections more feasible. It is also useful to make comparisons, whether of certain methodologies or algorithms (Congalton and Green, 1999).

When performing an accuracy assessment, reference images are mandatory to compare to the land cover classifications. Reference images should be retrieved as close as possible to the satellite images, even though reference images 5-15 years older are often used, assuring a lack of major earthly changes during this time period (Congalton and Green, 1999).

Numerous types of accuracy assessments can be applied to remote sensing data. One method is a 'random sampling,' in which a set number of reference points is applied to a reference image, with the analyst depicting the land cover category of these reference points. These reference points are compared to the supposed land cover class in the final classification. This process distinguishes whether reference point land covers when applied to the reference image correspond to the same land cover on the classified image. Congalton and Green (1999) suggest a minimum of 50 random points for each land cover class. Tømmervik et al. (2003) used between 124 and 506 points in each image (13 total classes) for their accuracy assessments, comparing errors from land cover maps of 1973, 1979, 1988, 1994, and 1999. An accuracy of 85% is deemed the baseline for a suitable assessment (Anderson et al., 1976), even though this may fluctuate for certain applications in which 85% might be too harsh or too lenient (Congalton and Green, 1999).

Displaying an error matrix is a common approach for an accuracy assessment, and is often used in conjunction with the 'random sampling' discussed above. According to Congalton and Green (1999), the error matrix is a square grid containing the number of pixels that correspond to a certain class in one classified image, when compared to the number of pixels corresponding to a certain class in another image. Generally, one image serves as the reference image while the other image represents a final classified image. This process effectively utilizes a classification for each category, applying commission errors (placing pixels into a class that is

incorrect) as well as omission errors (failing to place an area in the proper class). The Kappa analysis (synonymous with the KHAT statistic) is often performed on these error matrices, similar to a Chi-square statistic. The Kappa analysis calculates the correspondence between the relationship of the classified image and the reference image. The main diagonal in the error matrix must correspond to the 'chance agreement,' as shown by the totals in the row and the column pixel amounts. The KHAT statistic indicates whether a relationship lies between the reference image and the classified image, and helps display that the classification was not random (Congalton and Green, 1999).

5.1.6 Research Question

By analyzing the vegetation indices and Tasseled Cap Transformations for July 20, 2004, and July 7, 2005, together with the land cover classifications, the determination can be made as to how Ivan affected this area, mostly in terms of destruction to the forests.

5.2 Methodology

Two Landsat 5 images were used for this study, dated 20 July 2004 (path 020, row 039, GeoTiff format) for the pre-hurricane image, and 7 July 2005 (path 020, row 039, GeoTiff format) for the post-hurricane image. The post-hurricane image was taken about 9 ½ months after the hurricane to ensure that all of the vegetation affected by the storm surge was dead. Analyzing a post-storm image several months after the hurricane is not uncommon (see Ayala-Silva and Twumasi, 2004). Summer dates were also desirable, because of the reassurance that all trees depicted as dead are indeed dead and not solely losing their leaves seasonally.

The remote sensing study was performed by a complex classification process, utilizing both unclassified and classified classification schemes. A Tasseled Cap Transformation and an NDVI were also performed to clearly depict the aftermath of this storm. The analyzed reference

images were inclusive of Gulf Shores (1997), Orange Beach (1992), along with DOQs of the study area soon after the hurricane (28 September 2004) and from September 2006.

Layer stacking was necessary to group all of the bands into a single image. The images must be subset to focus on the research location of the three coastal lakes (Lake Shelby, Middle Lake, and Little Lake). The images were subsequently input into an eccentricity model followed by a radiance/reflectance model for atmospheric and radiometric correction, both supplied by Mr. Dewitt Braud of Louisiana State University. This input is required in order to calculate the correct sun angle and Julian calendar date. The process ensured an accurate output, calibrated to the time of day that the images were taken and the amount and angle of incoming sunlight. Geometric correction was performed on the pre- and post-hurricane image, to ensure that the images are aligned for proper and reliable output not only to these images, but reference images as well. The geometric correction for the pre- and post hurricane images was performed to less than a pixel accuracy, suitable for this analysis. These raw images (Figure 13, 14) were now aligned and ready for classification processes.

The process began with a supervised method. This was chosen to allow the author to choose Areas of Interest (AOIs) of familiar locations in and around Gulf State Park. These AOI signatures were interpolated into a signature editor, in which each signature was evaluated in terms of homogeneity (standard deviation less than 10% of the mean) and normality (histograms do not possess more than one peak). Probabilities for each class were assigned in terms of the estimated area of the study site, and were later normalized. This signature file was subsequently run through a supervised classification, using a maximum likelihood decision rule. A threshold file was created representing unclassified pixels, for all classified pixels were derived from the outcome of the supervised classification. This threshold file was applied in a later step.

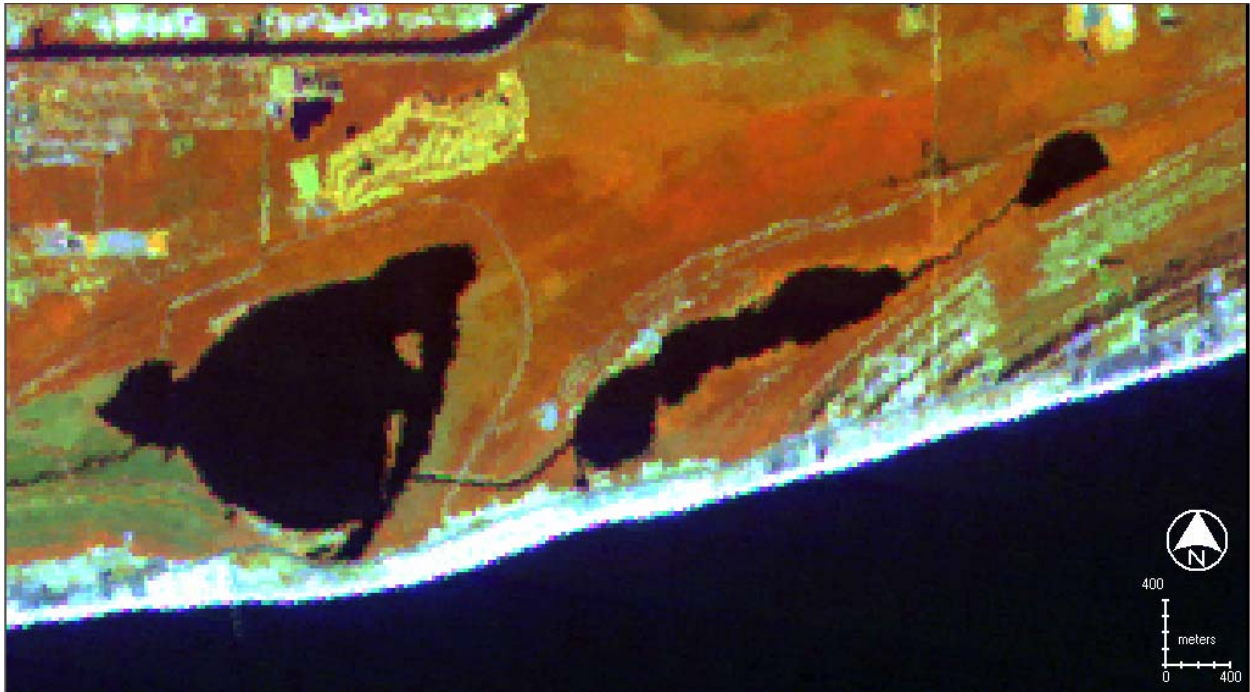


Figure 13: Pre-hurricane raw image (4,5,3 band combination).



Figure 14: Post-hurricane raw image (4,5,3 band combination).

Subsequently, an unsupervised algorithm (ISODATA) was run on this threshold file. This created a signature file of 25 classes. This method was chosen to allow ERDAS Imagine to act as an aid in deciphering particularly complex classes. These signatures were again checked for proper normality and homogeneity statistics. Eventually, the signatures were run through an additional supervised classification algorithm. This second process applied the same threshold file, which was created from the initial supervised classification. These classes were soon named accordingly to the respective class.

These two images were subsequently placed into a model to join them. Since classified pixels in the supervised image became unclassified in the unsupervised image (and vice versa), these images fit well to create a 4-bit thematic image. This was performed by using the Model Maker in ERDAS Imagine. The final image was recoded appropriately, and the clump/eliminate functions were used to reduce out-of-place pixels, by grouping and eliminating any unwanted pixels of at least 2 hectares.

A matrix function was performed between the final classified images to represent any land cover changes between the two images. The area of focus involves changes in forest-forested swamp regions to a transitional area (dead/highly damaged vegetation). Accuracy assessments were performed on both pre- and post-hurricane images to ensure precise land cover evaluations. The results are portrayed by a confusion matrix (showing errors of omission and commission), along with the respective accuracy percentages and kappa figures.

Land cover classifications were chosen after careful consideration (see Anderson et al., 1976). The pre-hurricane image consisted of five classes: forest, non-forested wetland, barren, urban, and water. Each of these represented Level I classifications (see Anderson et al., 1976), except for non-forested wetland (Level I classification is solely 'wetland'). Level I classification

land cover names are common with Landsat data, due to rather coarse resolution when compared to other high-powered sensors. The post-hurricane image included all five of these classes, with an additional class of transitional areas (highly damaged forest).

Water classes included such areas in the images as the Gulf of Mexico and the three lakes at Gulf State Park. Large amounts of water were visible on the post-hurricane Tasseled Cap image, but most were not due to the hurricane. The Mobile weather station reported that on 6 July 2005 (a day prior to the Landsat image process), an estimated 6.34 inches (16.1 cm) of rainfall was recorded (National Climatic Data Center, 2005). Areas that were not new water classes were determined with additional ground truthing and aerial photography.

Barren classes were mostly composed of the vast beach bordering the Gulf of Mexico. They also included the beach dunes south of Little Lake, and the sand pits toward the northwest corner of the image. The urban areas included the major business 'strip' alongside the main beach, along with subdivisions and other areas of business and commerce. A golf course was also included in this urban class, due to its being 'built-up' land (see Anderson et al., 1976). The term 'non-forested wetland' indicated that the considered wetland areas were devoid of significant land cover. 'Non-forested' was necessarily emphasized in order to avoid confusion with forested areas, discussed later in this paper.

Forest, in terms of classification, was composed of dense forested areas north of the three lakes, along with areas of slightly sparser vegetation, indicated by higher elevation north of these denser areas. It also included areas generally classified as forested wetland. Grouping of this forested area class was inclusive of both forest and forested wetland for three main reasons. First, and most importantly, a major reason for performing this land cover classification was to delineate the approximate area of major forest damage. The importance of depicting the forested

areas correctly must be stressed. However, discerning a 'wet' land cover for these areas was not pertinent. Second, and also important, the Landsat sensor was not ideal for differentiating accurately between these two land covers, due to the close similarities in spectral signatures for Gulf State Park. Third, the proper accuracy assessment results would be greatly compromised by this difficulty. It is imperative to cluster classes that can be grouped when appropriate (Anderson et al., 1976).

For the post-hurricane image, 'transition areas' were forested regions classified with major tree mortality and the highest degree of damage. Tree mortality in these regions was approximately 50% at the least, while in most areas tree mortality was much higher. This area was also characterized by a completely destroyed understorey. Conversely, the post-hurricane image indicates that the forested areas which were not classified as 'transition areas' experienced marginal or no damage. The tree mortality was <50%, while most areas had much less than 50% damage. The majority of the damage occurred in the understorey. These areas were not considered to be in 'transition' because the majority of the trees were healthy, the canopy was mostly intact, and the leaves/needles were green and healthy, even though a few dead trees for these areas were not uncommon.

5.3 Results and Discussion (Pre-hurricane)

5.3.1 NDVI

Primarily, the entire vegetated area of Gulf State Park has a medium-high NDVI value (approximately >0.4), due to the high density of green, healthy leaves. Conversely, areas depleted of healthy, green leaves, such as non-forested wetlands, urban areas, and beaches, have lower values (<0.4). It is clear from this image that in conjunction with aerial photography, the region displayed lush, green forest areas prior to Hurricane Ivan. The image (Figure 15) is also useful

in deciphering which stands of forest are the densest: generally, north and east of both Middle Lake and Little Lake. Large portions of the forested area in these regions have an NDVI value of at least 0.6.

5.3.2 Tasseled Cap Transformation

This image (Figure 16) is very distinct in differentiating between varying types of land cover, especially when the 1,2,3 band combination is utilized. The ‘greenness’ of the tasseled cap may be seen in the forested regions, composed of different shades of light green. The ‘brightness’ of the tasseled cap may be seen from areas of high reflectivity or albedo, such as the beach north of the Gulf of Mexico, the beach dunes south of Little Lake, or the sand pits at the northwest corner of the image. The “wetness” may be witnessed from the blue color of the water of the three main lakes, along with small lakes including the elongated lakes at the eastern side of the image.

5.3.3 Land Cover Classification

In the final classification (Figure 17), the landscape mimics the land cover in the pre-hurricane raw image. The surrounding areas of the lakes are generally composed of lush vegetation, either forests or forested wetlands (green color). The western portion just outside of Lake Shelby is non-forested swamp, along with the area to the east of the lake (light green shade). Scattered patches of urban developments (light blue) are located in the northern section of these subset images, along with the area just north of the beach ridges. A series of sand dunes (light yellow) are clearly shown south of Little Lake, which stretch south to Middle Lake.

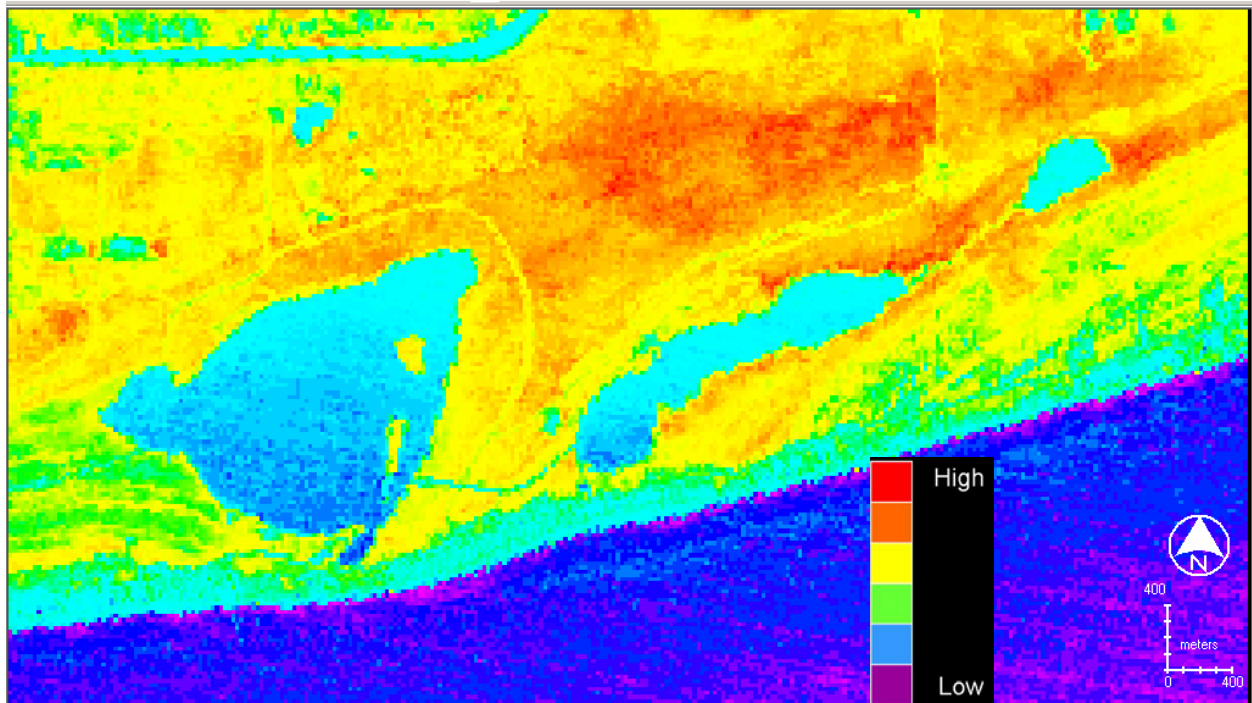


Figure 15: Pre-hurricane NDVI - ranging from purple (-0.2) to red (0.6).

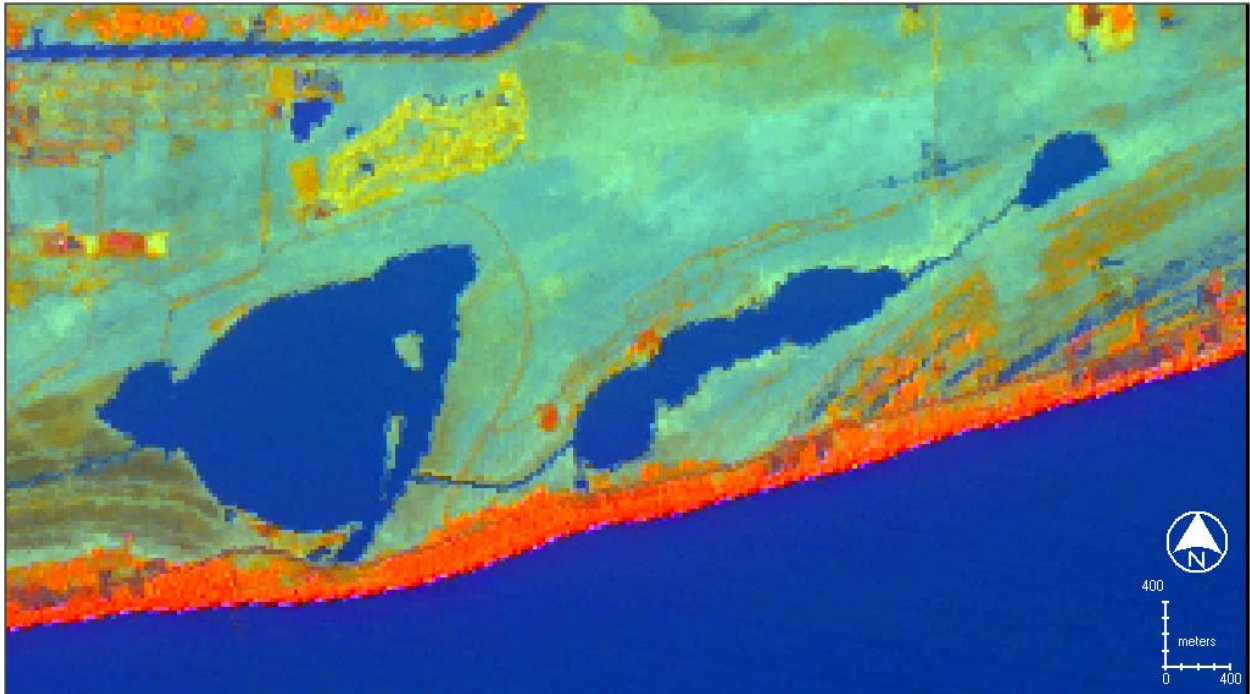


Figure 16: Pre-hurricane – Tasseled Cap Transformation (1,2,3 band combination).

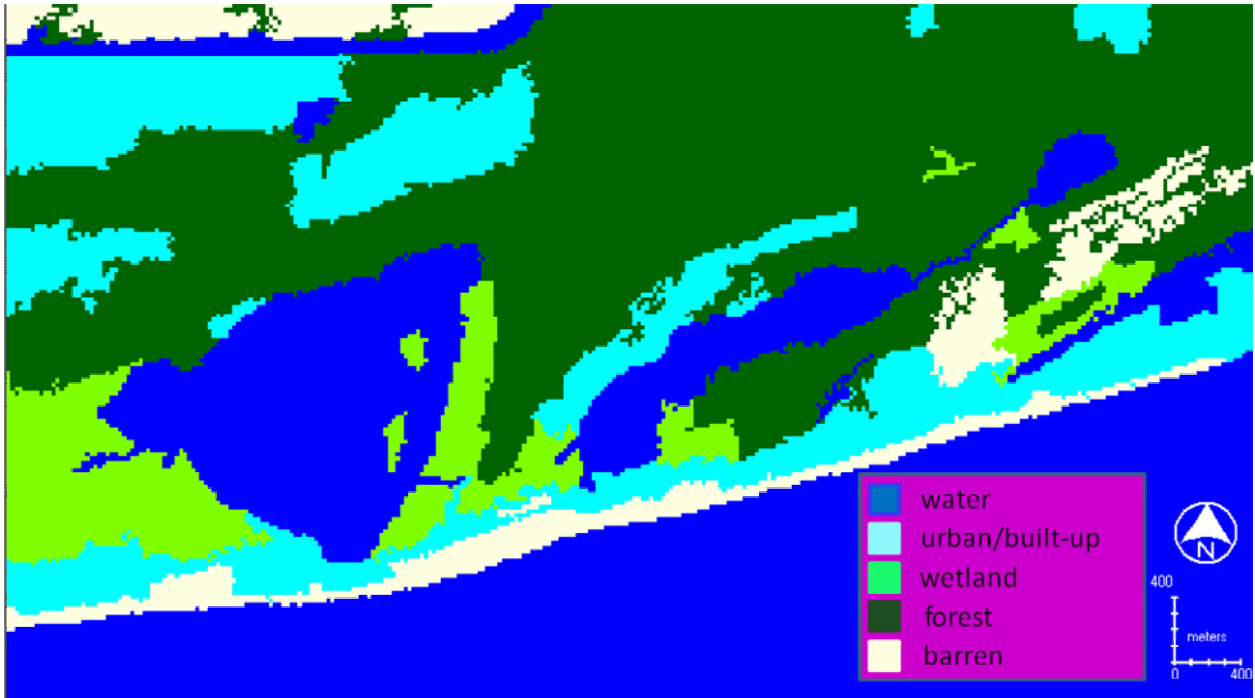


Figure 17: Pre-hurricane classification (two hectare elimination).

5.3.4 Accuracy Assessment

The overall accuracy of 83.20% is sufficient for this project. It may be noted that this figure is lower than the proposed 85% baseline (Anderson et al., 1976), mainly due to the fragmented landscape south of Little Lake. This location is expected to be the major cause for error.

Of the 250 total stratified random points used in the accuracy assessment (50 for each class), 208 (83.20%) are classified correctly. Producer accuracy indicates the preciseness of pixels from the analyst and from the classification process. The producer's accuracies are summed (Table 6). For instance, the forested area has 66 total units of forest, according to the reference images. The analyst (myself) classified 47 units correctly, leading to 71.21% (47/66).

The user accuracies are the number of accurate pixels divided by the class's total number of pixels. For instance, for forested areas, 47 pixels are classified correctly. This is divided by the number of total pixels classified as the 'forested area' class (50), leading to user accuracy of 94.00% (47/50). These statistics can be summed up by stating that in terms of the ground cover at this study area in Gulf State Park, 71.21% of the time the producer can say a region that is a forested area on the ground is classified accordingly, while a user interpreting this map will notice that 94.00% of the time a certain area will be a forested area on the ground if it is forested area on the map (see Congalton and Green, 1999; Lillesand et al., 2004).

The confusion matrix offers an in-depth approach to understanding sources of error. For instance, Table 6 reveals clearly any classes that are in major confusion with each other. For an example of interpretation, the forest class is analyzed. Since nondiagonal column figures represent omission errors, it can be interpreted that 19 pixels were mistakenly omitted from the forest class, and thereby should be included in that category. Furthermore, nondiagonal row

Table 6: Accuracy assessment results for the pre-hurricane classified image.

Classified Name	REF DATA					Reference Totals	Classified Totals	Number Correct	Producers Accuracy	Users Accuracy	Kappa
	W	B	U	F	NFW						
water	49	0	0	1	0	57	50	49	85.96%	98.00%	0.9741
barren	5	34	4	6	1	40	50	34	85.00%	68.00%	0.619
urban	1	4	42	2	1	49	50	42	85.71%	84.00%	0.801
forest	0	1	2	47	0	66	50	47	71.21%	94.00%	0.9185
non-forested wetland	2	1	1	10	36	38	50	36	94.74%	72.00%	0.6698
Overall:									83.20%	0.79	

figures represent commission errors. It is determined that three pixels were placed in the forest class incorrectly (see Lillesand et al., 2004).

In addition, the kappa statistics are listed (Table 6). The kappa statistic, as stated above, measures the agreement between the classified image and the reference image(s). These values generally range from -1 to 1 (Congalton and Green, 1999). According to Landis and Koch (1977), a kappa statistic of $0.61-0.80$ indicates a “substantial” agreement between the Landsat image and the reference images, while a kappa statistic of $0.81-1.00$ indicates an “almost perfect” agreement between these images. Therefore, it is clear that the agreement is rather high for all categories of this analysis, particularly the most pertinent category in this analysis: forested areas.

5.4 Results and Discussion (Post-hurricane)

5.4.1 NDVI

The area of greatest mortality (north of Middle Lake and the campground) exhibits NDVI values (approximately 0.2) similar to non-forested wetland areas just west of Lake Shelby. This is indicative of the typical slightly swampy ground cover of this region, showing a complete lack of healthy trees due to the storm. High NDVI values (approximately >0.4) exist mostly in areas of higher elevation, an important factor in limiting tree mortality. A major area exhibiting this geography is toward the northern edge of the image, in which the elevations are at least 16 feet, and can increase up to approximately 25 feet. Therefore, mortality is virtually non-existent. Although the elevation is somewhat lower, a similar circumstance exists completely surrounding Little Lake. The elevations here are approximately $11-15$ feet. Many trees survived the storm to the north and east of Lake Shelby, even though these areas are much lower in elevation. Tree survival here is believed to be due to the road, which served as a barrier to impede storm surge.

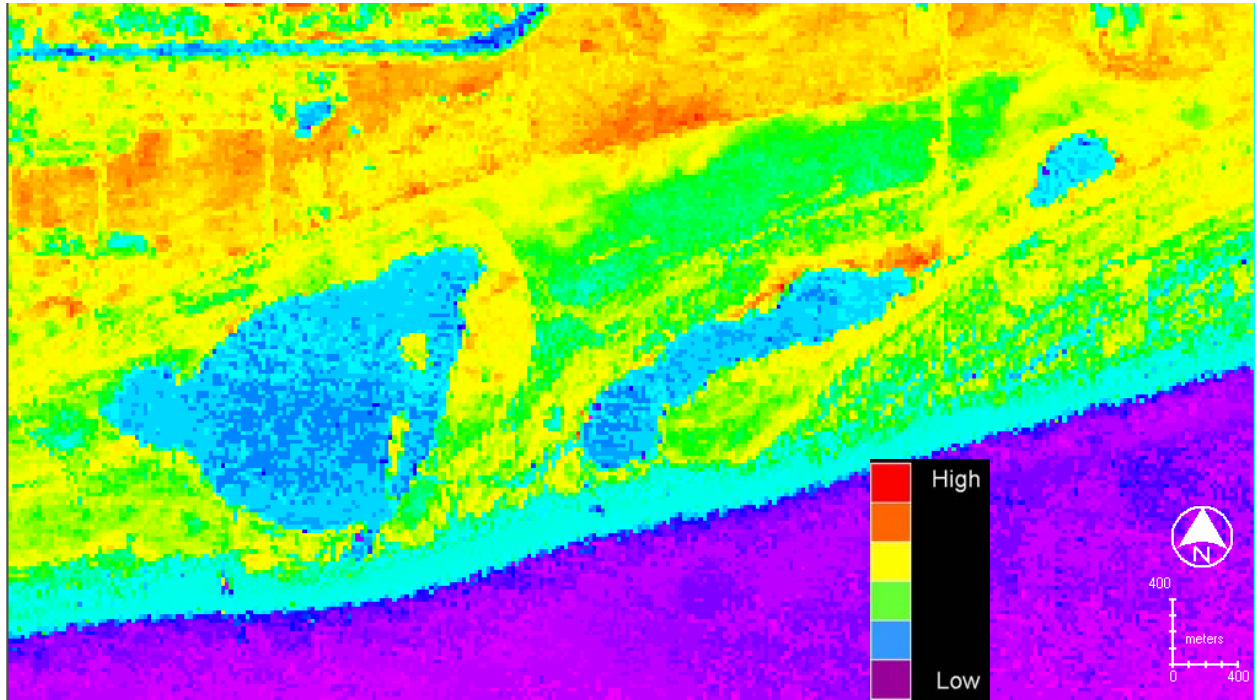


Figure 18: Post-hurricane NDVI – ranges from purple (-0.5) to red (0.7).

5.4.2 Image Differencing

This image (Figure 19) results from subtracting the NDVI values of the pre-Ivan image from the after-Ivan image. Areas in green indicate regions of stability or minimal change. The areas of higher elevations correspond with the green shades, indicating there is no change (values near 0). The areas of highest change to the forest are blue, especially the darker blue shades. The darker blue shades (high negative values) represent areas of nearly 100% tree mortality; lighter blue shades also indicate a high mortality rate. This differencing image is used in conjunction with ground truthing and vegetation plots to assess the approximate definition or degree of damage of the numerous values/shades of this portrait.

5.4.3 Tasseled Cap Transformation

The Tasseled Cap (Figure 20) is another form to view the vegetation damage, designated by means of a darker green shade. The Tasseled Cap detects water; a small portion east of Lake Shelby is blue in shade. This shading is believed to be from a rainshower, not from Hurricane Ivan. This rainshower is also believed to have caused the high amount of flooding in the non-forested wetland west of Lake Shelby. It is also possible that this Tasseled Cap indicates the increase in sand/barren area (mostly due to urban destruction), by the increase in “red” areas just north of the Gulf of Mexico, when compared with the pre-hurricane Tasseled Cap (see Stone et al., 1996).

5.4.4 Land Cover Classification

The post-hurricane image (Figure 21) offers stunning contrasts to the pre-hurricane image. For instance, the healthy vegetation behind the three lakes has been replaced by a high forest damage-transition area, mainly due to the storm surge of Hurricane Ivan. There also appears to be an increase in sand, especially along the coast where urban areas were destroyed.

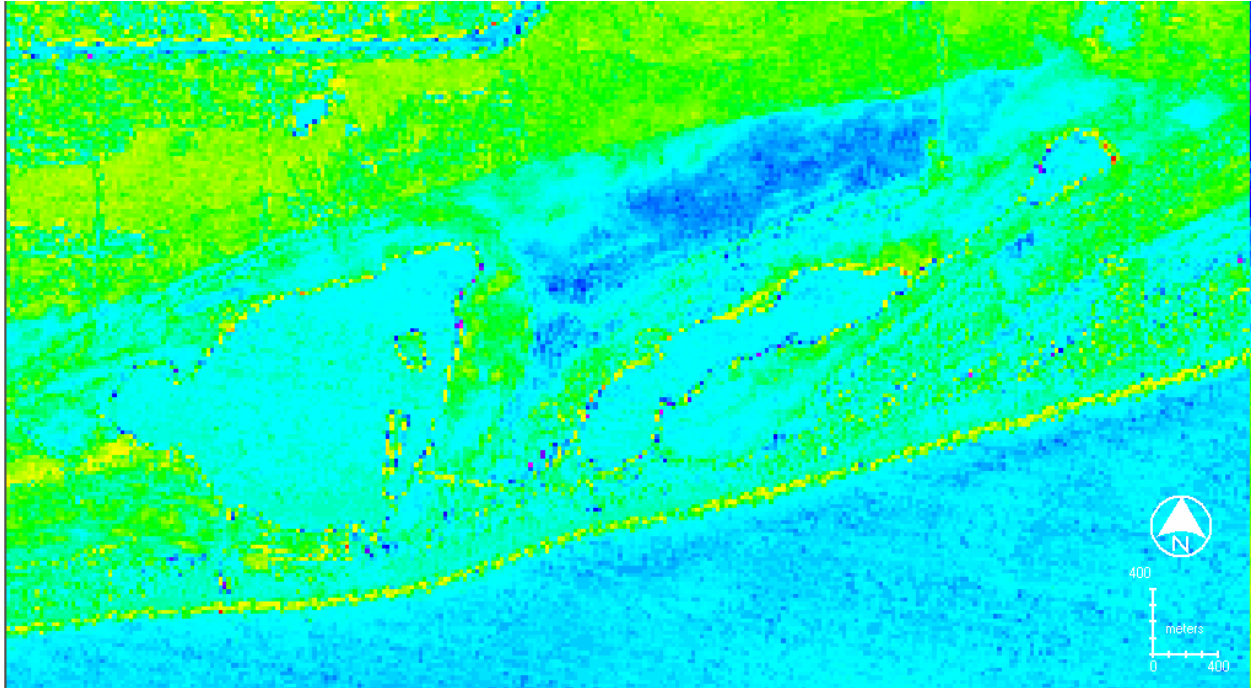


Figure 19: Image differencing (NDVI). Notice major vegetation index differences in forested region north of the Shelby Lakes (depicted with blue shades).

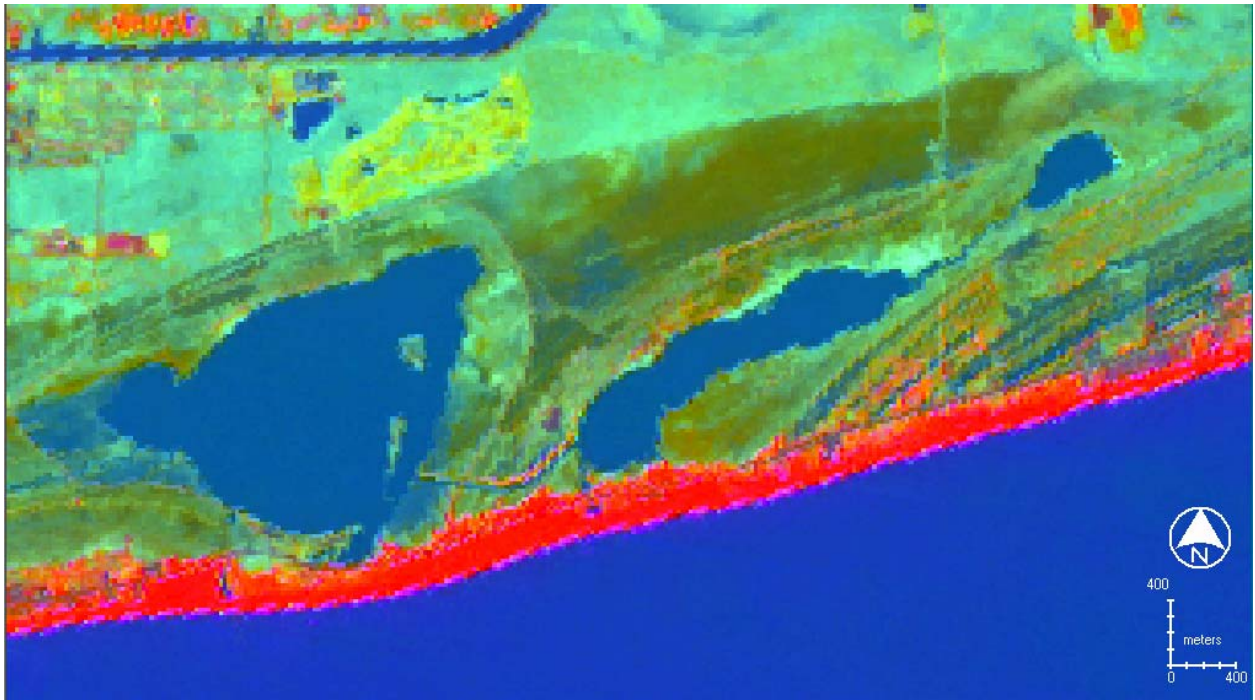


Figure 20: Post-hurricane – Tasseled Cap Transformation (1, 2, 3 band combination).

This could signify not only the transport of sand to this area from the storm surge, but also the loss of urban areas, which would provide the shifting sand a new area from the storm surge creating overwash sand lobes.

Interestingly, the area farther north of the lakes is unaffected by the hurricane/storm surge. This is evidently due to its higher elevation. This area is between 20-25 feet above sea level. This image, together with the NDVI and Tasseled Cap, reveals an area of destroyed vegetation immediately south of Middle Lake, which provides an indication of the storm surge extent. Thus the remote sensing data lend further support to the occurrence of a major overwash sand layer in Middle Lake and even stretching east to Little Lake (see Chapter 6). The destroyed area directly north of the three lakes is approximately 3-5 feet in elevation, with some locations extending to 7 feet. A similar scenario is also portrayed in an elongated strip of land bordering north and south of Little Lake. This small strip of vegetation did remain alive despite Hurricane Ivan. This is believed to be due to a higher elevation, approximately 13 feet, in contrast to lower elevations around, as identified by dead vegetation.

5.4.5 Accuracy Assessment

The overall accuracy of 82.67 % is suitable for this analysis. In this study, 300 points are analyzed (50 more than the pre hurricane image, due to the addition of the 'transition area' class). Of these 300 pixels, 248 pixels (or 82.67%) are correctly classified. The accuracies are summarized below (Table 7).

In terms of producer accuracy, for example, the forested area had 53 total units, according to the reference images. This analyst classified 42 units correctly, leading to a 79.25% number (42/53). For the user accuracies, 42 pixels are classified correctly for forested areas. This is divided by the number of total pixels that were classified under the 'forested area'

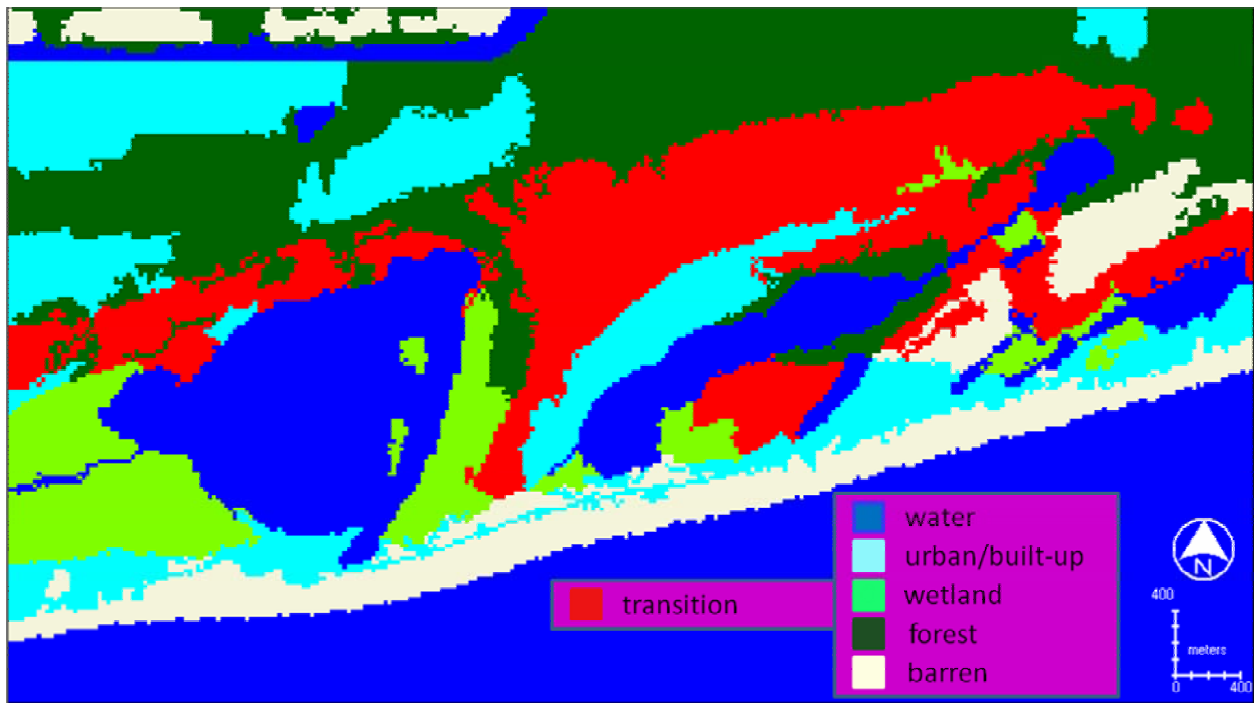


Figure 21: Post-hurricane land cover classification (two hectare elimination). The transition area is an area of high forest mortality, at least >50%.

class (50), leading to user accuracy of 84.00% (42/50). These statistics can be summed up by stating: In terms of the ground cover at this study area in Gulf State Park, 79.25% of the time the producer can say a region that is a forested area on the ground is classified accordingly, while a user interpreting this map will notice that 84.00% of the time a certain area will be forested area on the ground if it is forested area on the map (see Congalton and Green, 1999; Lillesand et al., 2004). Similar to the producer's accuracies, the user accuracies are importantly high in the most analyzed portions of the image, i.e. forest and transition (highly damaged) areas.

Furthermore, the kappa statistic (previously defined) for the post-hurricane image is 0.7920. The 0.7920 kappa stat is suitable for this classification. For this project, the most important land cover classes, forest and transition, display sound kappa statistics (0.8057 and 0.7360, respectively).

5.4.6 Matrix Image/Major Changes in Land Cover

The focused land cover classes in the pre-hurricane image and post-hurricane image are summarized in Table 8. The major focus is forest damage. Approximately 1108 hectares of forest/forested swamp are in the pre-hurricane image, while only 622 hectares (approximately 56%) of forest/forested swamp are stable in the post image. Similarly, approximately 484 hectares exhibit of major tree damage (transition area). Interestingly (yet not surprisingly), the "barren" class increase from 194 hectares to 288 hectares is indicative of demolished urban buildings, coupled with the spread of sand from the overwash fans (Figure 22).

5.5 Sources of Error

Error is prevalent in all land cover classifications for many reasons. These classification processes were subject to different types of error. For instance, the area between Little Lake and the Gulf of Mexico is a highly fragmented landscape, with scattered areas of swale lakes, urban

Table 7: Accuracy assessment results for the post-hurricane classified image.

Class Name	REF DATA						Reference Totals	Classified Totals	Number Correct	Producers Accuracy	Users Accuracy	Kappa
	W	B	U	F	T	NFW						
water	48	0	0	0	1	1	53	50	48	90.57%	96.00%	0.9514
barren	2	38	3	2	0	5	45	50	38	84.44%	76.00%	0.7176
urban	0	4	40	2	3	1	47	50	40	85.11%	80.00%	0.7628
forest	1	1	3	42	1	2	53	50	42	79.25%	84.00%	0.8057
transition	1	2	0	6	39	2	50	50	39	78.00%	78.00%	0.736
non-forested wetland	1	0	1	1	6	41	52	50	41	78.85%	82.00%	0.7823
Overall:										82.67%	0.792	

areas, sand dunes, non-forested wetlands, and forested patches. The 30 X 30 meter pixel is too coarse of a resolution to define these complex boundaries precisely. In addition, the wet landscape due to the rainshowers in the post-hurricane image (discussed previously) made it increasingly difficult to differentiate forested areas (including forested wetland) from non-forested wetland, due to the similarity in spectral signatures. Finally, many urban areas (especially residential areas with a high volume of trees) did not have similar spectral signatures to urban centers on Highway 182, nor did their signatures in these residential areas meet homogeneity or normality requirements. Therefore, in certain cases the AOI tool was used to draw certain boundaries which can create error.

Table 8: Comparing total land area of pre-hurricane to post-hurricane, with the total area and percent increase or decrease noted. The main focus is the destruction to the forest class.

<u>land cover</u>	<u>pre-Ivan (hectares)</u>	<u>post-Ivan (hectares)</u>	<u>change (hectares)</u>	<u>percent change</u>
barren	194	288	94	48%
urban	470	427	-43	-9%
forest	1108	622	-486	-44%
transition	0	484	484	N/A

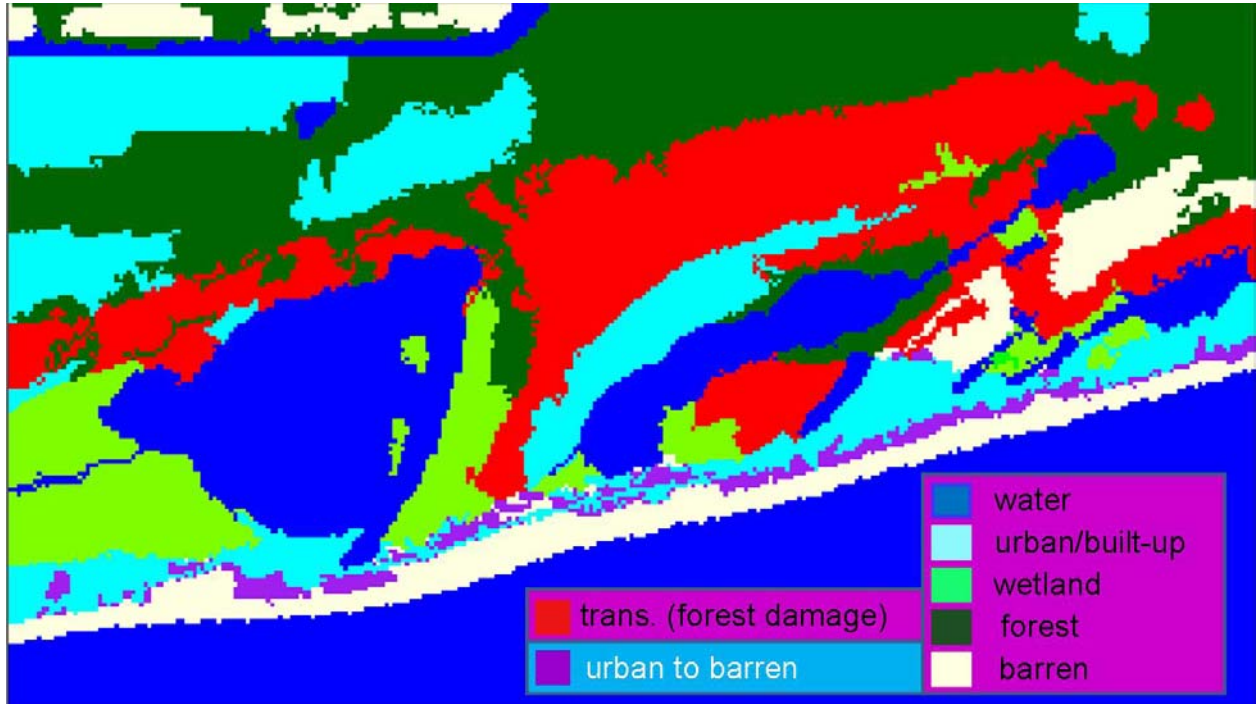


Figure 22: Matrix image, focusing on transition area (major forest damage) and urban transition to barren, indicating building loss to currently a sandy or undeveloped area.

Chapter 6: Sedimentary Impacts

6.1 Introduction

After analyses of land cover classifications (Chapter 5), sedimentary impacts derived from the three lakes at Gulf State Park were analyzed, along with their immediate vicinity. Results of the vegetation survey and remote sensing study (Chapter 4, 5) already suggested that storm surge was the main cause of tree mortality and ecological damage in the park. Therefore, a sand signature from Hurricane Ivan was highly probable at this Gulf Shores location.

Gulf Shores is located in southern Alabama, bordering the Gulf of Mexico. The region has a climate characterized by relatively hot and humid summers, while the spring and fall seasons are typically cooler, especially at night. The monthly average temperature in July and August is 81°F (27°C), while the average temperature in January is 50°F (10°C) (The Weather Channel, 2007).

Gulf State Park is one of Alabama's state-owned nature preserves. Three lakes comprise Gulf State Park: Lake Shelby, Middle Lake, and Little Lake. All three lakes lie behind a barrier beach, located to the immediate south. Lake Shelby contains three small islands composed primarily of non-forested swamp: Grass Island, Alligator Island, and South Island. Lake Shelby's southernmost point lies about 0.15 miles (0.24 km) from the coast, compared to approximately 0.17 miles (0.27 km) and 0.82 miles (1.32 km) for Middle Lake and Little Lake, respectively. Lake Shelby is connected to Middle Lake by a man-made waterway constructed in the 1960s (Liu and Fearn, 1993). Middle Lake and Little Lake are connected by Middle River. Lake Shelby has a river outlet connected to Little Lagoon to its west, a relatively large water body approximately 7.6 miles (12.23 km) long. Lake Shelby is north of beach dunes (Figure 23) approximately 2-4 meters in elevation (Liu and Fearn, 1993). Local residents and visitors, drawn



Figure 23: Sand supply (between Gulf of Mexico and Shelby Lakes).

by the scenic beauty of the lakes, as well as their affinity for fishing and swimming, frequent these waters.

The lake surroundings are eclectic in appearance. The barrier beach forms the southernmost boundary, separating the Gulf of Mexico and Gulf State Park. Highway 182 runs parallel to the beach, aligned on the north and south sides by condominiums, hotels, apartment buildings, restaurants, shirt shops, subdivisions, and other businesses in a tourist-based economy. To the north of these urban areas lies a plethora of natural environments, creating a diversified landscape at Gulf State Park. The numerous walking trails in Gulf State Park provide a tour through the many landscapes of the park, from non-forested swamp to forested swamp and intermittent sand dunes. The Alabama State Parks Department has immense information regarding these trails. The trails are lined with many different types of trees, mostly pines. However, live oak and holly trees mark the landscape, with palmettos and muscadine grape vines, ferns, and mosses also in the area. As of October 2006, the trails were still closed due to the damage from Hurricane Ivan (Alabama State Parks, 2004).

6.2 Methodology

Ground truthing and remote sensing analysis indicates the ecological and geophysical damage Hurricane Ivan inflicted on this area. Due to the storm's direct hit on these lakes, a major breach occurred in Middle Lake. Therefore, a storm signature in Middle Lake was expected. It was uncertain if a storm signature could be detected in the sediments of Lake Shelby (minor breach occurred) or Little Lake.

Sediment cores were taken using two different methods. For the non-forested swamps and shallow lake areas, a Russian Peat Borer was used to extract the core. These cores were placed into a 2-inch white PVC pipe cut in halves lengthwise. These were subsequently wrapped

in plastic foil, followed by aluminum foil or duct tape. They were then labeled and transported back to Louisiana State University for further analysis.

Cores from deeper areas in the lake were extracted by using the Livingstone corer. This involves a 2-inch, clear PVC pipe with a sharp metal cutting-shoe attached to one end. A piston, connected to a long and sturdy cable, is inserted into the bottom of the plastic pipe. Its purpose is to create a suction, enabling the sediment to remain in the tube. From inflatable rubber boats equipped with plywood boards for support, the tubes are pushed into the lake bottom where the sediment is collected. The tubes are labeled accordingly, and finally transported back to Louisiana State University for further analysis. The bottoms of the cores were generally lodged in the metal cutting-shoe. To preserve these ends, these sections were placed in small plastic ‘whirl-pak’ bags and labeled accordingly. To determine the core locations, all points were saved on a global positioning system (GPS), to be interpolated into National Geographic’s TOPO! Software system for Alabama.

After the Livingstone cores were returned to Louisiana State University, they were cut longitudinally with a table saw and opened for visual inspection. Monofilament wire was used to help divide the core into two sections after the cut. A description was jotted down regarding the core’s lithology and sedimentary features. Photos were also taken of the core segments.

Loss-on-ignition (LOI) analysis is a vital procedure for sediment stratigraphic research. It involves heating sediment samples at 105°C, 550°C, and 1000°C in a Barnstead International F6000 furnace to determine the percentages of water, organics, and carbonate in the sample, respectively. Generally, the cores were sampled at consecutive one-centimeter intervals. This procedure is vital, as the output was depicted on a multiple line graph, with the x and y axes representing, respectively, the percentages (water, organics, or carbonate) and the depth intervals

of the core. High levels of water and organic contents generally indicate an organic mud or gyttja, while low levels generally depict the presence of sand or silt layers. These percentages can help reveal the sediment stratigraphy of the core by depicting changes in sediment types, such as gyttja, marl, clay, or sand. This information can be used to infer environmental changes in the lake and its immediate surroundings during the periods of sediment accumulation. More importantly, LOI data can aid in identifying sand layers even if they are not visible to the naked eye. For those sand layers that are visible to the naked eye, these data can help quantify them by labeling them with specific water, organic, and carbonate percentages.

LOI diagrams were created with TILIAGRAPH, and transferred to CANVAS where they were grouped with other cores from the same lake. Cores from Lake Shelby were taken in three rough south-to-north transects. The transects covered the southern, eastern, and western areas of the lake. For example, all Lake Shelby cores from the western area were grouped with each other, and plotted from south to north. Middle Lake cores were extracted in a cluster at the south and middle sections. For the LOI diagrams, cores are arranged in a rough SW to NE pattern parallel to the expected direction of the storm surge. For Little Lake, the core locations were scattered. They were also plotted in an approximate SW to NE pattern.

On the LOI diagrams, the overwash layers are labeled with arrows. Different labels were used to designate different degrees of certainty in the presence of the storm signature. Visible overwash sand layers are depicted with black arrows. Less prominent but still visible clay or silt layers with little or no sand content are portrayed with a purple arrow. Any clastic layer which is invisible yet its presence is suggested by the results of the LOI diagrams and confirmed by further probing (by touch) is represented with a blue arrow. Areas which appear to have an abnormal “dip” on the LOI curve but the presence of a storm signature cannot be confirmed by

touch or visual inspection are labeled with question marks. For the core stratigraphies, green, blue, and red colors were used for the water, organic and carbonate contents, respectively.

Six core samples were selected for AMS radiocarbon dating, which were done by Beta Analytic Inc. in Miami. These six samples are derived from cores ML-TV2 and ML-06. The samples are as follows: ML-TV2 (20 cm), ML-TV2 (55 cm), ML-TV2 (79 cm), ML-TV2 (100 cm), ML-06 (53 cm), and ML-06 (95 cm).

Between three total trips (August 2005, May 2006, and June 2006), 43 total cores were taken from Gulf State Park. All 43 cores were analyzed, but certain cores were used for LOI and included in this work due to their unique stratigraphies.

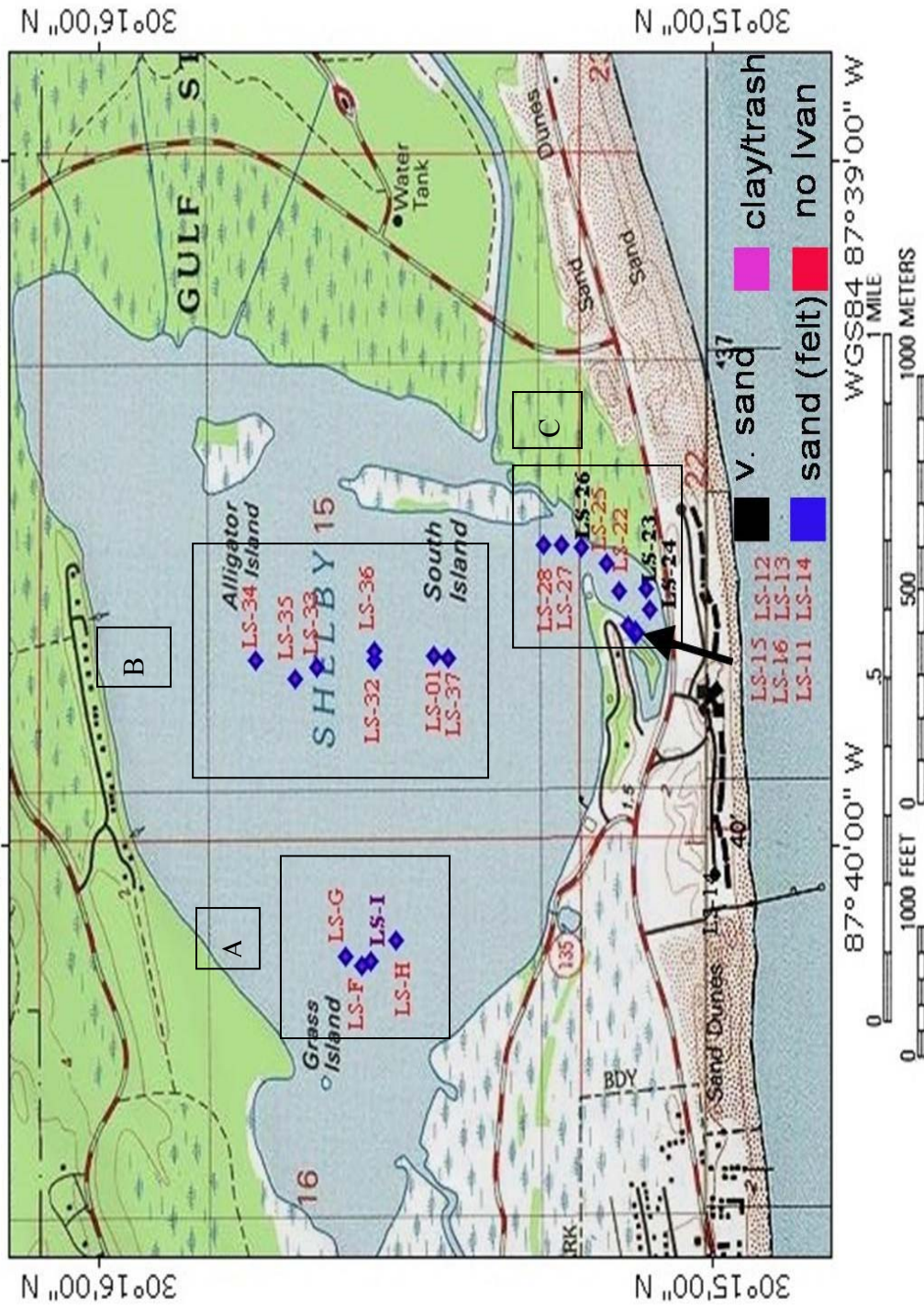
6.3 Results

6.3.1 Lake Shelby – Western Transect

Four cores were taken from this western transect (Figure 24). None of these cores contain a top sand layer attributable to Hurricane Ivan. With the exception of core LS-H (all sand), this area yields cores of similar stratigraphies that are correlatable, transversing from an organic mud in the upper part (lacustrine environment) to gray clay (lagoonal environment) in the lower part.

Core LS-I (88 cm) is representative of the cores in this transect. 0-7 cm is an organic detritus or ‘trash’ layer, in which twigs and leaves are common. It overlies a clay layer from 7-10 cm. The section from 10-65 cm has a very dark mud with visible sand layers at 15 cm and 65 cm. Gray clay comprises the remainder of the core. LOI data, confirmed by subsequent physical examination, suggest the presence of three additional clastic bands (Figure 25). Core LS-G (94 cm) is composed of a dark mud from 0-51 cm. The 10-12 cm segment is full of big shells. From 51-75 cm is a transition area of a lighter brown/red shade. The underlying sediment from 75 cm

printed on 03/17/07 from "shelbyplots.tpo" and "EVERYTHING_WITH_LAST_PLOT"
 87°40'00" W 30°16'00" N



Map created with TOPO!® ©2002 National Geographic (www.national Geographic.com/topo)

Figure 24: Lake Shelby core locations. A=western transect, B=eastern transect, C=southern transect. The sediment at the top of each core is designated by fonts of different colors (National Geographic TOPO Software).

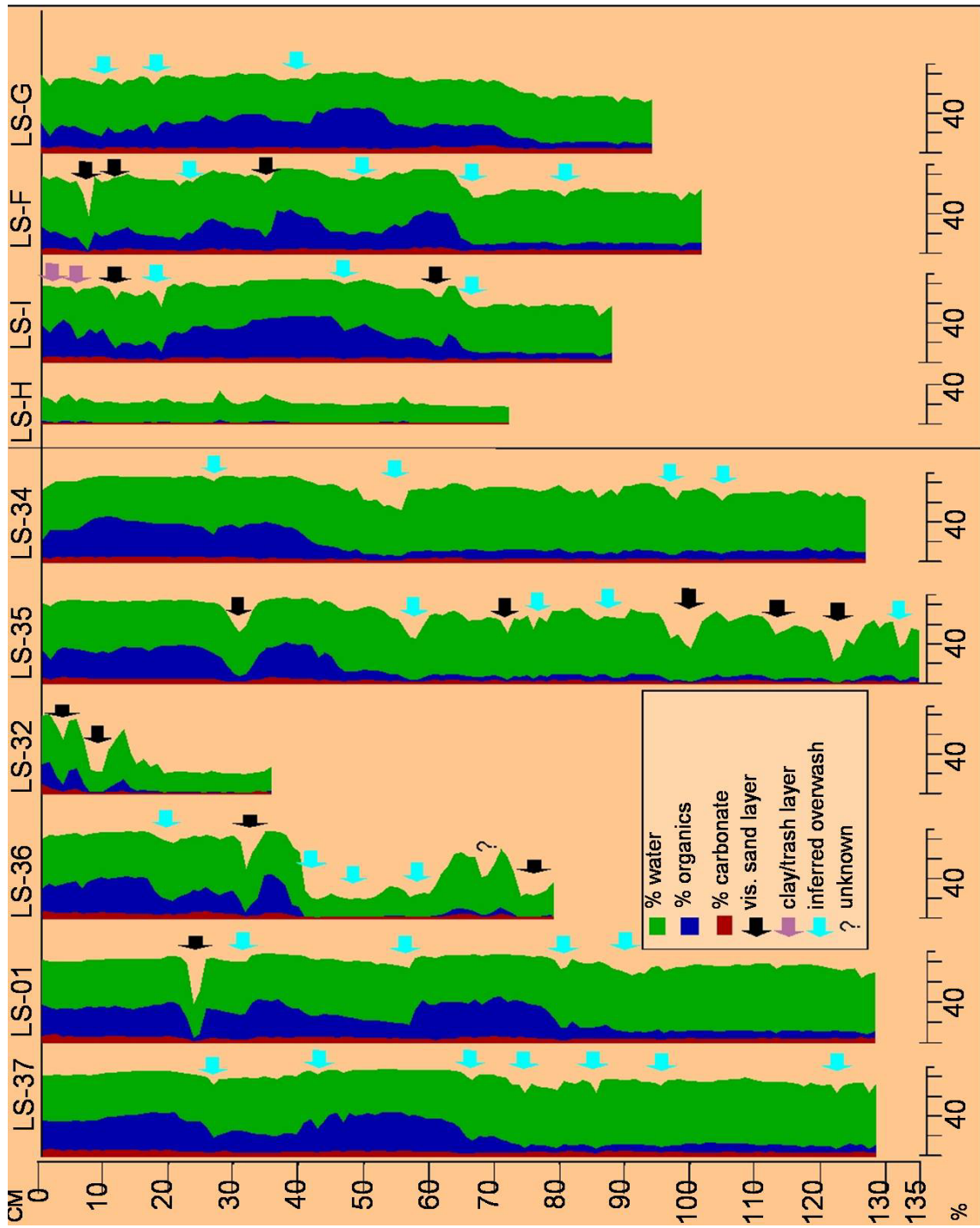


Figure 25: Lake Shelby LOI results (eastern and western transect). Cores on left side of vertical black line are from the eastern transect, while cores on the right side of the vertical line are from the western transect. The arrows depict hurricane events.

to the end of the core is gray clay, with a section of smaller shell fragments from 89-93 cm. LOI data, followed with an additional physical examination, show evidence of three indistinct clastic bands (Figure 25).

6.3.2 Lake Shelby – Eastern Transect

Seven cores are taken from this eastern transect (Figure 24). None of these cores contain a top prominent sand layer attributable to Hurricane Ivan. However, the top of certain cores (i.e. LS-35, LS-34) exhibit a slight “dip” on the LOI curves.

Core LS-01 (128 cm) is representative of the cores in this transect. The series from 0-29 cm contains a dark mud. A sizeable shell is present at 2 cm. A visible sand layer occurs at 23-24 cm. The 29-79 cm section contains a similar gyttja, but much sloppier in composition. A transitional segment from 79-93 cm becomes more grayish in color. Gray clay is prominent from 93-128 cm. LOI data, supported by subsequent examination, suggest the presence of four indistinct clastic layers (Figure 25).

Core LS-35 (135 cm) is composed of a black mud from 0-29 cm. A sizeable shell is found at 10-11 cm. A visible sand layer occurs at from 29-35 cm. The mud becomes somewhat lighter in color from 35-47 cm. From 47-56 cm is transitional toward gray clay, which occurs in the rest of the core from 56-135 cm. Four more visible sand layers are present at 73, 98-101, 111-115, and 120-123 cm. LOI data followed with an additional physical examination shows the presence of four additional clastic bands in the lower half of the core (Figure 25).

6.3.3 Lake Shelby – Southern Transect

Thirteen cores were taken from this southern transect (Figure 24). Certain cores are primarily composed of sand, while other cores have sections of high organic content. Ultimately, this is not an ideal location of the lake to search for the sedimentary signature of

Ivan, due to the predominance of sand in most cores. This indicates the area was affected by many hurricanes historically other than Ivan.

Core LS-12 (35 cm) is representative of cores in this area of predominantly sand deposition (Figure 26). This core is entirely composed of sand. The top 12 cm are composed of lighter sand than the rest of the core. From 12-28 cm is a darker sand without laminations. Lighter sand exists again from 28-35 cm. Despite this lighter sand, it is difficult to decipher these as overwash deposits, due to the high sand content throughout this core and potential frequent disturbance.

Alternatively, core LS-22 (60 cm) is representative of a core in this southern transect higher in organic content (Figure 27). The section from 0-39 cm contains a very dark mud abundant in plant fibers. A small piece of wood is visible from 12-14 cm. Due to the difference in sediment make-up for this section, it is deemed a “trash layer.” The section from 39-59 cm contains a slightly darker mud.

6.3.4 Middle Lake

Eight cores were taken from Middle Lake (Figure 28). Certain cores do contain a prominent top sand layer, while others lack this top sand signature. Most cores were taken in the southern portion of this lake, but a few cores were extracted from the middle area.

ML-01 (120 cm) is an example of a core with a prominent top sand layer (Figure 29). A thin layer of black mud occurs at the core top from 0-3 cm. A prominent white sand layer is present at 3-12 cm, which embeds a shell at 10-11 cm. An organic mud exists from 12-42 cm. This section starts very dark at 12 cm, and gradually turns lighter toward 42 cm. Two faint visible sand layers exist in this section (17 cm and 35 cm). From 42-52 cm another prominent sand layer exists. Darker sand is found from 52-62 cm. Another visible sand layer is seen

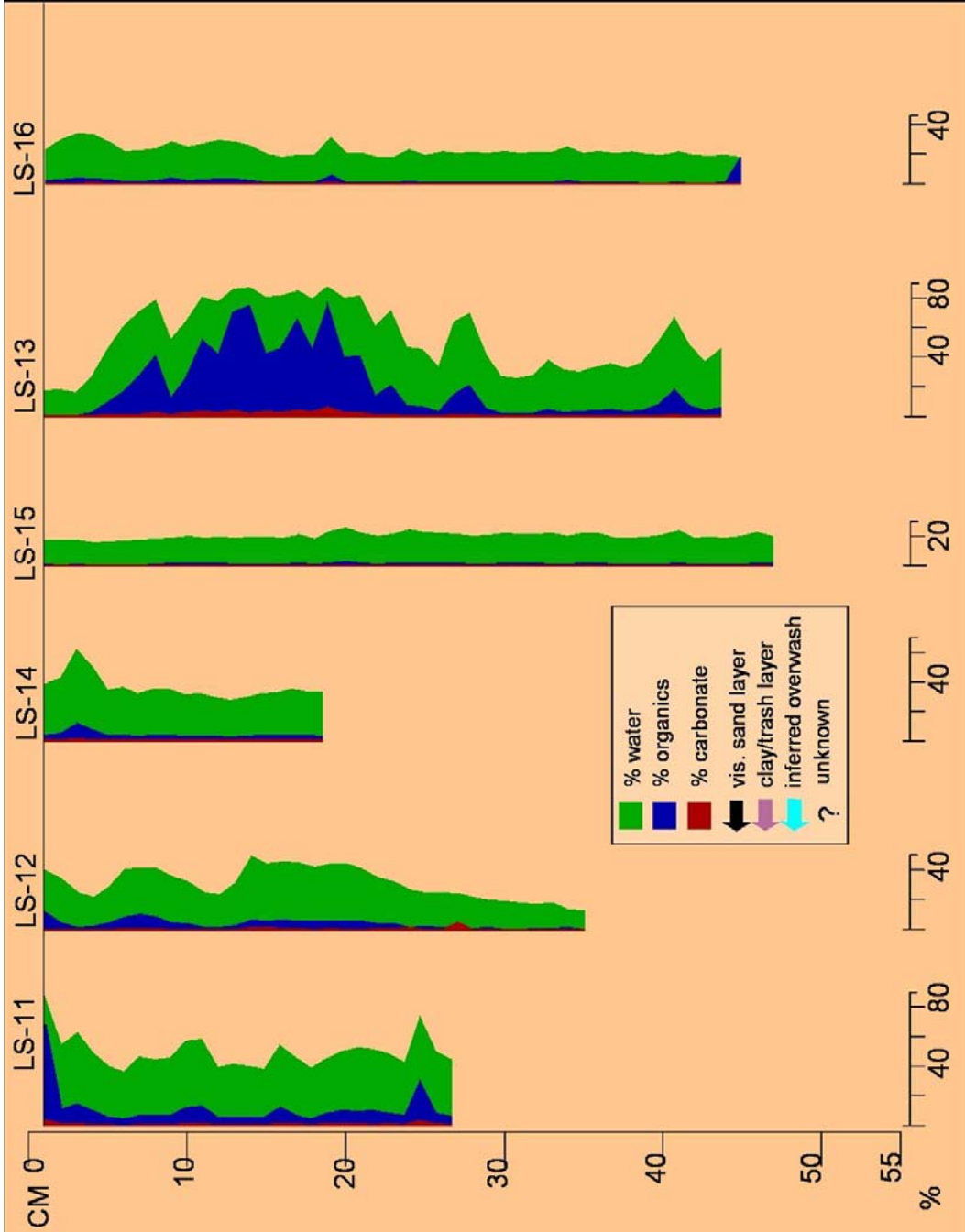


Figure 26: Lake Shelby LOI results (southern transect).

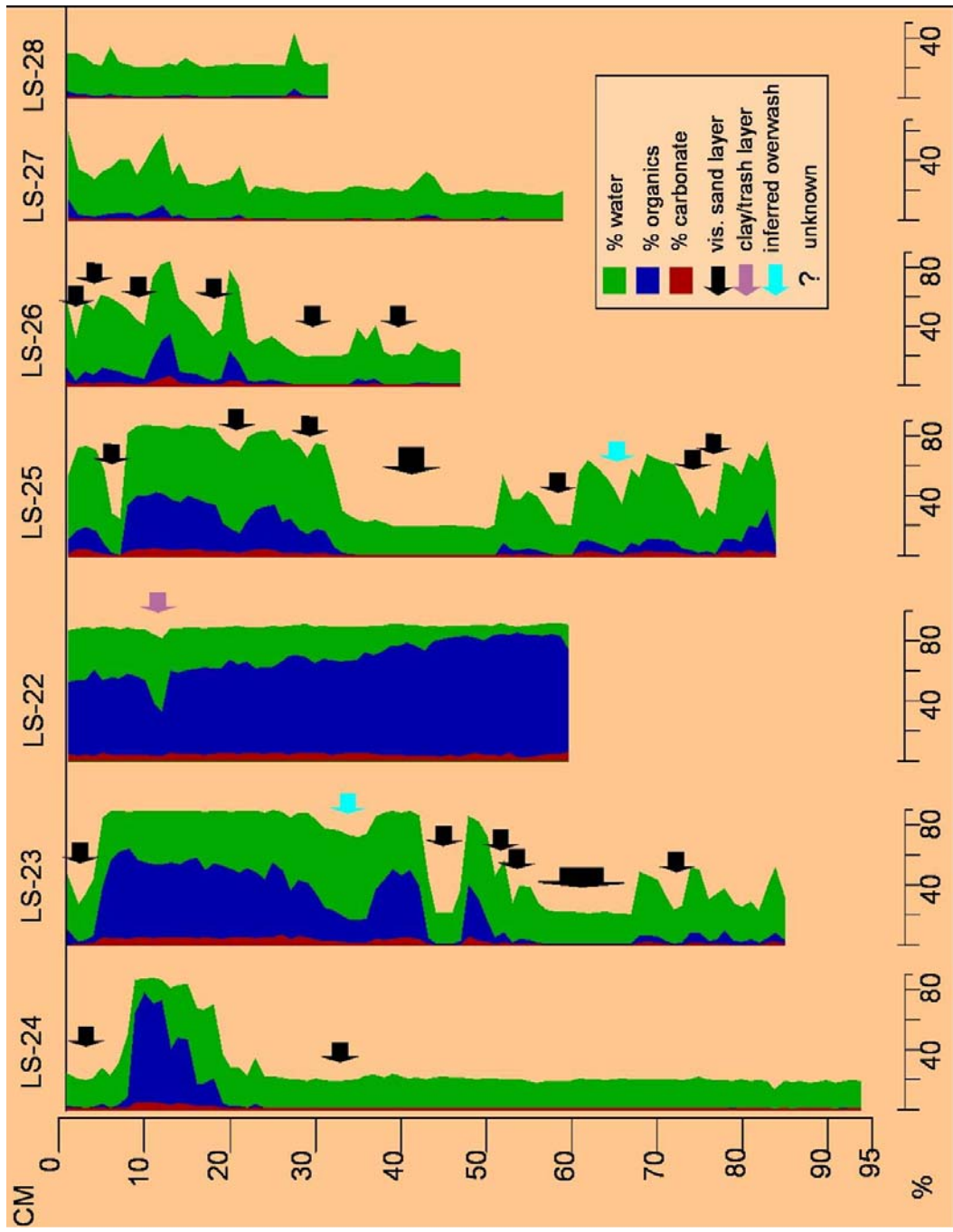
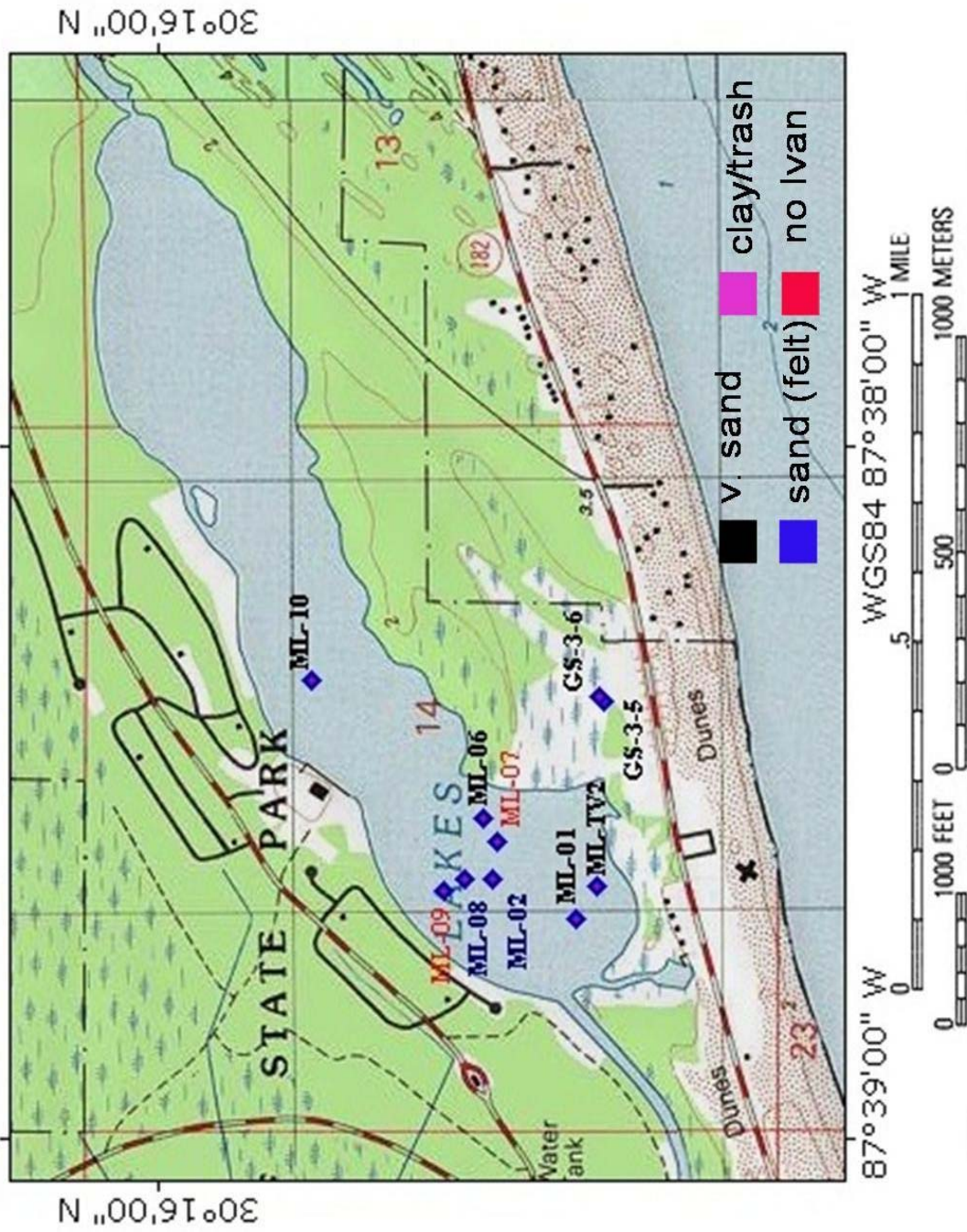


Figure 27: Lake Shelby LOI results (southern transect). The arrows depict hurricane events.

printed on 03/17/07 from "littlake.tpo" and "EVERYTHING_WITH_LAST_PLOT
 WGS84 87° 38'00" W



Map created with TOPO!® ©2002 National Geographic (www.nationalgeographic.com/topo)

Figure 28: Middle Lake (and vicinity) coring locations. The sediment at the top of each core is designated by fonts of different colors (TOPO software).

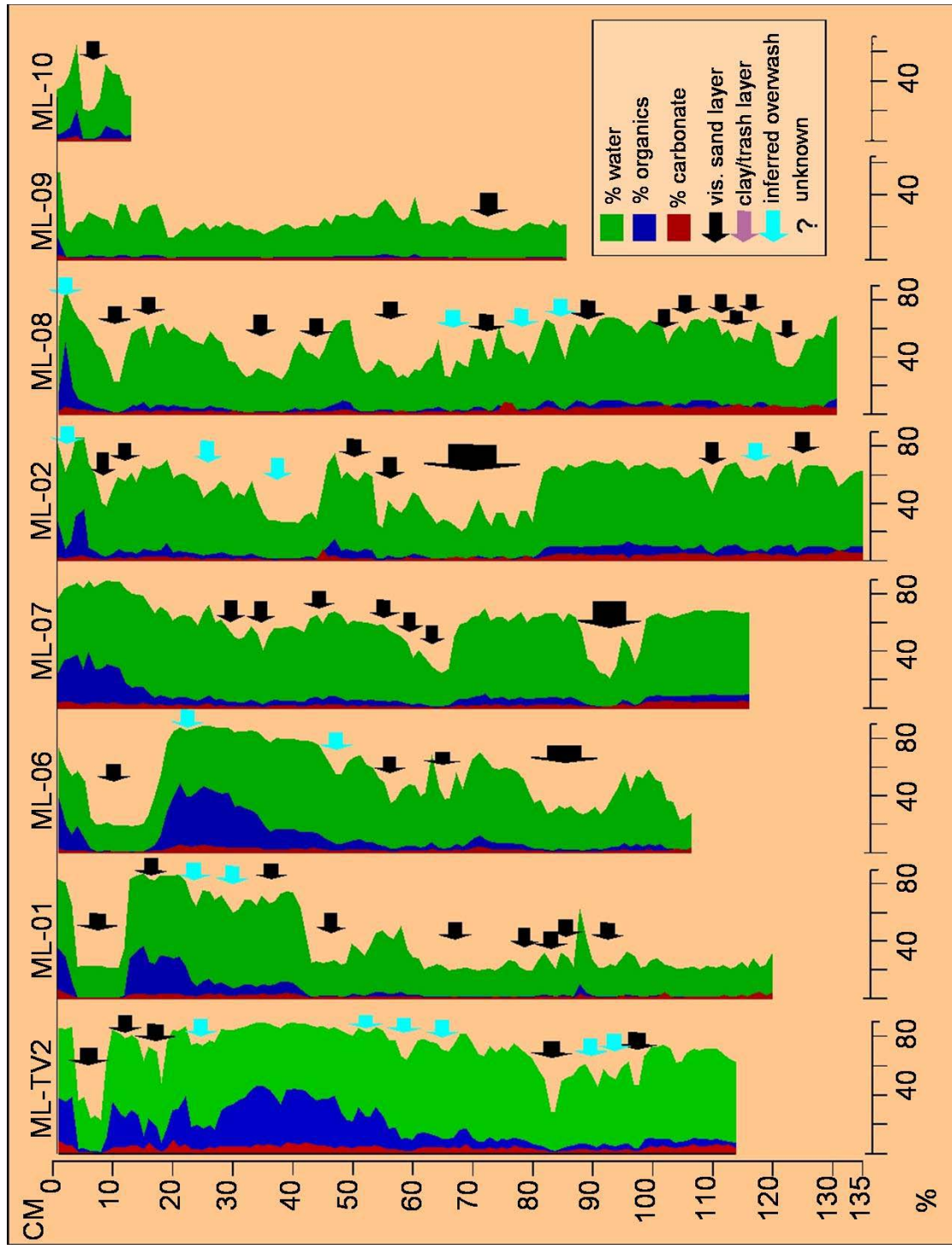


Figure 29: Middle Lake Lake LOI results. The arrows depict hurricane events.

from 62-77 cm. An additional visible sand layer is found at 78-79 cm, along with another one at 85 cm and 87 cm. There is a small section of high water content (89 cm), with a visible sand layer below it (89-93 cm). Gray sand comprises the remainder of the core. LOI data followed with an additional physical examination shows the presence of two additional sand layers (23 cm and 31 cm).

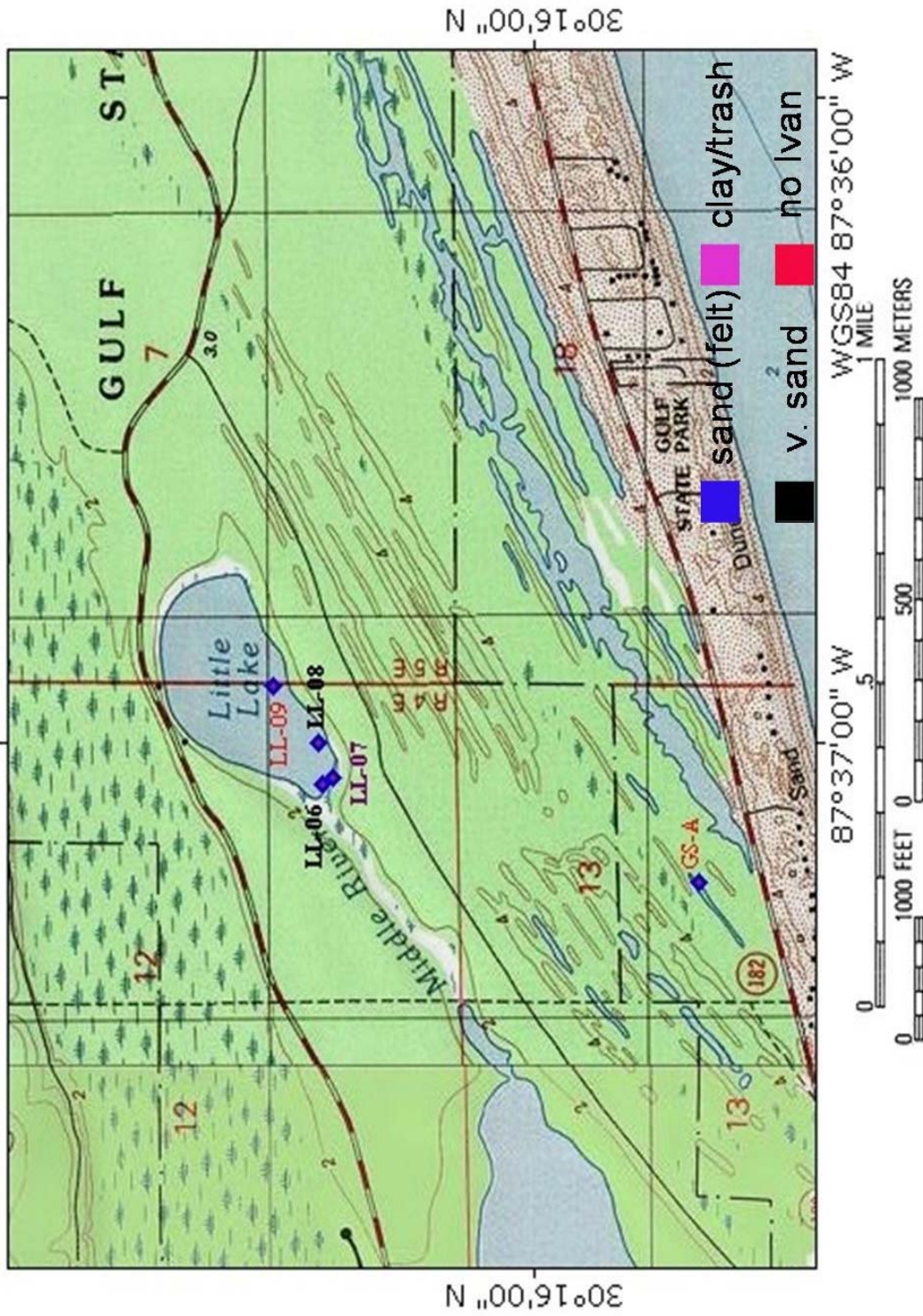
ML-07 (116 cm) is an example of a core lacking a storm layer at the top (Figure 29). A brown mud occurs at the top from 0-7 cm. A lighter band follows at 7-8 cm. A section similar to the top brown mud occurs at 8-12 cm. Gray clay is found from 12-33 cm. A visible sand layer is found at 29-32 cm and 34 cm. From 33-67 cm is gray clay similar to that above, but slightly sandier in touch. Visible sand layers are found at 44-45 cm, 55-56 cm, 59 cm, and 62-65 cm. Darker gray clay characterizes the section at 67-99 cm. An additional visible sand layer is found from 87-99 cm. Lighter gray clay occurs from 99-116 cm.

6.3.5 Little Lake

Four cores were taken from Little Lake (Figure 30). Certain cores contain a top sand layer, while other cores do not. Cores are taken toward the southern end of the lake.

LL-06 (110 cm) does contain a sand layer at the top. The top 5 cm is detrital gyttja rich in coarse plant fibers, with minimal sand content. A sand layer is present from 5-9 cm. Gyttja occurs again at 9-18 cm. Another visible sand layer is found at 18-22 cm, along with fragments of tree bark. A layer of plant debris characterizes the 22-26 cm section, which is also reflected by the high organic percentages on the LOI curve. Immediately underlying this plant detrital layer, a visible sand layer is found at 26-29 cm. Dark detrital gyttja occurs in the 29-33 cm section again, overlying a visible sand layer at 33-37 cm. Another layer of plant debris occurs from 37-42, immediately above a visible sand layer at 42-45 cm. Dark gyttja occurs from 45-57

map printed on 03/17/07 from "littlake.tpo" and "EVERYTHING_WITH_LAST_PLOT_TRIP
 WGS84 87°37'00" W



Map created with TOPO!® ©2002 National Geographic (www.nationalgeographic.com/topo)

Figure 30: Little Lake (and vicinity) core locations. The sediment at the top of each core is designated by fonts of different colors (National Geographic TOPO software).

cm, but sand becomes more abundant and visible from 52-56 cm. A coarse, darker sand exists from 57-60 cm. A lighter and finer sand layer again occurs from 60-68 cm. The remainder of the core consists of brown sand with numerous darker patches (Figure 31).

LL-09 (78 cm) does not contain a visible sand layer at the top. The top sediment (0-9 cm) is composed of gyttja rich in plant detritus. A section of dark detrital gyttja exists from 9-21 cm, with three visible sand layers (9-11 cm, 12-16 cm, and 17-19 cm). The remainder of the core is assorted patches of black and brown sand (Figure 31).

6.3.6 Non-forested Wetland

Two cores (GS 3-5 and GS 3-6) were taken from the non-forested wetland (marsh) south of Middle Lake (Figure 28). Both cores have a top sand layer. Core GS 3-6 (44 cm) is composed of black peat with many twigs at 0-4 cm. A mud/sand mixture occurs at 4 cm. The remainder of the core is very dark brown peat with an extremely low sand content and no laminations (Figure 32).

6.3.7 Swale Lakes

One short core (GS-A) was taken from an elongated swale lake between two parallel beach ridges south of Middle Lake and Little Lake (Figure 30). This core (11 cm) is primarily composed of white sand mixed with organic matter. Most of the lakes examined have a hard bottom difficult to penetrate with the Livingstone corer. The LOI data do not reveal more information than what could be deciphered from the visual inspection (Figure 32).

6.4 Discussion

6.4.1 Lake Shelby

Generally, cores from Lake Shelby do not contain an overwash sand layer at the top. Hurricane Ivan did not seriously breach the sand barrier between the Gulf of Mexico and Lake

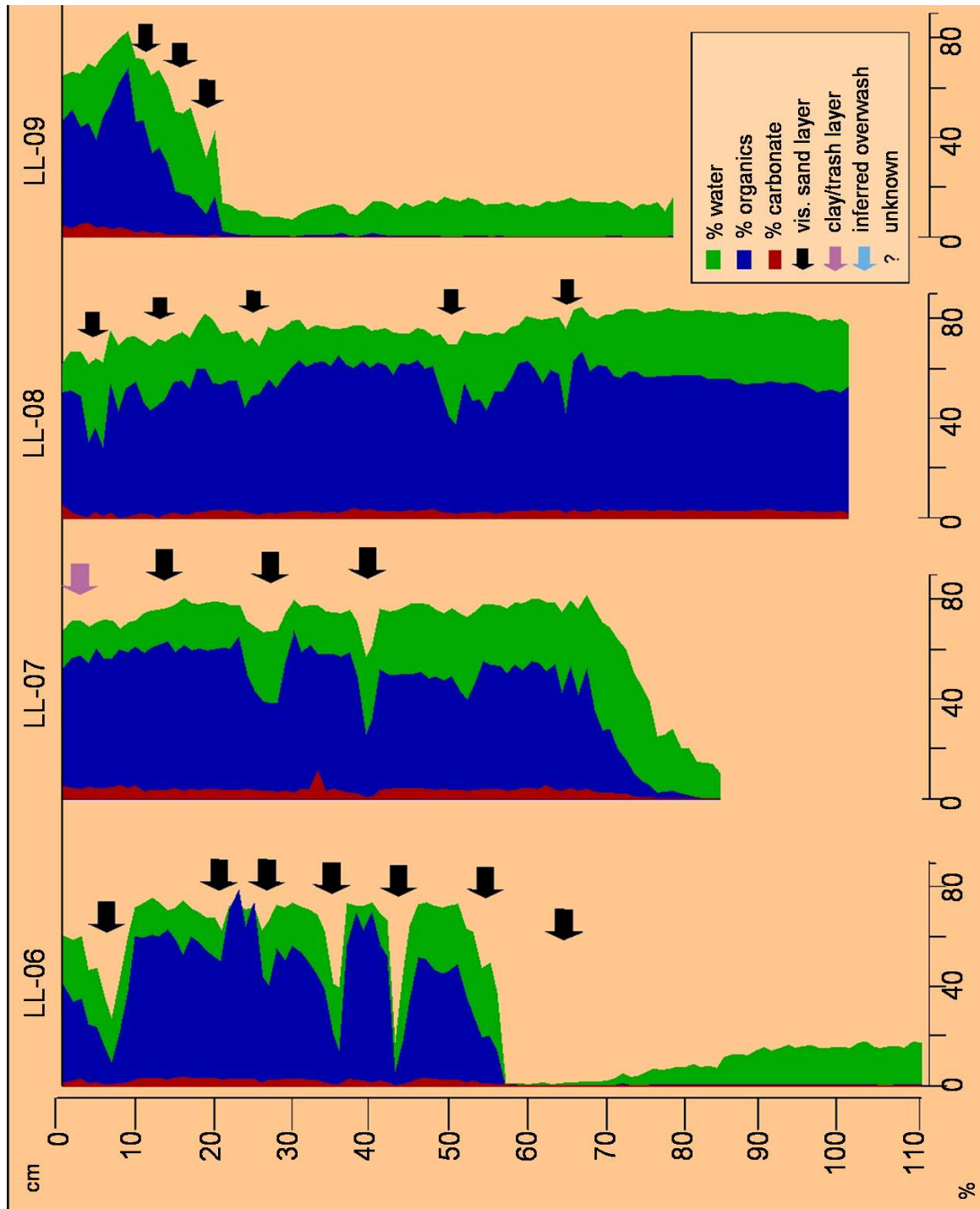


Figure 31: Little Lake LOI results. The arrows depict hurricane events.

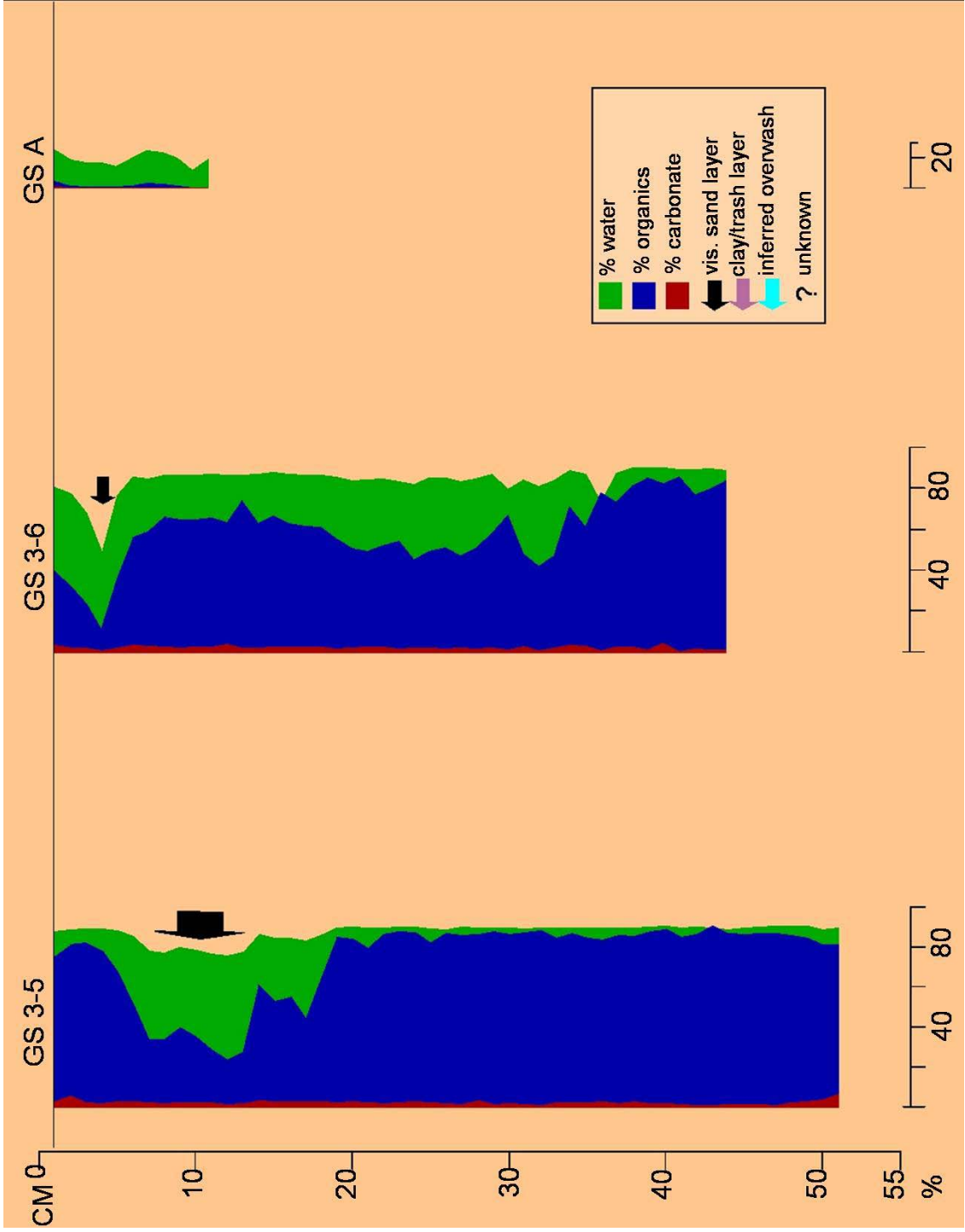


Figure 32: Non-forested wetland/swale lake LOI results. The arrows depict hurricane events.

Shelby. Therefore, transport of sand grains into the lake is limited to the southernmost part of the lake in the nearshore environment. Although a minor breach was created south of Lake Shelby (viewed from aerial photos/DOQs), it was probably not significant enough to transfer sand into the middle of this large water body, especially in the areas of the western and eastern transects. Moreover, the low-lying non-forested wetland to the west of Lake Shelby probably acted as a sediment trap for the incoming water during the storm surge, withholding the sand before it was transported further out to reach the lake. Furthermore, the many urban structures to the south of Lake Shelby could have hindered the movement of the incoming sand.

Certain cores in this western transect do show a slight dip in LOI values toward the top. Even though these are not visible sand layers, they are probably indicative of the minor disturbance caused by the Ivan storm surge. For example, core LS-I on the western transect contains a small clay layer at approximately 7 cm, under a “trash” layer consisting of twigs. Hurricane Ivan potentially caused this “trash layer,” and possibly even the clay layer. This is supported by the lack of this top dip in cores taken from many previous research trips in the late 1980s and 1990s (Figure 33).

A similar scenario exists for the eastern transect at Lake Shelby. The cores there do not contain a top visible sand layer attributable to Hurricane Ivan. However, slight dips in LOI values do occur toward the top of several cores. This indicates an increase in clay contents in the surface sediment, even though no distinct elastic layer is visible at the top. LS-35 and LS-34 are examples of this type of stratigraphy. As is the case of the cores in the western transect, the lack of a prominent top sand layer in Lake Shelby is mainly due to the absence of significant breach.

Cores taken from the southernmost part of Lake Shelby are typically dominated by sand and therefore not very useful in detecting the Ivan storm signature. Examples of such cores are

LAKE SHELBY CORE LOCATIONS

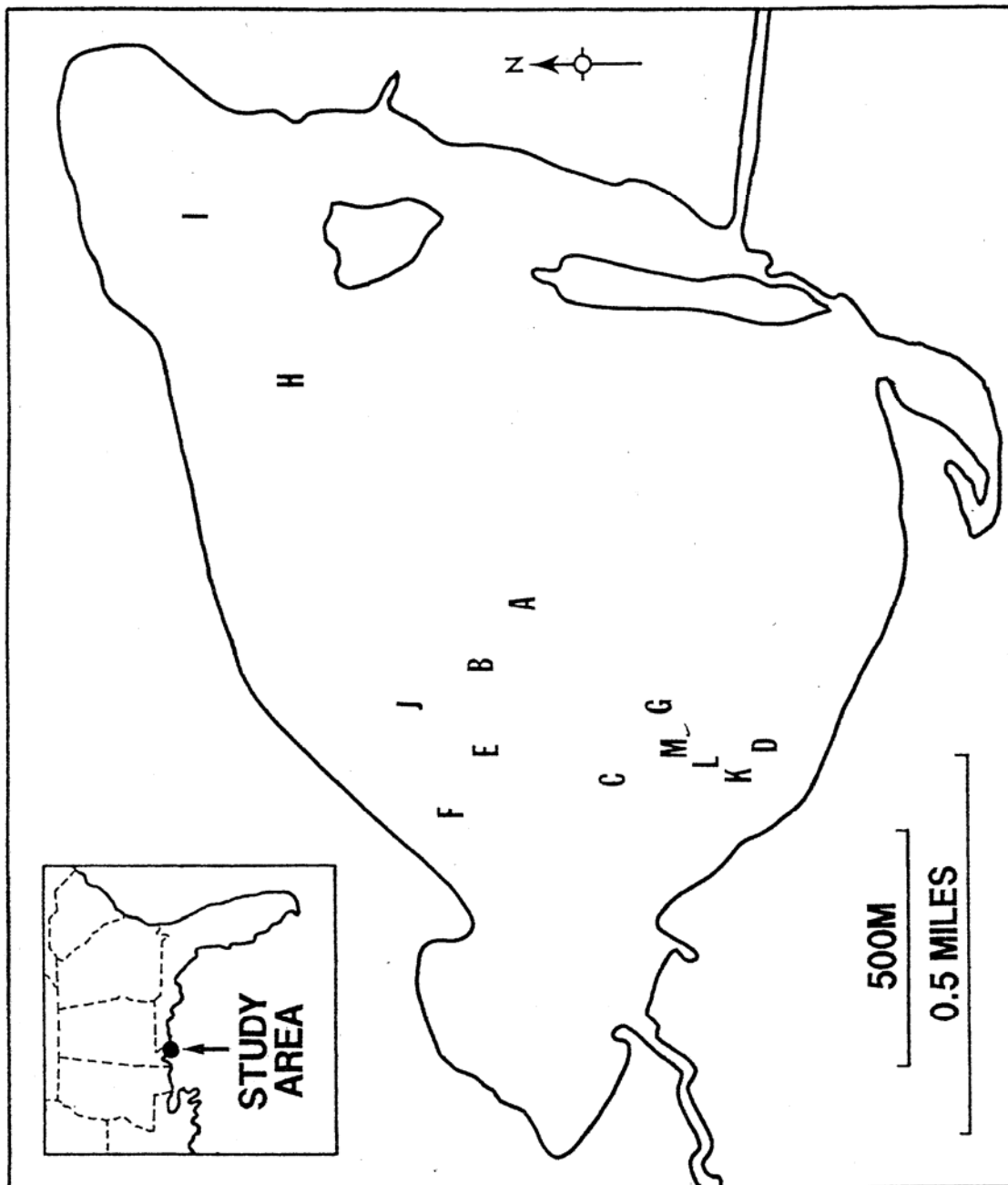


Figure 33: Location of cores taken from Lake Shelby in 1989 and the early 1990s (Liu, unpublished data).

LS-15 and LS-16. However, some of the cores from portions of this southern section do contain organic sediments indicative of a typical lake deposition. Examples of these cores are LS-13 and LS-23. LS-23, for example, has a top sand layer of approximately 5 cm in thickness which could be derived from Ivan. The top sand layer overlies almost 40 cm of detrital gyttja and peat. The lower part of the core is composed of many sand layers, with patches of gyttja and gray clay interspersed. Apparently, the sedimentary pattern of this southernmost part of the lakes is quite complex, which warrants more detailed investigation in the future.

6.4.2 Middle Lake

Middle Lake yields many cores with a clear, visible sand layer at the top (Figure 28). This sand layer is attributable to Ivan because of the major breaching known to have occurred at the southernmost portion of the lake. This breaching is believed to be one of the main processes carrying sand into the lake. Another process was probably overwash carrying sand over the non-forested wetland to the south/southwest section of Middle Lake. This reconstruction is based on the pattern of sedimentation observed from the cores. ML-06 (Figure 34), a core taken farthest away from the breach but closest to the wetland to the southeast of Middle Lake, has the thickest top sand layer (approximately 12 cm), compared with only 8 cm and 4 cm for ML-01 (Figure 35) and ML-TV2 (Figure 36), respectively. ML-10, farthest away from the breach, also has a prominent top sand layer attributable to Ivan (approximately 3 cm – Figure 37).

These top sand layers are interpreted to be deposited from Hurricane Ivan and not Hurricane Frederic (1979). The damage to Gulf State Park from Ivan surpassed damage inflicted from Frederic (Kelly Reetz, Gulf State Park naturalist, personal communications, 2005, 2006). This assertion is also supported by comparing cores taken before and after Ivan. Many lake cores were taken and analyzed in September 1989. All cores taken and analyzed failed to yield a top



Figure 34: Core ML-06. Notice top sand layer.



Figure 35: Core ML-01. Notice top sand layer.

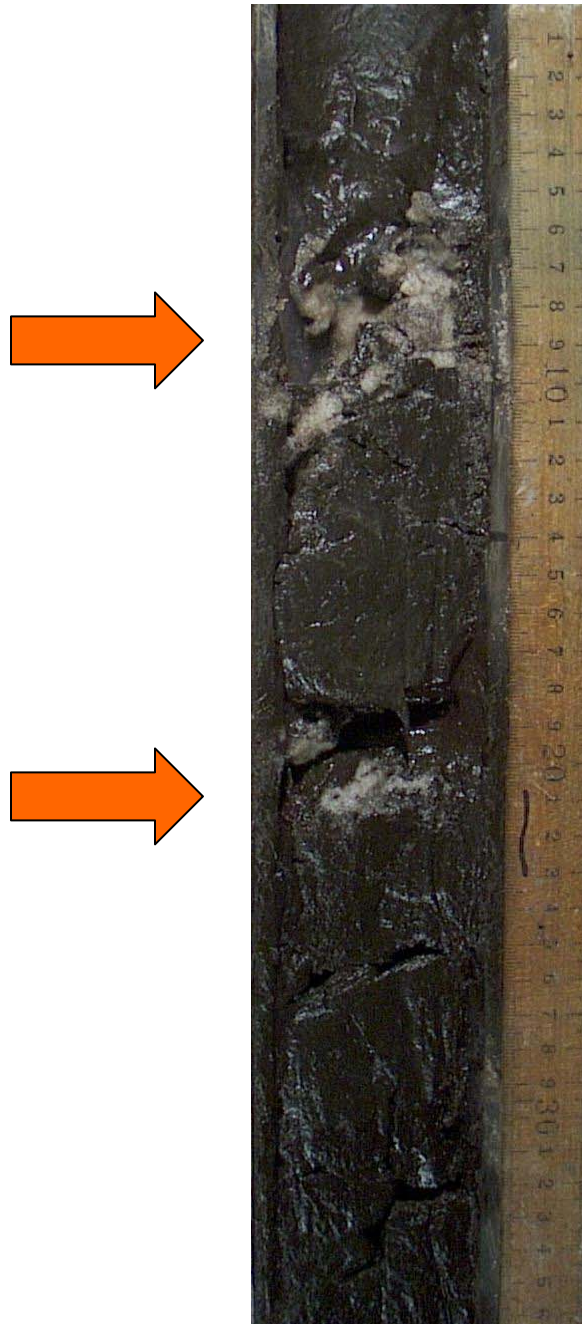


Figure 36: Core ML-TV2. Notice two top sand layers.



Figure 37: Core ML-10. Notice top sand layer.

sand layer attributable to any recent hurricane strike then, including Frederic of 1979. Two cores taken from that 1989 trip (M5G and M2D) were geographically close to two cores taken recently (ML-10 from August 2005 and ML-01 from June 2006). Both cores ML-10 and ML-01 contain a sand layer at the top, unlike the two cores taken from September 1989 before Ivan (Figure 38, 39).

The six AMS radiocarbon dates from cores ML-06 and ML-TV2 provide chronological control for the reconstruction of paleohurricane strikes for the region. Core ML-TV2 shows evidence of seven visible sand layers, and at least four inferred storm events (Figure 40). Therefore, at least eleven intense hurricanes were detected from this core. The radiocarbon date from the oldest sand layer dates to 2350 +/- 40 ¹⁴C years B.P. This is translated into approximately 2350 calendar years B.P. (Table 9). Therefore, a return period of approximately 213 years is established (Figure 40). This is similar to findings in Liu et al. (2003) for Little Lake. They found at least seven hurricane-induced overwash events in approximately 1250 years, for a similar return period (approximately 180 years).

6.4.3 Little Lake

Little Lake has yielded two cores (LL-06 and LL-08) with a top sand layer attributable to Ivan. LL-07 does not have a top visible sand layer, but a top “trash layer” attributable to Ivan. In a previous study of a core from Little Lake, Liu et al. (2003) did not find a top sand layer attributed to Hurricane Frederic. Additional coring of Little Lake (March 1990 and June 2003) also did not indicate evidence of a visible sand layer indicative of Hurricane Frederic. Therefore, it is suggested that these top sand layers occurring in cores LL-06 (Figure 41) and LL-08 are from Ivan’s storm surge, inundating the beach ridges just south of the lake.

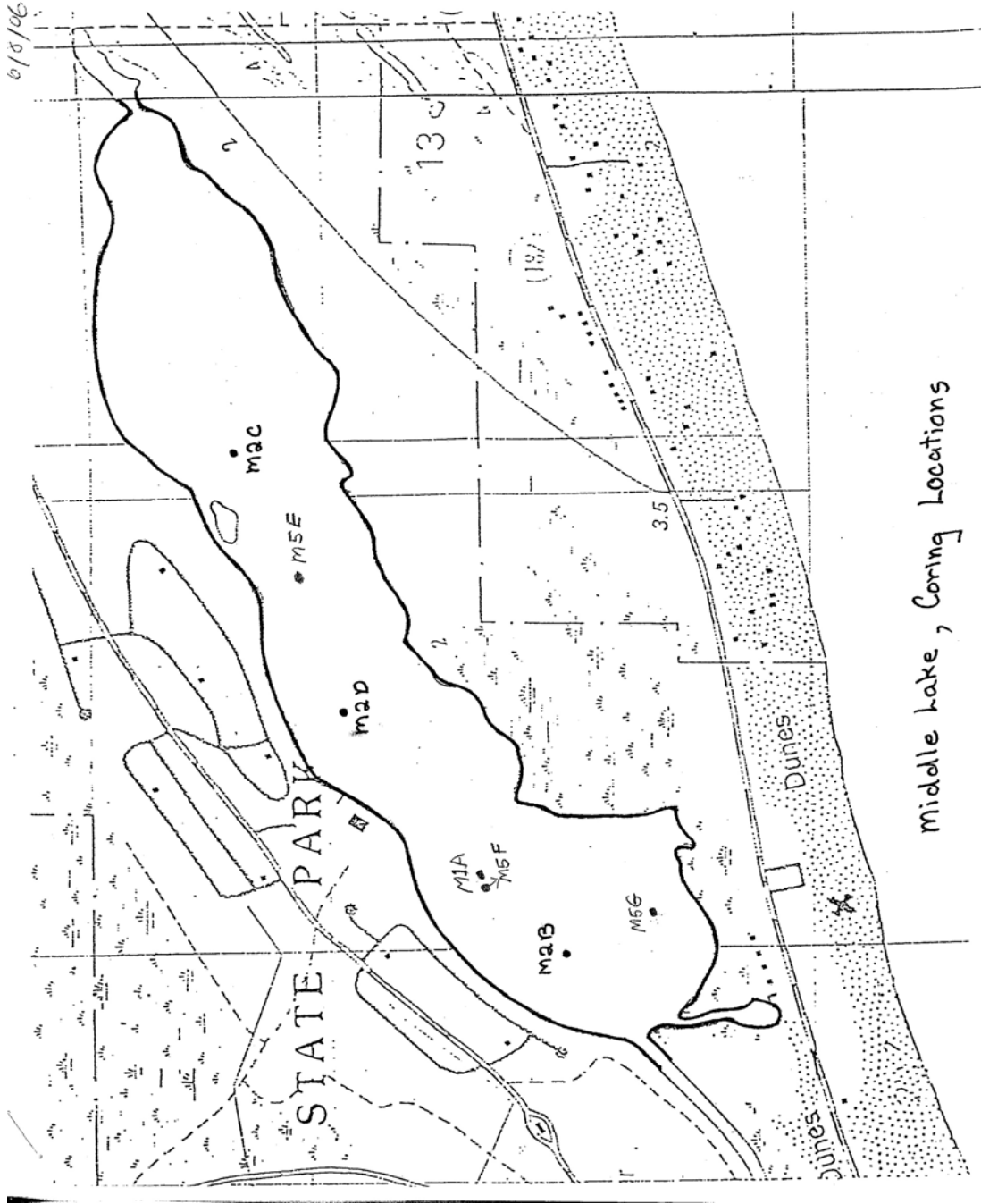


Figure 38: Cores taken from Middle Lake in September 1989 (Liu, unpublished data).

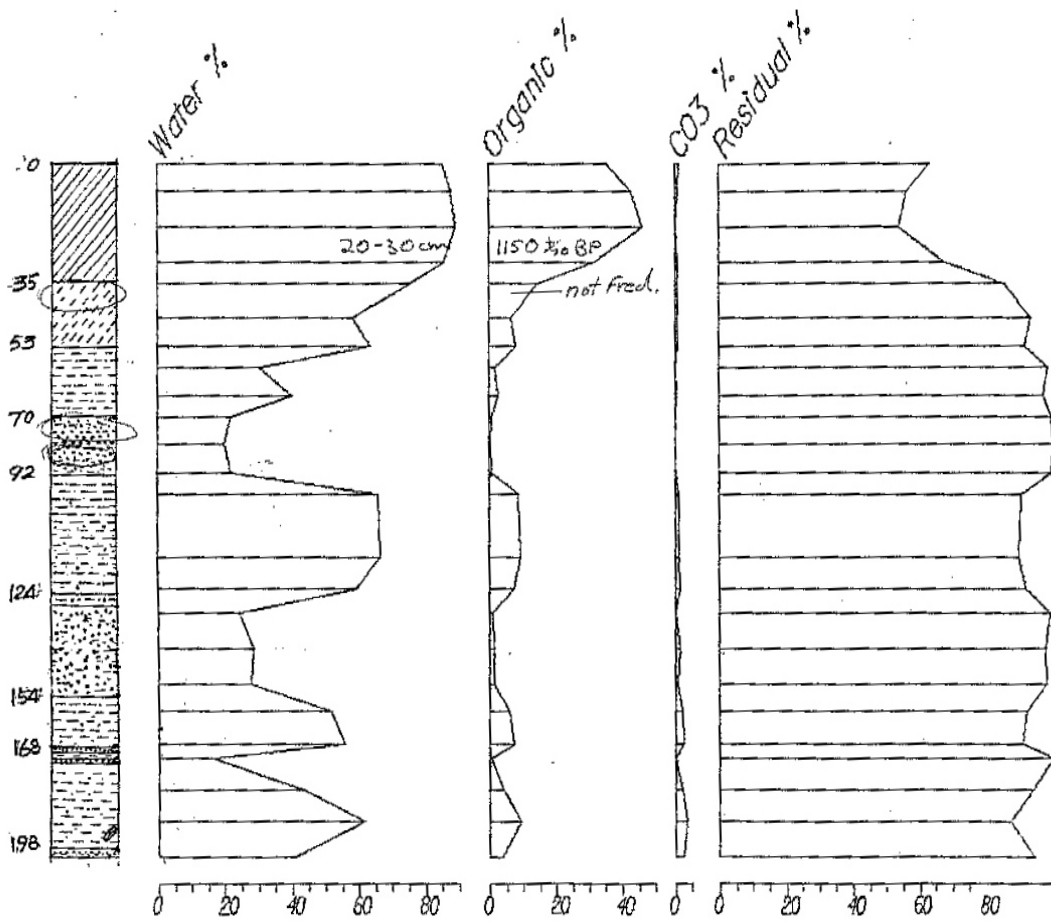


Figure 39: Loss on ignition results for core M2D. Notice the absence of top sand layer attributable to Hurricane Frederic (Liu, unpublished data).

Table 9: Radiocarbon dating results. Intercept, 1 sigma, and 2 sigma results are represented in calendar years before present (cal yr BP).

<u>Core</u>	<u>Sample</u>	<u>Conventional Radiocarbon</u>			<u>2 sigma result</u>
		<u>Age</u>	<u>Intercept</u>	<u>1 sigma result</u>	
ML-TV2	20 cm	720 +/- 40 BP	670	680-660	700-650 580-570
ML-TV2	55 cm	1330 +/- 40 BP	1280	1290-1260	1300-1180
ML-TV2	79 cm	1610 +/- 40 BP	1520	1540-1500 1500-1490 1470-1420	1570-1400
ML--TV2	100 cm	2350 +/- 40 BP	2350	2360-2340	2460-2330
ML-06	53 cm	1770 +/- 40 BP	1700	1720-1680 1670-1620	1810-1570
ML-06	95 cm	2480 +/- 40 BP	2690 2640 2610 2590 2500	2710-2470	2730-2360

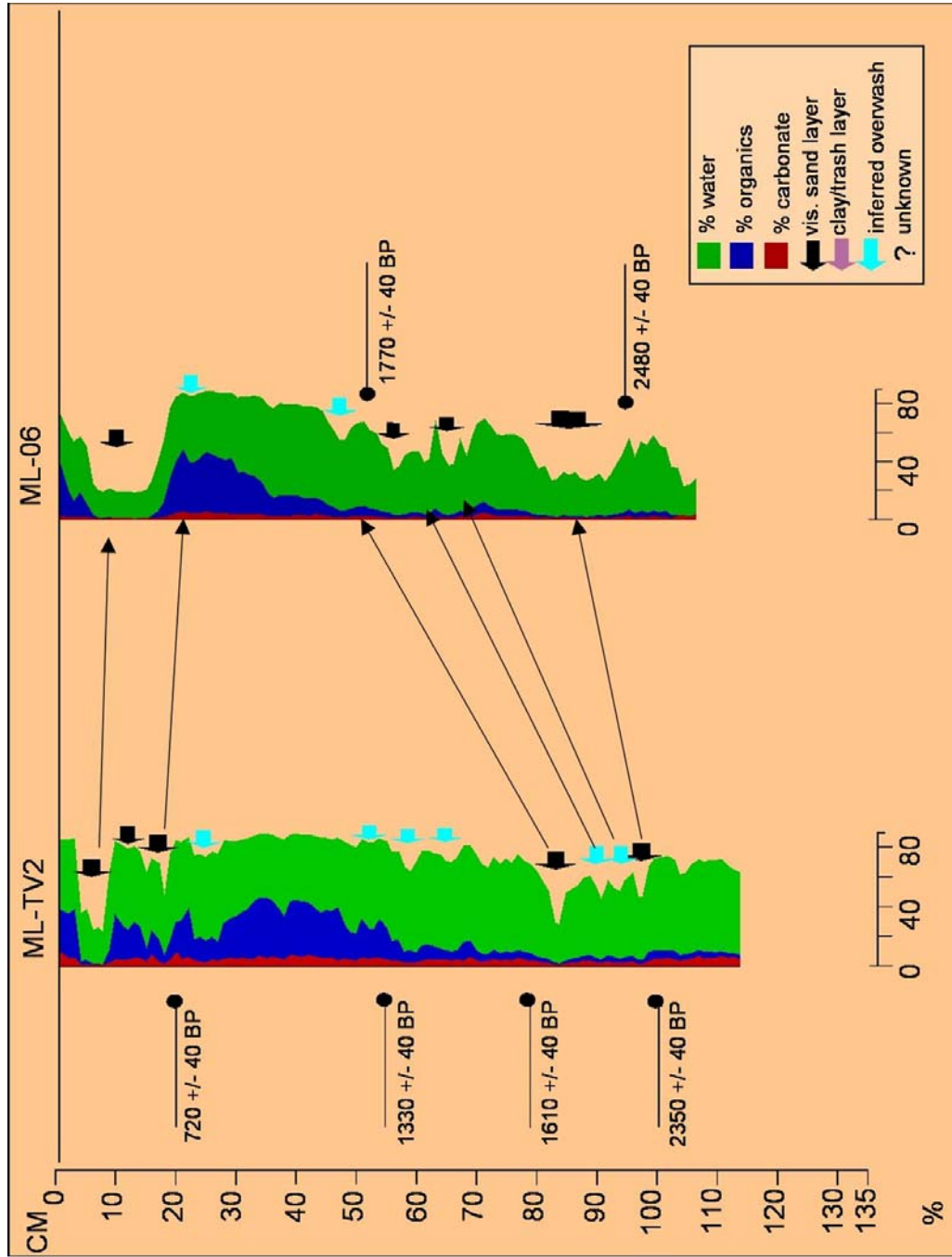


Figure 40: Radiocarbon dating results and possible storm correlations. All dates above are conventional radiocarbon dates.

6.4.4 Non-forested Wetland

Cores GS-3-5 and GS-3-6 both have a top sand layer believed to represent Ivan (Figure 42). These cores are almost due south of ML-06 (Figure 28), a core with a top sand layer. These data are therefore consistent with the interpretation that much sand was transported by storm surge entering Middle Lake from the southeast over the dune fields and wetlands, rather than directly through the breach to the south.

6.4.5 Swale Lakes

The core taken from the swale lake (GS-A) is not useful for paleotempestological research, due to its lack of organic lake deposition. Possibly, these swale lakes are too small for gyttja to accumulate. Also, human disturbance may have affected these lakes, as witnessed by the urban structures built between the lake and the highway.

6.4.6 The Role of Winter Storms

Could the top sand layers found in these lakes be due to a winter storm, such as the “Storm of the Century” of 1993, rather than Hurricane Ivan? This possibility is unlikely for several reasons. First, as stated in Liu and Fearn (1993), although winter storms are common on the Atlantic Coast, they are infrequent along the Gulf of Mexico coast. In addition, major hurricanes are typically associated with a much greater storm surge and higher wind speed than winter storms (Liu and Fearn, 1993). Specifically, even though this 1993 winter storm brought heavy snowfall to northern and central Alabama, the accompanying winds were only 40 to 55 miles per hour (NOAA’s National Weather Service, 2006), which were not sufficient to create a significant storm surge and overwash process in the vicinity of Lake Shelby.



Figure 41: Core LL-06. Notice top sand layer.



Figure 42: Core GS-3-6. Notice top sand layer.

6.5 Summary

Hurricane Ivan, a Category 3 hurricane at landfall, was not strong enough to deposit an overwash sand layer in the western and eastern transect areas of Lake Shelby. Data from this new study therefore support the contention by Liu and Fearn (1993) that older sand layers found in cores taken from the middle of Lake Shelby represent prehistoric hurricanes of Category 4 and 5 intensities.

The sediment in Middle Lake contains evidence of strikes by intense Category 3 hurricanes such as Ivan. This conclusion is supported by the presence of a distinct Ivan sand layer at the top of four cores taken from the southern end of the lake (ML-TV2, ML-10, ML-01, and ML-06), as well as cores with a top sand layer that is not distinct but with a presence confirmed by LOI data and physical examinations (ML-02, ML-08). The results from the radiocarbon dating indicate that the return period for intense Category 3-5 storms is about 213 years. This estimate is comparable to that established for Little Lake (Liu et al., 2003).

In agreement with Liu et al. (2003), Little Lake contains the sedimentary evidence of intense Category 3 hurricanes, in the form of visible sand layers. This evidence can be found in two cores (LL-06 and LL-08) that contain visible sand layers at the top attributable to Ivan, and the core LL-07 that contains a top trash layer of coarse organic detritus.

Chapter 7: Conclusions

From the sedimentary, vegetational, and remote sensing analyses, several major conclusions can be drawn.

The vegetation analysis provides important ground truth to document the ecological impacts of Hurricane Ivan. By choosing sampling plots at different elevations at Gulf State Park, the spatial pattern of tree mortality can be surveyed and the results can shed light on the question of whether wind damage or storm surge flooding was the primary cause of tree mortality. The data were analyzed by correlation coefficients and a logistic regression. The Pearson's r suggests that the chance of survival for trees increases with increasing elevation. These results are consistent with the interpretation that storm surge was the primary cause of tree mortality at Gulf State Park. The saltwater can linger at sites with very low (3-5 foot) elevations. By contrast, if wind damage were a major catalyst at Gulf State Park, the pattern of forest damage would be more geographically continuous, and not concentrated in the lower elevation areas.

The remote sensing analysis was a useful tool to reveal the ecological impacts at the landscape scale. This investigation offers a "bird's-eye" view using Landsat 5 images, NDVIs, and a hybrid classification scheme for the pre- and post-hurricane land cover changes. The study shows that the hurricane-induced salt water inundation caused catastrophic forest damage to the vast forests north of the coastal lakes. In conjunction with this forest loss, the increase in barren areas was also noteworthy. The most significant changes in land cover from the pre- to post-hurricane image are the increase in barren (from 194 to 288 hectares) and decrease in forest (1108 to 622 hectares) land cover types. The remote sensing study further suggests that a sand layer attributable to Ivan would be found in the Shelby Lakes, due to the clear damage to the landscape from the storm surge.

By analyzing sediment in Lake Shelby, Middle Lake, Little Lake, the non-forested wetland south of Middle Lake, and the “swale lakes” south of both Middle and Little Lake, it was determined that Ivan’s impact was distributed unevenly in these areas. A clear sand layer attributable to Ivan was not found in the center of Lake Shelby. This can be due to many factors, such as distance from the beach system, the large size of the lake, and the lack of major breach. This is in agreement with Liu and Fearn (1993) who suggested that the middle of Lake Shelby only has clear overwash layers from Category 4 or 5 events.

Middle Lake yields four cores with visible sand layers attributable to Ivan. Core ML-TV2, the only core from Middle Lake with two top sand layers, had at least 11 overwash layers, yielding a return period of approximately 213 years. Due to the results of this study, it is suggested that Middle Lake’s threshold can include visible sand layers from Category 3 storms. A similar scenario exists for Little Lake, which yielded two cores with visible sand layers attributable to Ivan. Little Lake can support visible overwash layers from Category 3 storms, in agreement with Liu et al. (2003). Despite its greater distance to the beach and dune system, the sand dunes immediately to the south can be an additional source of sand.

The cores taken from the non-forested wetland south of Middle Lake show evidence of Ivan in the form of visible sand layers. These aid in deciphering how the storm surge entered this area, apparently continuing north to deposit the thickest overwash deposit at ML-06. A core taken from a swale lake was not useful, due to the lack of organic deposition in a very small and shallow lake.

More research is warranted for this area. More cores should be taken from key areas within each lake. This includes, but is not limited to, eastern Middle Lake (where few cores were taken) and the non-forested wetland west of Lake Shelby (where no cores were taken). The

eastern part of Middle Lake offers an intriguing area for future research. A sand signature from Ivan is questionable. This is due to the increased distance from the major sand supply along the Gulf of Mexico coast, and the lack of sand dunes to the south of this area. This is the major reason that Little Lake's threshold supports Category 3 storms, which is possible yet unlikely for eastern Middle Lake. Furthermore, it is possible that Ivan left a sand imprint south of Lake Shelby's western transect. This is due to its southern location and its proximity to the minor breach. Finally, a land cover classification, along with NDVI /image differencing could be performed with a Landsat image more recent than July 2005 to discover any recent changes to the landscape, most notably any forest recovery.

Bibliography

- Agresti, A. (1996). An Introduction to Categorical Data Analysis. New York: Wiley.
- Alabama State Parks. (2004). Gulf State Park Trails. Retrieved <Jan 09, 2007> From <http://www.alapark.com/parks/feature.cfm?parkid=22&featureid=15>.
- Anderson, J.R., Hardy, E.E., Roach, J.T., and Witmer, R.E. (1976). A land use and land cover classification system for use with remote sensor data. Washington, U.S. Government Printing Office.
- Anthes, R.A. (1982). Tropical cyclones: their evolution, structure and effects. Meteorological Monographs, 19(41). American Meteorological Society, Boston, Massachusetts, USA. -
- Ayala-Silva, T. and Twumasi, Y.A. (2004). Hurricane Georges and vegetation change in Puerto Rico using AVHRR satellite data. International Journal of Remote Sensing, 25(9): 1629-1640.
- Batista, W.B., and Platt, W.J. (2003). Tree population responses to hurricane disturbance syndromes in a south-eastern USA old-growth forest. Journal of Ecology, 91: 197-212.
- Bellingham, P.J., Tanner, E.V.J., and Healey, J.R. (1995). Damage and responsiveness of Jamaican montane tree species after disturbance by a hurricane. Ecology, 76: 2562-2580.
- Boose, E.R., Foster, D.R., and Fluet, M. (1994). Hurricane impacts to tropical and temperate forest landscapes. Ecological Monographs, 64: 369-400.
- Boucher, D.H., Vandermeer, J.H., Yih, K., and Zamora, N. (1990). Contrasting hurricane damage in tropical rain forest and pine forest. Ecology, 71: 2022-2024.
- Bove, M.C., Elsner, J.B., Landsea, C.W., Niu, X., and O'Brien, J.J. (1998). Effect of El Niño on U.S. landfalling hurricanes, revisited. Bulletin of the American Meteorological Society, 79: 2477-2482.
- Brokaw, N.V.L., and Walker, L.R. (1991). Summary of effects of caribbean hurricanes on vegetation. Biotropica, 23: 442-447.
- Cahoon, D.R., Reed, D.J., Day Jr., J.W., Steyer, G.D., Boumans, R.M., Lynch, J.C., McNally, D., and Latif, N. (1995). The influence of Hurricane Andrew on sediment distribution in Louisiana coastal marshes. Journal of Coastal Research, 21: 280-294.
- Christensen, R. (1997). Log-Linear Models and Logistic Regression. (2nd ed.). New York: Springer.

- Climate Prediction Center. (2007). Monitoring and Data: ENSO Impacts on the U.S. Retrieved <7 Feb 2007> From http://www.cpc.noaa.gov/products/analysis_monitoring/ensostuff/ensoyears.shtml.
- CNN. (2004). Ivan's stormy trek floods Southeast. Retrieved <11 Jan 2007> From <http://www.cnn.com/2004/WEATHER/09/16/hurricane.ivan>.
- Cohen, J. (1988). Statistical Power Analysis for the Behavioral Sciences. (2nded.). Hillsdale: Erlbaum.
- Congalton, R.G., and Green, K. (1999). Assessing the accuracy of remote sensed data: principles and practices. Boca Raton: Lewis.
- Cooper-Ellis, S., Foster, D.R., Carlton, G., and Lezberg, A. (1999). Forest response to catastrophic wind: Results from an experimental hurricane. Ecology, 80: 2683-2696.
- DeCoster, J. (2004). Data Analysis in SPSS. Retrieved <01 Dec 2006> From <http://www.stat-help.com/notes.html>.
- Dilley, A.C., Millie, S., O'Brien, D.M., and Edwards, M. (2004). The relation between Normalized Difference Vegetation Index and vegetation moisture content at three grassland locations in Victoria, Australia. International Journal of Remote Sensing, 25(19): 3913-3928.
- Donnelly, J.P., and Webb III, T. (2004). Back-barrier sedimentary records of intense hurricane landfalls in the northeastern United States. In: Murnane, R., and Liu, K.-b (Eds.): Hurricanes and Typhoons: Past, Present, and Future. New York: Columbia University Press, 58-95.
- Doyle, T.W., Keeland, B.D., Gorham, L.E., and Johnson, D.J. (1995). Structural Impact of Hurricane Andrew on the forested wetlands of the Atchafalaya basin in south Louisiana. Journal of Coastal Research, 21: 354-364.
- Dunn, G.E., and Miller, B.I. (1964). Atlantic Hurricanes (Revised Edition). Baton Rouge, Louisiana, USA: Louisiana State University Press.
- Dymond, C.C., Mladenoff, D.J., and Radeloff, V.C. (2002). Phenological differences in Tasseled Cap indices improve deciduous forest classification. Remote Sensing of Environment, 80: 460-472.
- Elsner, J.B., and Kara, A.B. (1999). Hurricanes of the North Atlantic. New York: Oxford Univ. Press.
- Emanuel, K. (2005). Divine Wind: The History and Science of Hurricanes. New York: Oxford Univ. Press.

- Franklin, J.L. (2005). 2004 Atlantic hurricanes: A season of devastation. Weatherwise, March/April, 52-61.
- Garson, G.D. (1998). Logistic Regression. Retrieved <01 Dec 2006> From <http://www2.chass.ncsu.edu/garson/pa765/logistic.htm>.
- Gresham, C.A., Williams, T.M., and Lipscomb, D.J. (1991). Hurricane Hugo wind damage to southeastern U.S. coastal forest tree species. Biotropica, 23(4a), 420-426.
- Healey, S.P., Cohen, W.B., Zhiqiang, Y., and Krankina, O.N. (2005). Comparison of Tasseled Cap-based Landsat data structures for use in forest disturbance detection. Remote Sensing of Environment, 97: 301-310.
- Hosmer, D.W. and Lemeshow, S. (2000). Applied Logistic Regression: Second Edition. New York, John Wiley and Sons.
- Ichii, K., Maruyama, M., and Yamaguchi, Y. (2003). Multi-temporal analysis of deforestation in Rondônia state in Brazil using Landsat MSS, TM, ETM+, and NOAA AVHRR imagery and its relationship to changes in the local hydrological environment. International Journal of Remote Sensing, 24(22): 4467-4479.
- Jin, S., and Sader, S.A. (2005). Comparison of time series tasseled cap wetness and the normalized difference moisture index in detecting forest disturbances. Remote Sensing of Environment, 94: 364-372.
- Kovacs, J.M., Wang, J., and Blanco-Correa, M. (2001). Mapping disturbances in a mangrove forest using multi-date Landsat TM imagery. Environmental Management, 27 (5): 763-776.
- Kuemmerle, T., Radeloff, V.C., Perzanowski, K., and Hostert, P. (2006). Cross-border comparison of land cover and landscape pattern in Eastern Europe using a hybrid classification technique. Remote Sensing of Environment, 103: 449-464.
- Landis, J.R., and Koch, G.G. (1977). The measurement of observer agreement for categorical data. Biometrics, 33: 159-174.
- Latifovic, R., Zhu, Z.-l., Cihlar, J., Giri, C., and Olthof, I. (2004). Land cover mapping of North and Central America – Global Land Cover 2000. Remote Sensing of Environment, 89: 116-127.
- Leica Geosystems. (2003a). ERDAS Field Guide – 7th Edition. Atlanta.
- Leica Geosystems. (2003b). ERDAS Imagine Tour Guides. Atlanta.
- Lillesand, T.M., Kiefer, R.W., and Chipman, J.W. (2004). Remote Sensing and Image Interpretation – 5th Edition. New York, Wiley.

- Liu, K.-b. (2004a). Principles, methods, and examples from Gulf coast lake sediments. In: Murnane, R. and Liu, K.B. (Eds.): Hurricanes and Typhoons: Past, Present, and Future. New York, Columbia University Press, 13-57.
- Liu, K.-b. (2004b). Paleotempestology: Geographic solutions to hurricane hazard assessment and risk prediction. In: D. Janelle, B. Warf, and K. Hansen (Eds.), WorldMinds: Geographical Perspectives on 100 Problems. Dordrecht, Kluwer Academic Publishers, 443-448.
- Liu, K.-b. (2007). Paleotempestology. In: Elias, S. (Ed.): Encyclopedia of Quaternary Science. Amsterdam, Elsevier, 1978-1986.
- Liu, K.-b. and Fearn, M.L. (1993). Lake-sediment record of late Holocene hurricane activities from coastal Alabama. Geology, 21: 793-796.
- Liu, K.-b. and Fearn, M.L. (2000a). Holocene history of catastrophic hurricane landfalls along the Gulf of Mexico coast reconstructed from coastal lake and marsh sediments. In: Ning, Z. and Abdollahi, K. (Eds.): Current Stresses and Potential Vulnerabilities: Implications of Global Change for the Gulf Coast Region of the United States. Baton Rouge, Franklin, 38-47.
- Liu, K.-b. and Fearn, M.L. (2000b). Reconstruction of prehistoric landfall frequencies of catastrophic hurricanes in northwestern Florida from lake sediment records. Quaternary Research, 54: 238-245.
- Liu, K.-b., Lu, H., and Shen, C. (2003). Assessing the vulnerability of the Alabama Gulf coast to intense hurricane strikes and forest fires in the light of long-term climatic changes. In: Ning, Z.H., Turner, R.E., Doyle, T., and Abdollahi, K. (Lead Authors). Integrated Assessment of the Climate Change Impacts on the Gulf Coast Region. Baton Rouge, GCRCC, 223-230.
- Loope, L., and Duever, M. (1994). Hurricane impact on uplands and freshwater swamp forest. Bioscience, 44: 238-248.
- Lopez, O.R., and Kursar, T.A. (2003). Does flood tolerance explain tree species distribution in tropical seasonally flooded habitats? Oecologia, 136: 193-204.
- Lugo, A.E., and Scatena, F.N. (1996). Background and catastrophic tree mortality in tropical moist, wet, and rain forests. Biotropica, 54: 238-245.
- Myers, R.K., and van Lear, D.H. (1998). Hurricane-fire interactions in coastal forests of the south: a review and hypothesis. Forest Ecology and Management, 103: 265-276.
- NASA Earth Observatory. EO Library: Measuring Vegetation (NDVI and EVI). Retrieved <Jan 10, 2007> From http://earthobservatory.nasa.gov/Library/MeasuringVegetation/measuring_vegetation_2.html.

- National Climatic Data Center. (2005). Local Climatological Data: Mobile, AL. Retrieved <03 Feb 2007> From www1.ncdc.noaa.gov/pub/orders/F888050E-B0C1-2B5A-2020-6AC728446ADE.PDF.
- National Geographic TOPO! Software. Alabama. [CD-ROM]. Place of publication unknown: USGS, date unknown.
- National Hurricane Center (2004). Tropical Cyclone Report: Hurricane Ivan. Retrieved <01 Nov 2006> From <http://www.nhc.noaa.gov/2004ivan.shtml>.
- National Oceanic and Atmospheric Administration. Hurricane Ivan – September 2-26, 2004. Retrieved <16 Jan 2007> From <http://www.hpc.ncep.noaa.gov/tropical/rain/ivan2004.html>.
- National Weather Service. (2006). NOAA's National Weather Service – Birmingham, Alabama. Retrieved <16 Jan 2007> From http://www.srh.noaa.gov/bmx/significant_events/2004/09_16_Ivan/ivan_path.php.
- NOAA Coastal Services Center. (2006). Historical Hurricane Tracks. Retrieved <09 Jan 2007> From <http://maps.csc.noaa.gov/hurricanes/viewer.html>.
- NOAA's National Weather Service. (2006). Top 10 Weather Events in the 21st Century for Alabama. Retrieved <10 Jan 2007> From http://www.srh.noaa.gov/bmx/significant_events/climate/top10.php.
- Otvos, E.G. (2004). Beach aggradation following hurricane landfall: Impact comparisons from the two contrasting hurricanes, northern Gulf of Mexico. Journal of Coastal Research, 20(1): 326-339.
- Pezeshki, S.R. (1994). Plant responses to flooding. In: Wilkinson, R.E. (ed.). Plant environment interactions. New York, Dekker: 289-321.
- Platt, W.J., Beckage, B., Doren, R.F., and Slater, H.H. (2002). Interactions of large-scale disturbances: Prior fire regimes and hurricane mortality of savanna pines. Ecology, 83(6): 1566-1572.
- Ramsey III, E.W., Hodgson, M.E., Sapkota, S.K., and Nelson, G.A. (2001). Forest impact estimated with NOAA AVHRR and Landsat TM data related to an empirical hurricane wind-field distribution. Remote Sensing of Environment, 77: 279-292.
- Reilly, A.E. (1991). The effects of Hurricane Hugo in three tropical forests in the U.S. Virgin Islands. Biotropica, 23: 414-419.
- Rice, M.D., Lockaby, B.G., Stanturf, J.A., & Keeland, B.D. (1997). Woody debris decomposition in the Atchafalaya River basin of Louisiana following Hurricane disturbance. Soil Science Society of America Journal, 61: 1264-1274.

- Risi, J.A., Wanless, H.R., Tedesco, L.P., and Gelsanliter, S. (1995). Catastrophic sedimentation from Hurricane Andrew along the southwest Florida coast. Journal of Coastal Research, 21: 83-102.
- Saksa, T., Uuttera, J., Kolström, T., Lehikoinen, M., Pekkarinen, A., and Sarvi, V. (2003). Clear-cut detection in boreal forest aided by remote sensing. Scandinavian Journal of Forest Research, 18: 537-546.
- Sheshkin, D.J. (1997). Handbook of Parametric and Nonparametric Statistical Procedures. CRC: New York.
- Simpson, R.H., and Riehl, H. (1981). The Hurricane and Its Impact. Louisiana State University Press: Baton Rouge.
- Stone, G.W., Armbruster, C.K., Grymes III, J.M., and Huh, O.K. (1996). Researchers study impact of Hurricane Opal on Florida coast. EOS, 77: 81.
- Stone, G.W., Walker, N.D., Hsu, S.A., Babin, A., Liu, B., Keim, B.D., Teague, W., Mitchell, D., and Leben, R. (2005). Hurricane Ivan's impact along the northern Gulf of Mexico. EOS, 86, 497-508.
- Tanner, E.V.J., Kapos, V., and Healey, J.R. (1991). Hurricane effects on forest ecosystems in the Caribbean. Biotropica, 23(4a): 513-521.
- Tedesco, L.P., Wanless, H.R., Scusa, L.A., Risi, J.A., and Gelsanliter, S. (1995). Impact of Hurricane Andrew on south Florida's sandy coastlines. Journal of Coastal Research, 21: 59-82.
- The Weather Channel. (2007). Monthly Averages for Gulf Shores, AL. Retrieved <09 Jan 2007> From <http://www.weather.com/weather/wxclimatology/monthly/USAL0254>.
- Tømmervik, H., Høgda, K.A., and Solheim, I. (2003). Monitoring vegetation changes in Pasvik (Norway) and Pechenga in Kola Peninsula (Russia) using multitemporal Landsat MSS\TM data. Remote Sensing of Environment, 85: 370-388.
- United States Department of Commerce. (2006). Hurricane Katrina: August 23-31, 2005. NOAA. Retrieved <11 Jan 2007> From <http://www.weather.gov/om/assessments/pdfs/Katrina.pdf>.
- United States Geological Survey. (2004). Hurricane Ivan Impact Studies. Retrieved <16 Jan 2006> From <http://coastal.er.usgs.gov/hurricanes/ivan/photos/index.html>.
- Walker, L.R. (1991). Tree damage and recovery from Hurricane Hugo in Luquillo Experimental Forest, Puerto Rico. Biotropica, 23: 379-385.

Whigham, D.F., Olmsted, I., Cano, E.C., and Harmon, M.E. (1991). The Impact of Hurricane Gilbert on trees, litterfall, and woody debris in a dry tropical forest in the northeastern Yucatan Peninsula. Biotropica, 23(4a): 434-441.

Zimmerman, J.K., Everham, E.M., Waide, R.B., Lodge, D.J., Taylor, C.M., and Brokaw N.V.L. (1994). Responses of tree species to hurricane winds in subtropical wet forest in Puerto Rico: implications for tropical tree life histories. Journal of Ecology, 82: 911-922.

Vita

Thomas Anthony Bianchette was born in Warren, Michigan (an immediate suburb of Detroit), on April 16, 1983. He spent his adolescence playing video games, shooting hoops, and pestering his parents. During high school, he played baseball at the varsity level for two years for Hartland High School in Hartland, Michigan, and was a member of the 2000 Hartland Eagle team which reached the state semifinals for the first time in school history, only to suffer a heartbreaking defeat to Detroit Catholic Central, 12-11. He later played junior college baseball at Mott Community College in which he fell on hard times, disagreed with the coach, and slowly lost interest in the game he loves.

It was then he took an Introduction to Regional Geography class with Mr. Andrew Huddy, and was quickly infatuated with the world, especially the physical environment, in front of him. Tom finished his two years at Mott, and subsequently transferred to Western Michigan University, where he received his Bachelor of Science degree in 2005. He left Michigan behind, and followed his professor (and friend) Dr. Greg Veeck's advice, and moved to Baton Rouge, Louisiana, to work on his Master of Science degree in geography. Tom will continue his studies in the doctoral program of oceanography/coastal sciences in the Fall of 2007.